UNIVERSITY OF
KWAZULU-NATAL

INYUVESI
YAKWAZULU-NATALI

An *in vitro* assessment of functionalized gold nanoparticles in anticancer drug delivery

By

Lorenzo Lance David

Master of Science

at

University of KwaZulu-Natal

College of Agriculture, Engineering and Science
School of Life Sciences
Department of Biochemistry

Supervisor: Prof M Singh

DECLARATIONS

COLLEGE OF AGRICULTURE, ENGINEERING AND SCIENCE
DECLARATION 1 - PLAGIARISM

I, Mr Lorenzo Lance David declare that:

1. The research reported in this thesis, except where otherwise indicated, and is my original research.

2. This thesis has not been submitted for any degree or examination at any other university.

3. This thesis does not contain other persons' data, pictures, graphs or other information, unless specifically acknowledged as being sourced from other persons.

4. This thesis does not contain other persons' writing, unless specifically acknowledged as being sourced from other researchers. Where other written sources have been quoted, then:
   a. Their words have been re-written but the general information attributed to them has been referenced
   b. Where their exact words have been used, then their writing has been placed in italics and inside quotation marks, and referenced.

5. This thesis does not contain text, graphics or tables copied and pasted from the Internet, unless specifically acknowledged, and the source being detailed in the thesis and in the References sections.

Signed

Declaration Plagiarism 30/01/2017 FHDR Approved

COLLEGE OF AGRICULTURE, ENGINEERING AND SCIENCE
DECLARATION 2 - PUBLICATIONS

DETAILS OF CONTRIBUTION TO PUBLICATIONS that form part and/or include research presented in this thesis (include publications in preparation, submitted, *in press* and published and give details of the contributions of each author to the experimental work and writing of each publication)

Not Applicable

Signed: ---------- Date: ----------

I, Prof M Singh as supervisor of the MSc study hereby consent to the submission of this MSc Dissertation.

Signed: ---------- Date: 30/01/2017

CMC Feb 2012

ABSTRACT

The science of nanotechnology that is involved in the treatment, diagnosis, monitoring and control of diseases is commonly referred to as nanomedicine. Nanomedicine is set to revolutionize drug delivery and development, especially for diseases such as cancer which is on an upward spiral. Technologies involving the manipulation of materials at an atomic level are shaping the direction of conventional therapeutic approaches, promising to improve areas of delivery, entrapment and sustained release. Gold nanoparticles (AuNPs), present with unique characteristics on the nano-scale, exhibiting low toxicity, high biocompatibility, ease of surface design and unique optical properties. The combination of these factors promotes the extensive study for their use as drug and gene delivery vectors. Conventional chemotherapeutic drugs are limited in their efficacy, relating to factors of poor biodistribution, rapid *in vivo* degradation and lack of specificity. The nature of conventional therapeutic approaches gives rise to undesirable and often severe side effects, determining the duration and intervals between treatments. A development of a targeted drug delivery system, able to improve distribution and bioavailability to cancerous tissue whilst offering low off target cytotoxicity and a controlled release profile under appropriate conditions is urgently required.

This study entails the chemical synthesis of AuNPs and their subsequent functionalization with two cationic polymers, chitosan and poly-l-lysine. Encapsulation and linear binding of respective polymers to 5-fluorouracil (5-FU) was investigated. Physico-chemical characterization studies were carried out on all synthesized nanoparticles and nanocomplexes through UV-visible spectroscopy, TEM, FTIR, ICP and Nanoparticle Tracking Analysis (NTA). All nanoparticles and nanocomplexes appeared as polydispersed, small (<105 nm) spherical particles, with nanocomplexes exhibiting good colloidal stability (high positive zeta potentials). From the two polymers utilized and the two binding methods evaluated, the encapsulation method with chitosan exhibited superior 5-FU binding and release capacity, with a controlled release pattern observed over a selected period of time. The cytotoxicity trends of all nanocomplexes were investigated using the MTT and SRB cell viability assays in three human cancer cell lines, viz. Caco-2 (colon adenocarcinoma), HEPG2 (hepatocellular carcinoma), MCF-7 (breast adenocarcinoma) and a non-cancer cell line, HEK293 (embryonic kidney). The AuNP nanocomplexes were able to exhibit significant dose dependent anticancer activity, with a specificity towards the cancer cell lines. A comparative study of AuNP-polymer:5-FU nanocomplexes against control polymer:5-FU complexes revealed that the Au containing nanocomplexes elicited greater anticancer activity, highlighting the versatility of gold nanoparticles in therapeutic drug delivery.

Overall, the above characteristics and biological activity show the immense potential of these AuNPs as suitable anticancer drug carriers *in vitro*, and with further studies and optimizations they could be extended to clinical cancer therapy.

Key Words: Nanomedicine, gold nanoparticles, drug delivery, 5-fluorouracil, chitosan, poly-l-lysine, anticancer activity.

Dedication

This thesis is dedicated to my late grandfathers
Mr Nelson David and Mr Thumba Naicker. Thank you for all your support, guidance and love. I could have not asked for better role models.

ACKNOWLEDGEMENTS

I wish to express my sincere gratitude and appreciation to the following persons and institutions:

- None of this would have been possible without the strength and guidance I have received from above and for that I would like to firstly thank God.
- To Professor Singh, thank you for all your effort which has gone into this thesis. Your guidance, patience and support has been invaluable throughout this entire process.
- To my family, Terence, Rose and Leighton David, I want to acknowledge all your help, guidance and support in every sense throughout the years. I could never thank you enough.
- To Shandre Pillay, thank you for all your support and motivation over the years, for always being there when I needed you.
- To Stephanie Pillay, thank you for putting up with me through this process and for your help and motivation.
- To all of my colleagues at the non-viral gene delivery lab University of KwaZulu-Natal. Thank you for all of the help, guidance and motivation, this work would not be possible without you.
- The **University of KwaZulu-Natal** for supporting my research and providing me with the facilities that I needed to achieve my goals.
- The **National Research Foundation (NRF)** for funding this research initiative.

PREFACE

This thesis is presented as a compilation of 5 chapters.

Chapter 1	Introduction and project Aims
Chapter 2	Literature Review
Chapter 3	Research Results 1
Chapter 4	Research Results 2
Chapter 5	Conclusion and Future Work

CONTENTS

Chapter 3. Chitosan functionalized gold nanoparticles in the delivery of the anticancer drug, 5-Fluorouracil, *in vitro.*

Chapter 4. An *in vitro* study of poly-l-lysine functionalized gold nanoparticles in anticancer drug delivery

---

ABBREVIATIONS

AuNP's	**Gold Nanoparticles**
5-FU	**5-Fluorouracil**
NTA	**Nanoparticle Tracking Analysis**
Caco-2	**Colon adenocarcinoma**
HEPG2	**Hepatocellular carcinoma**
MCF-7	**Breast adenocarcinoma**
HEK293	**Embryonic kidney**
CS-AuNP's	**Chitosan conjugated gold nanoparticle**
Mw	**Molecular weight**
mM	**Millimolar**
g	**Grams**
DMSO	**Dimethyl sulfoxide**
FBS	**Fetal bovine serum**
gml	**Grams per ml**
M	**Molar**
ml	**Milli litre**
nm	**Nanometre**
SPR	**Surface plasmon resonance**
TEM	**Transmission electron microscopy**
FTIR	**Fourier transform infra-red analysis**
µl	**Micro litre**
PLL	**Poly-l-lysine**
PLL-AuNP's	**Poly-l-lysine conjugated gold nanoparticles**

LIST OF FIGURES

LIST OF TABLES

Abstract

The science of nanotechnology that is involved in the treatment, diagnosis, monitoring and control of diseases is commonly referred to as nanomedicine. Nanomedicine is set to revolutionize drug delivery and development, especially for diseases such as cancer which is on an upward spiral. Technologies involving the manipulation of materials at an atomic level are shaping the direction of conventional therapeutic approaches, promising to improve areas of delivery, entrapment and sustained release. Gold nanoparticles (AuNPs), present with unique characteristics on the nano-scale, exhibiting low toxicity, high biocompatibility, ease of surface design and unique optical properties. The combination of these factors promotes the extensive study for their use as drug and gene delivery vectors. Conventional chemotherapeutic drugs are limited in their efficacy, relating to factors of poor biodistribution, rapid *in vivo* degradation and lack of specificity. The nature of conventional therapeutic approaches gives rise to undesirable and often severe side effects, determining the duration and intervals between treatments. A development of a targeted drug delivery system, able to improve distribution and bioavailability to cancerous tissue whilst offering low off target cytotoxicity and a controlled release profile under appropriate conditions is urgently required.

This study entails the chemical synthesis of AuNPs and their subsequent functionalization with two cationic polymers, chitosan and poly-l-lysine. Encapsulation and linear binding of respective polymers to 5-fluorouracil (5-FU) was investigated. Physico-chemical characterization studies were carried out on all synthesized nanoparticles and nanocomplexes through UV-visible spectroscopy, TEM, FTIR, ICP and Nanoparticle Tracking Analysis (NTA). All nanoparticles and nanocomplexes appeared as polydispersed, small (<105 nm) spherical particles, with nanocomplexes exhibiting good colloidal stability (high positive zeta potentials). From the two polymers utilized and the two binding methods evaluated, the encapsulation method with chitosan exhibited superior 5-FU binding and release capacity, with a controlled release pattern observed over a selected period of time. The cytotoxicity trends of all nanocomplexes were investigated using the MTT and SRB cell viability assays in three human cancer cell lines, viz. Caco-2 (colon adenocarcinoma), HEPG2 (hepatocellular carcinoma), MCF-7 (breast adenocarcinoma) and a non-cancer cell line, HEK293 (embryonic kidney). The AuNP nanocomplexes were able to exhibit significant dose dependent anticancer activity, with a specificity towards the cancer cell lines. A

comparative study of AuNP-polymer:5-FU nanocomplexes against control polymer:5-FU complexes revealed that the Au containing nanocomplexes elicited greater anticancer activity, highlighting the versatility of gold nanoparticles in therapeutic drug delivery.

Overall, the above characteristics and biological activity show the immense potential of these AuNPs as suitable anticancer drug carriers *in vitro*, and with further studies and optimizations they could be extended to clinical cancer therapy.

Key Words: Nanomedicine, gold nanoparticles, drug delivery, 5-fluorouracil, chitosan, poly-l-lysine, anticancer activity.

Chapter 1

Introduction and Project Aims

Chapter One

1.1 Introduction

Cancer, a chronic worldwide disease, is characterized by uncontrolled cell division, mainly due to genetic aberrations[1]. The mechanism through which cancer develops, for many years has divided researchers due to the complexity of the disease. However, with the increased research into the genetics and biology of cancer, this is slowly unravelling, implicating genetic alterations, cell signaling pathways, replication and avoidance of apoptosis[2]. Current methods of treatment are dependent on the outcomes of clinical and pathological staging[3], and include surgical resection, if the tumor is located in an area which is operable, followed by radiation or chemotherapy, to kill the remaining cancer cells[4]. Each method carries their own measure of risk.

Chemotherapy involves the use of cytotoxic drugs, with the aim of targeting rapidly dividing cells, a fundamental characteristic of cancer cells[5]. Conventional anticancer drugs used in the treatment of cancer do provide some benefit, however, they show no specificity towards the tissue they act upon, resulting in severe and unwanted side effects[6], such as hair loss, anemia, and lowering of the white cell blood count, which further drain strength from already ailing patients. Recent research has indicated that chemotherapeutic agents may also stimulate an antitumor immune response[7], however a safer and targeted system would serve patients better. In addition to these side-effects, repeated administration of treatment is common, but does not guarantee remediation of cancer. The non-specificity of action, low levels of accumulation of the drug at the target site and their rapid metabolism in the body shortly after administration, are all obstacles which scientists must overcome if we are to successfully treat cancer and related diseases[8].

Hence, there is much room for treatment options to be improved upon. Essentially, drug delivery is what governs the effectiveness of therapeutic agents[9] and a better understanding of the field will go a long way in improving the lives of the millions of patients, who are in battle with this dreaded disease. The potential of classical and novel therapeutic agents is limited by their ability to be delivered both safely and efficiently to targeted tissue[10]. Further research must be conducted to gain a better understanding of the inner workings of efficient drug delivery systems[11]. Over the years, a multitude of delivery agents have been studied, both for their safety and efficacy in

delivering their payloads to the targeted tissue. Many have shown promise *in vitro,* but have suffered setbacks due to unforeseen interactions and hurdles in *in vivo* studies. For these reasons, new methods for cancer therapy, especially in the field of nanotechnology are being developed, in the hope that they present with better outcomes.

While nanotechnology has revolutionized areas of our lives such as entertainment and transport, they also show promise in advancing the fields of science and medicine. Nanotechnology is dedicated to developing, designing, constructing, and employing materials at the nanometer scale. Nanoparticles are advantageous, in that their characteristics can be altered to suit the desired requirement, without changing their actual chemical composition[12]. Gold is a precious metal, coveted for its luster, color and its value. Its favorable characteristics and the facile synthesis of gold nanoparticles, have led to their use as potential therapeutic agents and drug and gene delivery carriers.

This study focused on chemically synthesizing gold nanoparticles via the citrate reduction method, conjugation of gold nanoparticles(AuNPs) with the cationic polymers, chitosan and poly-l-lysine via the methods of encapsulation and linear binding, and complete characterization of nanoparticles and nanocomplexes using physico-chemical methods. It was anticipated that the combination of gold nanoparticles with the cationic polymers would produce delivery systems with greater anticancer activity than administration of the drug on its own, in the cell lines tested.

Cationic polymers were incorporated into the delivery vehicle due to their ability to stabilize the nanoparticles and serve as chemical linkers between the gold nanoparticle and the anticancer drug, 5-fluorouracil (5-FU). These polymers have high densities of positive charges and were expected to impart favorable characteristics to the AuNPs for biological applications. Both chitosan and poly-l-lysine were investigated for their ability to entrap 5-FU efficiently and to release the anticancer agent under specific pH conditions. The nanoparticle cytotoxicity's and apoptosis inductions were further evaluated.

1.2 Aim and objectives

This study aims to synthesize, and fully characterize AuNPs, polymer functionalized AuNPs and their nanocomplexes with the anticancer drug 5-FU. The study further aims to determine, the effectiveness of the AuNPs and functionalized AuNPs as an anticancer drug delivery systems.

The main objectives will be:

- To chemically synthesize and characterize AuNPs.
- To functionalize the AuNPs with chitosan and poly-l-lysine using two unique methods.
- To evaluate the conjugation of 5-FU to the AuNP systems by binding efficiency studies.
- To determine the pharmacokinetics of the AuNP delivery systems with regards to controlled drug release and final drug delivery.
- To establish a cytotoxicity profile for the delivery systems in four selected cell lines, and determine if any apoptosis induction was achieved.

1.3 Outline of thesis

This thesis was written in the format of an introductory chapter followed by a literature review, two research papers and a concluding chapter.

Chapter 1 is a brief introduction and background to the research topic, and provide the aims, objectives and outline of the thesis.

Chapter 2 provides a detailed review of the literature. It also highlights the use of gold nanoparticles in delivery of therapeutic agents and what generated interest in this study. It highlights some of the commonly used techniques in the synthesis of gold nanoparticles, whilst also including information on stabilizing agents used, and the most likely mechanisms through which the nanoparticles enter the cells.

Chapter 3 and 4 are written in the form of research papers, involving chitosan and poly-l-lysine functionalization of AuNPs, respectively. It highlights the design and synthesis of gold nanoparticles, focusing on their characterization using UV-vis, TEM, ICP, NTA and FTIR. Drug binding, release studies, and *in vitro* cytotoxicity and apoptosis studies in four cell lined were

assessed. The papers compare the encapsulation and linear binding for each polymer, with discussion and interpretation of all results.

Chapter 5 concludes the thesis, highlighting and summarizing the results obtained. Future studies or recommendations are also outlined.

1.4 References

[1] Hoeijmakers, J. H. (2001) Genome maintenance mechanisms for preventing cancer, *nature 411*, 366-374.

[2] Hanahan, D., and Weinberg, Robert A. (2011) Hallmarks of Cancer: The Next Generation, *Cell 144*, 646-674.

[3] Brodeur, G. M., Seeger, R. C., Barrett, A., Berthold, F., Castleberry, R. P., D'Angio, G., De Bernardi, B., Evans, A. E., Favrot, M., and Freeman, A. I. (1988) International criteria for diagnosis, staging, and response to treatment in patients with neuroblastoma, *Journal of Clinical Oncology 6*, 1874-1881.

[4] Association, J. G. C. (2011) Japanese gastric cancer treatment guidelines 2010 (ver. 3), *Gastric cancer 14*, 113-123.

[5] Jain, M., Nilsson, R., Sharma, S., Madhusudhan, N., Kitami, T., Souza, A. L., Kafri, R., Kirschner, M. W., Clish, C. B., and Mootha, V. K. (2012) Metabolite profiling identifies a key role for glycine in rapid cancer cell proliferation, *Science 336*, 1040-1044.

[6] Chari, R. V. (2007) Targeted cancer therapy: conferring specificity to cytotoxic drugs, *Accounts of chemical research 41*, 98-107.

[7] Ménard, C., Martin, F., Apetoh, L., Bouyer, F., and Ghiringhelli, F. (2008) Cancer chemotherapy: not only a direct cytotoxic effect, but also an adjuvant for antitumor immunity, *Cancer Immunology, Immunotherapy 57*, 1579-1587.

[8] Ross, J. S., Schenkein, D. P., Pietrusko, R., Rolfe, M., Linette, G. P., Stec, J., Stagliano, N. E., Ginsburg, G. S., Symmans, W. F., and Pusztai, L. (2004) Targeted therapies for cancer 2004, *American journal of clinical pathology 122*, 598-609.

[9] Huang, X., and Brazel, C. S. (2001) On the importance and mechanisms of burst release in matrix-controlled drug delivery systems, *Journal of controlled release 73*, 121-136.

[10] Lu, Y., and Low, P. S. (2012) Folate-mediated delivery of macromolecular anticancer therapeutic agents, *Advanced drug delivery reviews 64*, 342-352.

[11] Sahoo, S. K., Dilnawaz, F., and Krishnakumar, S. (2008) Nanotechnology in ocular drug delivery, *Drug discovery today 13*, 144-151.

[12] Jain, P. K., El-Sayed, I. H., and El-Sayed, M. A. (2007) Au nanoparticles target cancer, *Nano Today 2*, 18-29.

Chapter 2

Literature Review

Chapter Two

2. Literature review

2.1 Drug delivery

Drug delivery is a captivating field of study, engaging the interest of researchers worldwide, both from an academic and industrial view point. This is largely due to the urgent need to address the many limitations associated with the delivery of drugs safely and efficiently, while minimizing their harmful side effects[1]. Drug delivery as a concept, can be summarized as the release of a bioactive agent, at a specific site under controlled and sustained release[2]. This definition however, is based on an ideal scenario and further research is required to meet the challenges of efficient drug delivery, thereby allowing classical and novel drugs to be used to their fullest potential. This can be achieved through the development and optimization of targeted and efficient drug delivery systems[3, 4].

It is of little consequence designing novel drugs or modifying classical formulations to increase activity, when the vectors responsible for their distribution remain ineffective[5]. Presently, many drugs are limited in their efficacy towards treating conditions due to issues of poor solubility resulting in chemotherapeutic agents being unable to penetrate biological membranes[6-8], requirement of high dosages leading to increased toxicity towards healthy tissue, low levels of accumulation at the target site, their nonspecific delivery and action[9], short plasma half-lives and rapid *in vivo* degradation[10]. The need to develop safe and efficient delivery vehicles has generated in great interest in the field, resulting in collaborations between researchers of various fields and disciplines[8].

In addition, the biology of solid tumors is such that cell division towards the center slows down drastically, effectively stopping, thereby limiting the ability of the chemotherapeutic agents to act. Furthermore, many chemotherapeutic agents are unable to penetrate deep into the tumor, limiting their effectiveness in eradicating the cancerous cells[11, 12]. A further obstacle includes the overexpression of P-glycoprotein on the surface of cancerous cells[13, 14]. This protein is termed a multidrug resistance protein, primarily as it prevents the accumulation of drugs within the cell, since this protein acts as an efflux pump, and contributes to drug resistance in cancer cells.[15, 16]

Presently the vast number of chemotherapeutic agents used in the treatment of cancer, work through destroying rapidly dividing cells[17], one of the fundamental characteristics of cancerous tissue . This targeting system is largely ineffective, as many types of tissue in addition to neoplastic cells are known to divide rapidly, including those present in the digestive tract, hair follicles and bone marrow[18, 19].

Current methods of treatment show little differentiation between cancerous and healthy tissue[20], the consequences being that such chemotherapeutic agents often result in unpleasant and severe side effects[21]. These include hair loss, anemia, decrease in white blood cells that leave patients vulnerable to infections through a suppressed immune system, organ dysfunction and mucositis that involve inflammation of the gastrointestinal tract lining. Such side effects limit the dose and intervals between treatments[22, 23].

An ideal targeted drug delivery system should possess the ability to bind the therapeutic agent, protect the drug from *in vivo* degradation, transport the drugs in a safe and efficient manner to a specific cell, tissue or organ and successfully release the anticancer agent under the appropriate conditions[24, 25], in comparison to classical methods, thereby reducing treatment costs through avenues including increased product shelf life and reduced concentrations needed to obtain positive outcomes[26, 27]. The development of unique drug delivery systems offers many advantages such as a greater degree of protection, whilst improving pharmacokinetics[28, 29]. This highlights the importance of developing novel drug delivery systems for the future, resulting in it being one of most important areas of drug research currently.

The rapid advancement of nanotechnology in recent years is likely to have a substantial impact on the discovery and emergence of new drug delivery systems. Due to recent advancements in the field, it is not beyond reason to suggest that nanoparticles are the future of drug delivery, having the potential to become valuable therapeutic and diagnostic tools due to their varied applications in research and medicine[30]. In addition, the ease of modification associated with many nanoparticles makes them attractive prospects for tailoring of treatment options for patients [31].

2.2 5-Fluorouracil

There are a variety of classical anticancer drugs, which have been developed over the years. However, 5-fluorouracil (5-FU) is widely accepted as being the backbone of many chemotherapeutic techniques in the treatment of patients with late stage colorectal cancer. 5-fluorouracil was introduced as a chemotherapeutic agent more than 4 decades ago, currently the drug remains one of the more favored options and is included in majority of adjuvant chemotherapy for late stage colon cancer. Most chemotherapeutic regimes involve the use of a combination of drugs, 5-fluorouracil is often used in combination with levamisole or leucovorin[32]. Studies have revealed that 5-fluorouracil based combinational chemotherapy improves the survival rates of patients with stage III colon cancer[33-35].

Effectively, 5-FU is an analogue of the naturally occurring pyrimidine uracil, it is an antimetabolite, as seen in Figure 2.1, it contains a fluorine group, covalently attached to an uracil molecule [36]. Research has previously demonstrated that rat hepatomas tend to favor incorporation of radiolabeled uracil when compared to normal tissue. These studies eluded to the fact that enzymatic pathways for the use of uracil and by extension analogs of uracil are different between cancerous and non-cancerous cells[37]. Building on this, with the inclination that analogs could be used for therapeutic purposes, researchers Heidelberger and colleagues synthesized 5-FU in 1957[38].

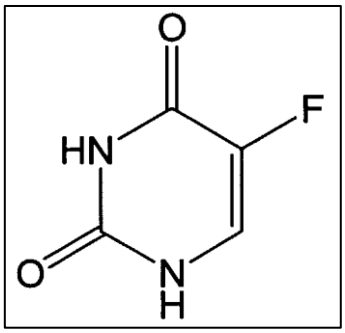

Figure 2.1 Molecular structure of 5-Fluorouracil.

Since 1957, great strides in elucidating the mechanism of action of 5-FU have been made. For 5-FU to express its cytotoxic ability, it requires cellular uptake and metabolic activation. 5-FU is an analogue of uracil, therefore it will be utilized and incorporated for the same transport processes

and enzymes involved in anabolism and catabolism[39]. Upon entry into the cell, 5-FU undergoes anabolism into its cytotoxic equivalent via a number of pathways. The enzyme thymidine phosphorylase catalyzes the reversible conversion of 5-FU to 5-fluoro-2'-deoxyuridine (FdUrd)[40, 41]. A second enzyme, thymidine kinase introduces a phosphate group onto the 5'-carbon present in the deoxyribose ring, resulting in 5-fluoro-2'deoxyuridine monophosphate (FdUMP). The *de novo* synthesis of thymidine 5'monophosphate from 2'-deoxyuridine-5'monophosphate is catalyzed by the enzyme thymidylate synthase. This is achieved through the transfer of a methyl group from 5,10-methlyenetetrahydrofolate. There have been two pathways identified in which 5-FU is converted into a ribonucleotide viz. firstly uridine phosphorylase converts 5-FU into FdUrd, followed by the enzyme uridine kinase which catalyzes the formation of 5-fluorouridine monophosphate. The second pathway involves the direct transfer of a ribose 5'monophosphate from 5'phosphoribosyl-1-pyrophosphate to a 5-FU molecule via the enzyme orotate phosphoribosyltransferase. The 5-fluorouridine monophosphate first undergoes conversion to 5-fluorouridine diphosphate then to 5-fluorouridine triphosphate by action of the enzymes nucleoside monophosphate and nucleoside diphosphate kinases. The latter is readily utilized by RNA polymerases, which incorporate it into RNA molecules.

One of the main mechanisms of action exhibited by 5-FU is the inhibition of thymidylate synthase through action of FdUMP. Some of the consequences of the inhibition of thymidylate synthase include depletion of thymidine 5'monophosphate and thymidine 5'-triphosphate. This results in DNA synthesis ceasing and interference with DNA repair. Whilst there is an argument that cells can overcome the inhibition of thymidylate synthase, through salvage of extracellular thymidine, the levels of thymidine present in human plasma are insufficient[42].

Like many classical chemotherapeutic agents, whilst it has shown to be very effective in destroying cancerous cells, it shows little specificity, resulting in the systematic destruction of both healthy and cancerous tissue. However, due to its effectiveness, it is still a drug of choice and in use presently. However, the drug is administered intravenously, primarily due to the unpredictable bioavailability of the drug when administered orally. Numerous studies have reported on the cytotoxicity of this drug towards healthy tissue. In many cases it was reported that 5-FU has resulted in mucositis[43, 44] and the alteration in microflora structure [45].

2.3 Nanotechnology

Advancement in the field of nanotechnology has greatly impacted many medical and industrial fields [46]. It involves the engineering and synthesis of materials, at a level of atoms and molecules[47]. Nanotechnology has been one of the most important influences on our social economy over the last century and can be compared to the effect the semiconductor or information technology has had over the years[48]. Recent advancements in the field has highlighted the possibility of breakthroughs in various areas including nanoelectrics, materials and manufacturing, biotechnology, medicine and healthcare. With such a vast array of possible applications, it comes as no surprise that expectations are high with many viewing nanotechnology as being the next industrial revolution[49, 50].

The use and interaction of nanotechnology with cellular and molecular components in medicine and healthcare is termed nanomedicine. The ability to manipulate matter at an incredibly small scale, often between 1 – 100 nm[51, 52], offers many advantages which are not exhibited by their bulk counterparts, such as the capability of deeply penetrating tumors, areas that are not accessible to individual molecules or bulk solids [53]. In addition, the creation of materials at this scale often results in unique and desirable chemical, physical and biological properties[54, 55].

At the nanoscale level, many semiconductors, metals and polymeric particles exhibit novel electronic, magnetic, structural and optical properties[56]. Such properties have enabled the science of nanotechnology to be applied across a variety of fields including diagnostics, therapeutics and imaging[57]. Nanotechnology has shown immense potential in being able to bind and transport drugs across those physiological barriers known to be difficult to traverse, such as the blood brain barrier. Researchers have shown that through coating nanoparticles with polysorbates, it is possible for drug loaded nanoparticles to be transported across the blood brain barrier, thereby enabling brain targeting after intravenous injection[58].

There is no doubt that nanotechnology is shaping the future especially in formulation of novel methods and application in science and medicine. Hence, it is now important to build frameworks for the application of nanotechnology in therapeutics.

2.4 Cancer

Cancer is a disease that has been around for thousands of years with the earliest known medical description dating back to 2500 BC, in ancient Egyptian text. It was described there as a "a bulging tumor in the breast, like touching a ball of wrappings". With regard to a form of treatment, it was written "There is none" [59].

Thousands of years later, we are still searching for an effective form of treatment, with cancer becoming one of the leading causes of mortality worldwide[60]. However, since then tremendous strides have been made in attempting to understand the genetics and biology of tumors, with the general consensus being, that cancer develops from both genetic instability and exposure of cells to different micro-environmental factors[61]. Simply, cancer is the uninhibited growth of cells, which results in cellular dysfunction due to the level of aggressive growth.

Cancer is known to follow a multi-stage process[62], from the initial emergence of cancer cells to clonal masses or tumors, and to the subsequent distribution of cancer cells from the primary tumor to distant organs or tissue via the blood and lymphatic systems through the complex processes of invasion and metastasis[63, 64]. Metastasis remains a challenge in terms of treatment and is a major cause of cancer related mortalities[65]. Cancer cells often undergo genetic mutations causing activation of their oncogenes and/or inactivation of their tumor suppressor genes, allowing the cells to evade growth suppressors, resist cell death, sustain proliferative signaling, encourage angiogenesis and replicative immortality and finally induce invasion and metastasis[66]. A schematic representation of the fundamental characteristics of cancer is shown in Figure 2.2. One of the many challenges faced by researchers in the effective treatment of cancer is the combination of complex signaling pathways and multiple mechanisms which permit cancerous cells to evade programmed cell death.

Drug delivery systems must meet certain requirements if effective cancer treatment is to be reached, viz. targeted delivery of the anticancer agent specifically to the tumor, thereby limiting cytotoxicity towards healthy tissue, increasing the bio-accessibility of the drug to the tumor tissues at the required concentrations, increasing circulation time of the drug, and protecting therapeutic agents from degradation[67].

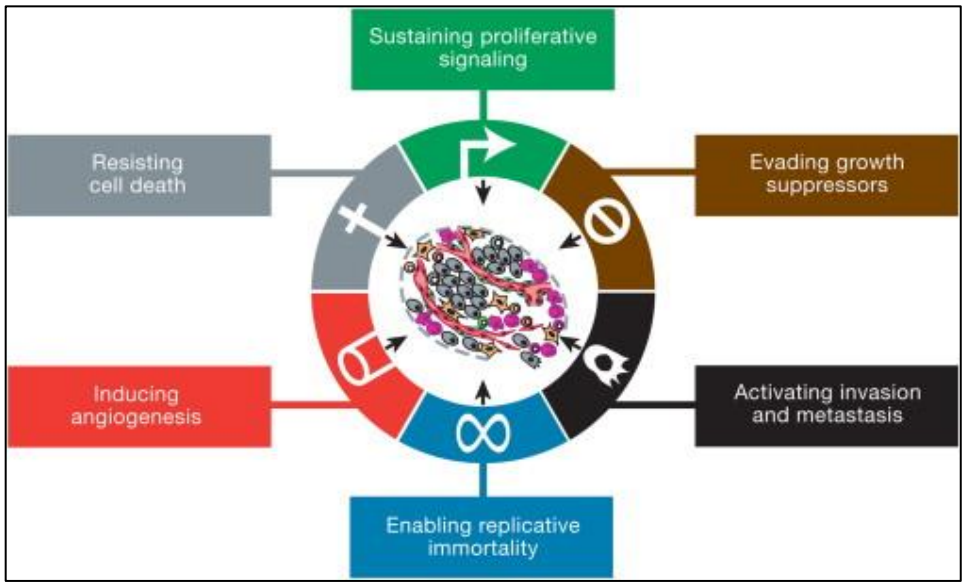

Figure 2.2: The hallmarks of cancer, processes enabling tumor formation and metastasis [61].

Colon cancer represents some of the highest mortality rates, and is the third most frequently diagnosed form of cancer with 1.36 million new cases reported in 2012 [60], and a prominent cause of mortality in both men and women worldwide. Standard treatment options involve surgery, and either chemotherapy or radiation or both[68]. These options have shown to be effective, however they often result in severe side effects in patients[69]. In addition, these treatment options come with their own level of peril, such as radiotherapy which can result in complications such as soft tissue necrosis[70] or spinal cord myelitis[71]. This highlights the need for non-invasive techniques in the treatment of cancer. Hence the challenge to formulate and design suitable drug delivery systems that can fulfill this need.

2.5 Gold nanoparticles: A brief history

Gold has fascinated man for centuries, wars have been waged and civilizations built around this precious metal. The history of gold dates back centuries, and during the middle ages it was believed that through experiments base metals could be converted into gold[72]. The quest to discover the secrets of creating gold laid down many of the principles of modern chemistry through discovering the physical and chemical properties of various substances[73].

As early at the 16th century, there was a belief among healers of the time, that if gold could be made drinkable, it would have therapeutic uses[74]. As such, many individuals who were able to

afford such luxuries began to drink gold and noticed that this gave their skin a sheen and which was highly desirable at the time. In ancient Egypt, 5000 years ago, gold was ingested to aid in mental, spiritual and purification of the body[75].

2.6 Gold in biomedical applications

Gold nanoparticles have emerged as potential drug and gene delivery vehicles due to their multitude of favorable characteristics, such as their ease of synthesis and ability to be chemically functionalized with various groups[76]. The ability to conjugate gold nanoparticles with a number of therapeutic agents such as peptides, proteins, nucleic acids and drugs, allows for them to be used in various biomedical applications such as diagnostics, imaging and therapeutics[77, 78]. However, for these nanoparticles to become effective in cellular applications, the nanoparticles must exhibit efficient delivery to targeted cells, including controlled release of the drugs or genes under specific conditions.

While *in vitro* studies are essential and will demonstrate the many capabilities of nanoparticles in delivering genes and drugs and other therapeutic molecules[79], when introduced *in vivo* they are likely to illicit possible immune responses[80, 81]. Hence, if nanoparticles are to safely and efficiently deliver their cargos, mechanisms must be created to negate these immune responses. This is not beyond comprehension, and with a thorough working knowledge of the various constraints involved, gold nanoparticles with purposefully designed morphologies and surface modifications, have the potential live up to current expectations[82].

Some of the many advantages of using gold nanoparticles in medicine is that they are bio-inert, essentially non-toxic and biocompatible, thereby making them an ideal choice as a starting material when designing a delivery vehicle[83]. Furthermore, gold nanoparticles with varying hydrodynamic sizes have been easily synthesized with controlled dispersity[84]. The favorable sizes of gold nanoparticles adds to their arsenal, as they have the ability to deeply penetrate cells and tissues, making their possible uses in medicine far-reaching[85]. In addition, they possess unique properties, such as their ability to absorb and significantly scatter visible and near-infrared light upon excitation of their plasmon oscillation[86]. These properties can be manipulated to control the release of drugs, which was first reported in 2000, where drugs bound to plasmonically active particles were successfully released by photo-activation[54, 87].

Many drug delivery systems involving gold have been formulated to release their payload in either one of two ways viz. through biologically controlled factors such as pH environment of the cell or through external stimuli such as the application of light or radio frequencies[88].

Modification of particles at the level of atoms and molecules, changes the substances properties often resulting in unique characteristics. These unique characteristics are what set gold nanoparticles apart from their opponents. Gold nanoparticles have been shown to possess a larger surface to volume ratio, in comparison to other particles[89]. This is attractive as a single nanoparticle of gold will be able to carry a larger capacity of drugs, therapeutic agents or targeting moieties, making them more efficient as delivery vectors.

In addition to the unique optical, magnetic[90] and catalytic properties[91] of gold nanoparticles, and their various sizes, they can be synthesized into a variety of shapes, such as rods, stars, diamonds or spheres. Their applications are vast, ranging from chemical processing, to drug[92] and gene delivery, and to imaging or diagnosis of cancer or other related diseases[93]. The introduction of cationic polymers to gold nanoparticles serves to further strengthen electrostatic interactions with drugs such as 5-Fluorouracil, enabling for a greater level of binding, in addition to increase stability in physiological conditions.

2.7 Gold nanoparticles and drug delivery

As mentioned earlier, gold nanoparticles have attracted attention in recent years due to their many unique properties. However, the ability to delivery drugs safely and efficiently to target sites such as the colon, lungs or brain requires more basic research. Gold nanoparticles, on their own, do not possess any targeting groups, or unique surface properties which allow them to be directed specifically to any tissue or to bind specific biomolecules such as nucleic acids. Their advantage lies in their ability to be functionalized with cell specific ligands, stabilizing agents[94] and polymers[92], among others. The ability to study the mechanism of functionalization, its optimization, and its effects on the bio-activity of gold nanoparticles may hold the key to successful drug delivery to a variety of tissues. In order for gold nanoparticles to be targeted, various ligands, aptamers, antibodies or proteins have been employed to modify the surface properties to provide target recognition[95].

However, this will not be limited to drug delivery, as better understanding of the inner workings of functionalization and targeting emerge, in theory any chemical or biomolecule may be introduced and delivered efficiently. Current research has illustrated that gold nanoparticles can be successfully functionalized using targeting ligands such as folic acid[96] and galactose[97]. Such functionalization results in the accumulation of nanoparticles in target cells, allowing for their use in various applications including therapeutics, diagnostics and imaging[57].

2.8 Surface plasmon resonance of gold nanoparticles

Gold is a metal which has fascinated man for centuries, and much of the attention it received stems from properties such as its depth of color, luster and resistance to oxidation. Gold nanoparticles possess unique optical properties which result in their intense color. The color of colloidal gold suspension is dependent on the shape and size of the nanoparticles, and their ability to interact with light results in these unique properties[98]. The shape of gold nanoparticles is important as it has an effect on the surface plasmon resonance(SPR), which in turn has an effect on the efficiency of the nanoparticles in various medical applications[99]. Through altering the shape of a nanoparticle, it is possible to adjust the SPR in the visible and near infrared regions. The surface plasmon resonance of spherical gold nanoparticles occurs in the middle of the visible wavelength, and by changing the shape from spheres to rods or nanoshells, it is possible to shift the SPR closer to the near-infrared (between 800-1200 nm)[100, 101]. Briefly, all metal nanoparticles possess a naturally occurring oscillating electromagnetic field, and the exposure of light to these nanoparticles results in an increase in the oscillation of the free electrons present in the metal. Due to the increased oscillation of the electrons, a charge separation occurs between the ionic lattice and the free electrons. The amplitude of the oscillation reaches a maximum at a specific frequency, resulting in the absorption of light[102]. This specific frequency can be determined through UV-vis analysis. There are several factors which are known to affect the surface plasmon resonance of a particle including the size, shape and composition of the specific metal in question. This unique ability, allows for these nanoparticles to be used in photothermal therapeutic schemes, such as the release of drugs once they have entered their site of action[103]. Furthermore, the presence of the gold nanoparticles can be confirmed using its SPR, with deviations from this occurring upon nanoparticle functionalization.

2.9 Surface modification and zeta potential

The surface chemistry of a nanoparticle is one of the determining factors directing their uses in specific applications. In the instance of drug delivery, a proper understanding of nanoparticle surface chemistry is imperative in determining whether successful conjugation can occur between biomolecules such as targeting ligands and the nanoparticle. Surface modification of nanoparticles with regard to drug delivery will determine the efficacy of the nanoparticle as a drug delivery vector.

Surface modification is important primarily for four reasons viz. (1) to increase the circulation time of the nanocomposite which can also be achieved by slowing down the removal of the nanocomposite via the reticulo-endothelial system, (2) to allow for the attachment of targeting ligands and therapeutic agents such as drugs, (3) to stabilize the nanoparticle and preventing aggregation and (4) to reduce any cytotoxicity that could arise from the original capping ligands[104].

The term zeta potential is used to describe the electro kinetic potential in a colloidal suspension. It is a measure of the magnitude of charges on a nanoparticle. The zeta potential is also an indication of the surface potential, and so determines the magnitude of the electrical double layer repulsion. It is possible to generate a net electrical charge through ionizing surface functional groups present is a suspension of nanoparticles such as gold. Zeta potential analysis is one of the few methods available for characterizing the interaction between the surface of the nanoparticle and the substance it is suspended[105]. Essentially, if all particles present in a colloidal solution have larger zeta potentials, either negative or positive in magnitude, this results in stronger forces of repulsion between the nanoparticles, thereby preventing aggregation. In comparison, if particles have low zeta potentials, then there will be a reduction in the repulsive forces which exist between nanoparticles, resulting in unwanted interactions and aggregation. Two factors which greatly affect zeta potential are pH and conductivity of the medium the nanoparticles are suspended in[106]. Zeta potential has been widely used in pharmaceutical formulations for evaluation of stability.

2.10 Synthesis of gold nanoparticles for drug delivery

Since the ability of gold nanoparticles to function as drug or gene delivery vehicles is largely dependent on their size, shape and structure, the ability to produce and manipulate gold nanoparticles, with specific requirements in mind is vital to their continued used in the biomedical

field. The two most commonly used methods for the synthesis of gold nanoparticles viz. citrate reduction and the polyol reduction method, are described below.

2.10.1. The citrate reduction method

The citrate reduction technique, introduced by Turkevich in 1951, remains one of the most common methods for synthesizing gold nanoparticles for biomedical applications. The method involves the reduction of gold (III) chloride trihydrate with a reducing agent such as Trisodium citrate. It is a simple and cost effective method, allowing for the synthesis of gold nanoparticles in which size can be parametrically controlled, through changing the ratio of sodium citrate to gold salt. Nanoparticles produced are relatively uniform in shape and size distribution.

The progress of the reaction can be monitored through observation of changes in color[107,108]. Initially the color will be a pale-yellow solution, transitioning to colorless, to dark blue, purple then finally a deep wine red hue. The color of the solution gives an indication of the size of nanoparticles present in the solution, with the change in color from blue to wine red being attributed to the reduction in size of the gold nanoparticles. Generally, the size of nanoparticles synthesized in this method range from 40 -100 nm, making it an ideal protocol for the synthesis of nanoparticles with biological applications in mind.

It has been shown that the citrate ions have a dual purpose in this reaction. Firstly, they act as a reducing agent, assisting in the reduction of Au^{3+} to Au^{0}, secondly they stabilize the nanoparticle through forming a layer of citrate ions around the surface of the nanoparticle[107, 109]. The citrate ions have a net negative charge, which they induce around the surface of the nanoparticle. This creates repulsive forces between the gold nanoparticles preventing undesirable interactions and aggregation. However, if the nanoparticles are suspended in a non-aqueous media, the nanoparticles will become unstable and aggregate. This is very undesirable and would limit the use of the nanoparticles in many applications.

2.10.2 Polyol reduction method

In this method, metal precursors such as oxides, nitrates and acetates are refluxed in ethylene glycol or polyols in the presence of a protecting polymer[110]. Essentially this is a reduction method

in which nanoparticles are formed by nucleation and growth from the solution, with polyol acting a solvent for the inorganic compound. It has been shown that the size of nanoparticles produced through this method can be modified by altering the pH of the solution, with a decrease in pH resulting in a decrease in the size of nanoparticles, much like how the addition of larger volumes of sodium citrate will result in smaller nanoparticles in the citrate reduction method described previously.

The above two methods have been successfully employed to synthesize gold nanoparticles of favorable characteristics, with the former being utilized in this study. However, the long-term stability of a colloidal solution is an important factor in creating efficient delivery systems, therefore a better understanding of the mechanisms by which the nanoparticles are stabilized is needed.

2.11 Polymer modification and stabilization of gold nanoparticles

The stability of gold nanoparticles (AuNPs) in forming efficient drug or gene delivery vehicles is of great importance, with research ongoing into methods to improve the bio-stability, biocompatibility and water solubility of AuNPs. Studies have shown that the addition of polymers to the surface of gold nanoparticles has resulted in greater stability. It has further been reported[111] that by replacing the surfactant bilayer using thiol-terminated methoxypoly (ethylene glycol) on gold nanorods allowed for the successful conjugation of anti-rabbit IgG.

Cationic polymers can serve as both a stabilizing agent and a cross linker in attaching therapeutic agents. The use of such cationic polymers has been shown to prevent the aggregation of gold nanoparticles, which is vital when the nanoparticles are exposed to an environment of high ionic strength. These cationic polymers have the added advantage of improving the cellular uptake of nanocomplexes, and increasing the overall circulation time of the nanocomposites *in vivo*[112, 113]. There are several strategies which can be employed to modify the surface of AuNPs, and can essentially be divided into covalent and non-covalent methods.

Covalent interactions of polymers with the surface of AuNPs will produce stronger bonds, which could be a disadvantage in some instances. If the therapeutic agent is bound too strongly to the surface of the nanoparticle, there may be issues associated with the efficient release of the agent at its target site of action[114]. To circumvent such issues, AuNPs can be modified to present with an

abundance of positive charges on their surface, through ionic interactions with ligands containing amine or acidic groups[115]. Functionalization of AuNPs with cationic polymers results in the formation of delivery vehicles which show a greater level of biocompatibility, lower toxicity and the ability to increase the load of therapeutic agents[116]. Two polymers which have gained much attention in recent years, viz. chitosan (CS) and poly-l-lysine (PLL), are attractive alternatives to both sterically stabilize nanoparticles and serve as cross linkers, allowing for many anionic therapeutic agents to be functionalized to the surface of gold nanoparticles. These polymers are not affected by the presence of electrolytes, therefore allowing for a more permanent method of stabilization. These two polymers that are utilized in this study are discussed below[117].

2.11.1 Chitosan (CS)

Chitosan is a naturally occurring carbohydrate polymer, which is obtained from the deacetylation of chitin (Figure 2.3). Chitin is primarily sourced from the exoskeleton of marine animals such as crabs and shrimps[118]. Similar in its structure to the polysaccharide cellulose, chitosan is also composed of a linear β-(1→4) linked monosaccharides. The difference in their structure is that chitosan contains 2-amino-2-deoxy-β-D-glucan residues, joined through glycosidic linkages. Resulting primary amine group, is what imparts the unique properties possessed by chitosan, making them desirable for biomedical applications.

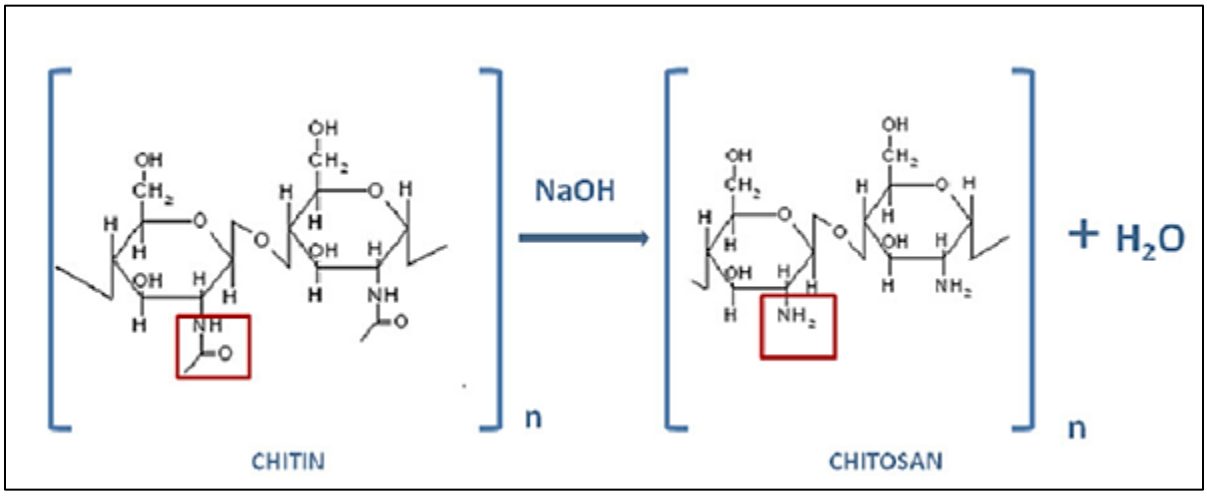

Figure 2.3 Scheme for the N-deacetylation of chitin into chitosan through hydrolysis[119]

Briefly, chitosan is synthesized through hydrolysis of the aminoacetyl groups of chitin in an aqueous alkaline solution. Chitosan presents with many desirable characteristics, which make it suitable for biological applications. Studies have shown that chitosan entraps bioactive molecules through several mechanisms viz. ionic crosslinking, chemical crosslinking and through ionic complexation. In addition, chemical modification of chitosan has been of great benefit in improving the association of bioactive molecules to polymers, whilst also generating a controlled drug release profile. Chitosan has been utilized in other delivery systems, including liposomes as a coating agent, due to their high affinity for the cell membrane, studies have concluded these characteristics of chitosan and their derivatives show promise as materials to form part of controlled drug and gene delivery systems[120, 121]. The functional groups present in chitosan, allows for simple conjugation of targeting ligands and therapeutic agents. Due to chitosan's high level of biocompatibility, it does not trigger allergic reactions. It is biodegradable and slowly degrades into harmless products including amino sugars, which are absorbed by the human body[122]. Other desirable characteristics include , presence of positive charges, mucoadhesive properties[123], low toxicity[124, 125], and high levels of adhesion and immunostimulating properties[126]. One of the limitations of chitosan is its insolubility at physiological pH due to its cationic nature, however due to the numerous advantageous properties they possess, many chitosan derivatives have been synthesized, with the aim if making them more compatible for biological applications, many of which have been successful[127].

It is important to note that many of the properties of chitosan depend on its molecular weight and viscosity[128]. Research has shown that, higher molecular weight chitosan is more suitable as food preservatives than those of lower molecular weight[129]**.** Studies have shown that the degree of acetylation and the molecular weight have a major influence on the biological and physiological properties exhibited by chitosan[130, 131]. The use of chitosan as an encapsulation or stabilization agent is dependent on the pH. At an acidic pH, the primary amine groups present in chitosan become protonated, resulting in chitosan being soluble in water**.** The degree of solubility is reliant on the distribution of the free amino and acetyl groups, with good solubility of CS solutions being reported in 1-3% acetic acid[126]. Chitosan and its derivatives have been studied for their potential as non-viral gene delivery vectors[132], while chitosan based delivery systems are also under investigation for development of gastrointestinal delivery systems[133]. The positive charge exhibited by chitosan, allows for the binding of anionic therapeutic agents such as 5-FU, as well

as conjugation to gold nanoparticles which present with a slightly negative charge on their surface. Interestingly close to physiological pH, the nanocomplex of chitosan and 5-FU will present with a positive charge, thus enabling their interaction with the cell membrane which is negatively charged, through electrostatic interactions.

2.11.2 Poly-l-lysine (PLL)

Poly-l-lysine (PLL) is a cationic linear polymer composed of the essential amino acid, lysine. It has been shown to interact favorably with cell membranes[134], facilitating their uptake. Figure 2.4 depicts the typical structure of PLL, a positively charged amino acid polymer which contains at minimum a single hydrobromide molecule (HBr) per lysine molecule. The presence of the hydrobromide, results in PLL occurring in a crystalline state, which assists in its high solubility in water.

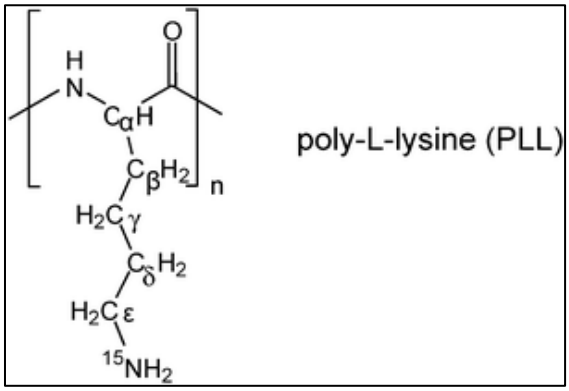

Figure 2.4 Chemical structure of poly-l-lysine[135]

Factors such as pH and temperature have been shown to affect the secondary structure of PLL, resulting in different conformations such as, random coils, α-helices and β-sheets. At a neutral pH, the conformation of PLL is an extended random coil, due to the repulsive forces which exist between the protonated amide groups[136]. These protonated groups are the primary contributing factors which allow PLL functionalization of AuNPs. The active amino groups, which are positively charged entities, ensure that PLL interacts readily with cell membranes, assisting in cell adhesion [137].

The functionalization of PLL onto the surface of gold nanoparticles will ensure that many of the desirable characteristics such as high biocompatibility, a flexible molecular backbone and good

solubility in water, are conferred to the functionalized molecule[138]. Functionalization of the AuNPs with PLL molecules, occur through interaction of the amino groups on the PLL molecule with carboxyl groups present on the surface of gold nanoparticles. The remaining free amino groups present on PLL can then serve to act as a cross linker[139], allowing for the conjugation of therapeutic molecules, eluding to the fact that PLL functionalized gold nanoparticles are promising drug delivery carriers.

2.12 Cellular uptake

Drug delivery systems act through two methods of distribution viz. passive and active targeting (Figure 2.5). Passive targeting is dependent on the physiochemical properties of the nanoparticle, including size, shape and surface charge of the particle[29]. This type of targeting takes advantage of characteristics such as leaky tumor vasculature, leading to the enhanced permeability and retention (EPR) effect and the tumor microenvironment, which was first reported by Matsumura and Maeda[21, 25, 140]. The nanoparticles can enter the site through passive diffusion or convection[141]. The EPR effect entails two components viz. altered biodistribution and increased plasma half-life of the nanocomplexes. The altered biodistribution involves the accumulation of nanocomposites at much greater concentrations in the tumor tissue, as opposed to healthy tissue, whilst the increased plasma half-life is due to the size of the nanocomposites containing the drug, being greater than the renal excretion threshold[142]. Passive targeting has the advantage of increasing the bioavailability of the drug at the tumor site, because in comparison to the vasculature of healthy tissue, tumors are known to present with gaps as large as 800 nm in their angiogenic blood vessels and a disorderly structure as seen in Figure 2.6.

It has been suggested that tumor angiogenic blood vessels are so leaky due to very high levels of vascular mediators such as brandykins, vascular endothelial growth factor, prostaglandins and nitric oxide to name a few. The combination of such infrastructure and poor lymphatic drainage induces the EPR effect[143]. However, a drawback of this type of targeting may also result in increased cytotoxicity across normal tissue, due to its non-targeting based approach.

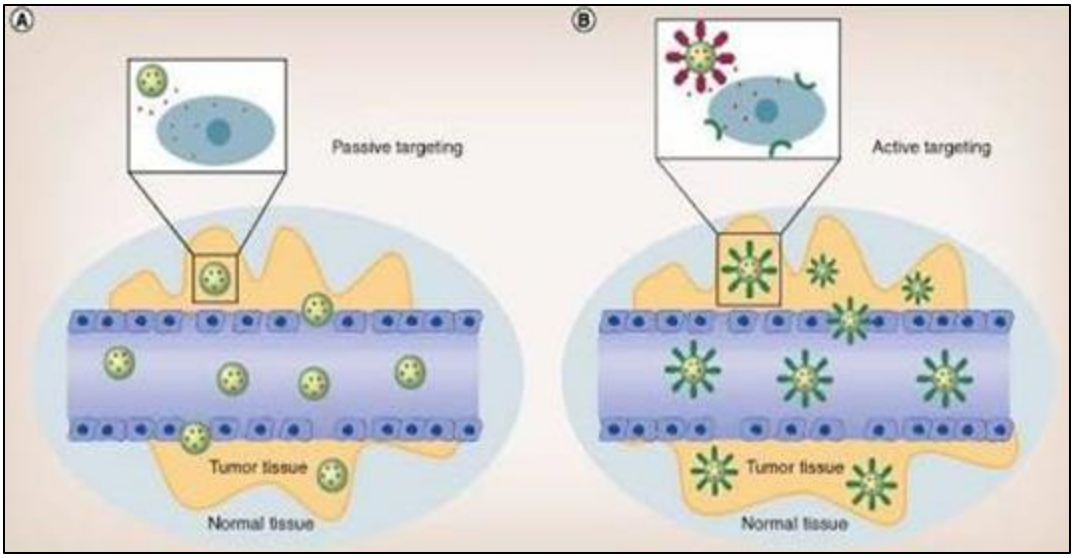

Figure 2.6 A scheme depicting drug delivery via active and passive targeting[144]

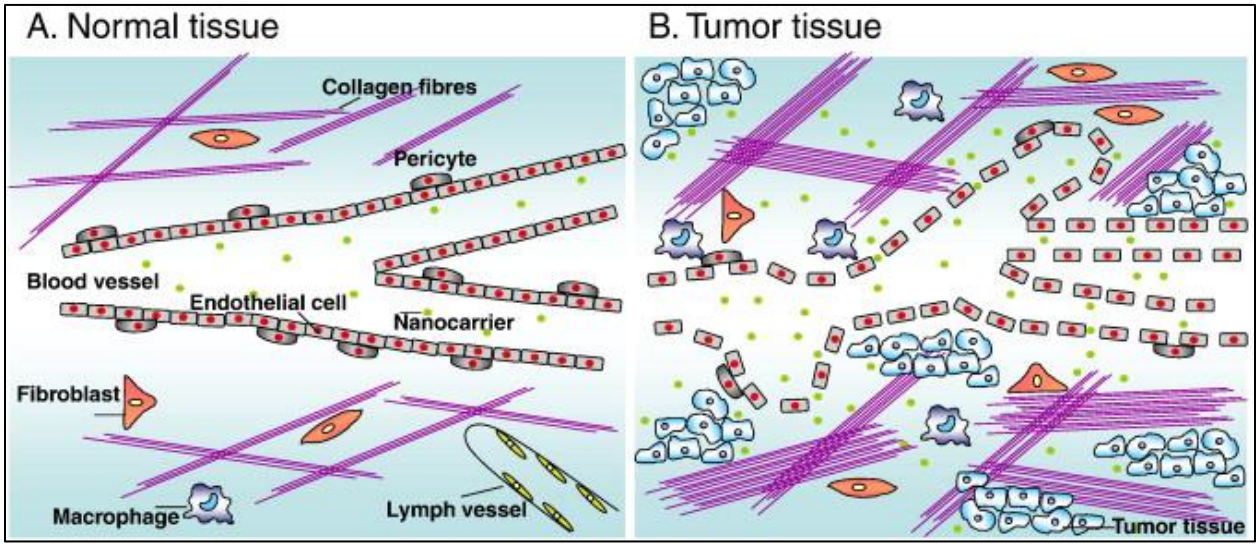

Figure 2.7: Differences in structure between normal and tumor tissue, assisting in the passive targeting due to enhanced permeability and retention effect[145].

In comparison, active targeting involves the functionalization of targeting moieties onto the surface of nanoparticles. These targeting ligands are selected by determining the type of receptor present and upregulated exclusively on specific tumor cells. Active targeting allows for greater accumulation of the therapeutic agent at the target site, as the nanoparticles are able to cross biological barriers based primarily on molecular recognition[146, 147]**.** Studies were carried out by Pun and coworkers on the influence of AuNP size, PEGylation and targeting ligands on targeted

and non-specific uptake[97]. They used gold nanoparticles of varying sizes ranging from 50 nm to 150 nm, functionalized with and without polyethyleneglycol (PEG5000), and to serve as targeting moieties they functionalized galactose residues onto the surface of the gold nanoparticles, for targeting asialglycoprotein receptors present on hepatocytes. They found that gold nanoparticles of 50 nm were internalized at a faster rate compared to unPEGylated nanoparticles of other sizes.

2.13 Biological barriers to drug delivery in tumors

The variation in biodistribution of chemotherapeutic drugs when delivered orally has resulted in many treatments introducing their drugs intravenously, as a result these drugs circulate the vascular system, reaching both healthy and cancerous tissue. Disadvantages of such a delivery method include increased cytotoxicity towards healthy tissue, resulting in severe side effects and the presence of numerous barriers both intracellular and extracellular before it is able to reach the tumor.

The initial obstacle faced by circulating nanocomposites is the reticuloendothelial system, and macrophages which circulate the blood stream[148], the sole purpose of which is to rid the body of objects not recognized as self. To avoid such an immune response, the nanocomposites need to be coated in a polymer layer which resists binding of proteins referred to as opsonins, via the process of opsonization. Opsonins are composed of several proteins including, but not limited to fibronectin, type I collagen and immunoglobulins. When the opsonin proteins encounter a foreign body, they adhere through a variety of interactions such as electrostatic, ionic and van der waals forces. Circulating macrophages identify the opsonin proteins coating the foreign body, followed by phagocytosis of the particle[149], therefore through the prevention of binding of opsonins, particles can circulate for longer in the blood stream.

Due to the rapid growth of cancerous tissue, tumor vasculature presents with a highly unorganized structure, coupled with an absence of smooth muscle resulting in varied blood flow. This poses a problem as the therapeutic containing nanocomposite will struggle to disperse through the tumor tissue[150]. Studies have shown that regions of the tumor with limited blood flow prove more resilient to the effects of chemotherapeutic agents[151].

The area within the tumor, referred to as the interstitium contains a combination of collagen and a viscous liquid[152]. With an increase in tumor size there is an increase of pressure, most of which is

contained towards the center. This buildup in pressure can be attributed to a number of factors including lack of lymphatic drainage and rapid cellular proliferation in a confined area[153]. Due to the increase in pressure, drug containing nanocomposites will find it difficult to penetrate deep into the tumor mass[152].

The exact mechanism by which nanoparticles are eventually removed from the body, is not fully understood, and requires further investigation. However, due to nanoparticles circulating the vascular system, it is thought that they accumulate in the spleen or are entrapped by macrophages[154]. The mechanism by which nanoparticles are taken into the cell, is also not fully understood, but an understanding of basic cellular uptake mechanisms eludes to endocytosis as being the main pathway. Phagocytosis usually involves the uptake of particles greater than 500 nm. However, most synthesized inorganic molecules fall within the range of 1-100 nm, and even with surface modifications they are unlikely to be in the range of 500 nm. It has been shown that when gold nanoparticles are incubated with cell culture media, serum proteins form an encapsulating layer around the nanoparticle. It is suggested that this layer is beneficial in the uptake of nanoparticles into cells[155]. These types of interactions could prove vital in understanding cellular uptake mechanisms better, facilitating the need for more research to be conducted in this area.

2.13 Intracellular Trafficking of nanoparticles

The mechanisms by which nanocomplexes are internalized into cells are not yet properly understood, however their entry from the extracellular space may occur via the main pathways such as nonspecific uptake, micropinocytosis or clathrin-coated pits capable of internalizing nanoparticles ranging from 10 to 300 nm[156] (Figure 2.7). Such pathways are known to transport particles into the cell, eventually leading to early endosomes. Alternatively, some nanocomposites may be transported via the endoplasmic reticulum or the golgi body, or from the early endosomes towards the lysosomes, often leading to their degradation. The preparation of most colloidal solutions often does not result in even size distribution. This factor could greatly influence the uptake of nanocomplexes into the cell, as size is related to their specific physiochemical properties. The obvious limiting factor in successfully delivering therapeutic agents into cells, is their cellular uptake. One can argue that for every delivery vehicle, there will be an ‘optimum’ size limit which exists, for delivery to selected cells and tissues, regulating their entry into the cell. It is suggested

that the low volumes of therapeutic agents reaching the desired cells are due to the inability of the delivery vector to escape the endosomal compartments, thus gaining entry into the cytoplasm. Therefore, many agents such as fusogenic peptides, which can disrupt the endosome have been suggested to be incorporated into the delivery systems. These peptides exist in a random coil conformation, however under the appropriate conditions, they can form an amphiphilic α-helical structure, which will result in endosomal disruption.

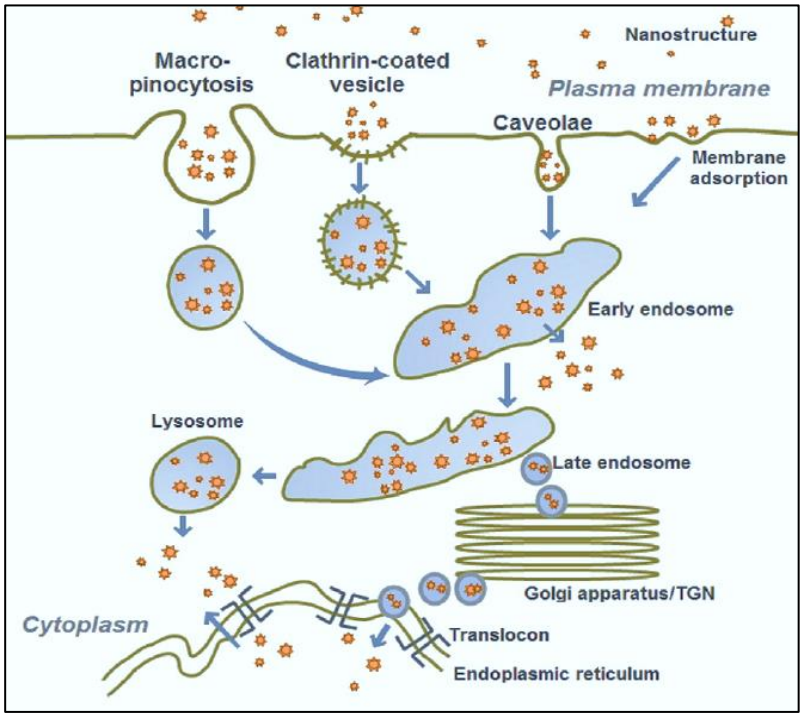

Figure 2.8 Possible endocytosis pathways for cellular uptake of nanocomplexes[157]

2.14 References

[1] Orive, G., Hernandez, R. M., Gascón, A. R. g., Domínguez-Gil, A., and Pedraz, J. L. (2003) Drug delivery in biotechnology: present and future, *Current opinion in biotechnology 14*, 659-664.

[2] Vallet-Regí, M., Balas, F., and Arcos, D. (2007) Mesoporous materials for drug delivery, *Angewandte Chemie International Edition 46*, 7548-7558.

[3] Mishra, B., Patel, B. B., and Tiwari, S. (2010) Colloidal nanocarriers: a review on formulation technology, types and applications toward targeted drug delivery, *Nanomedicine: Nanotechnology, biology and medicine 6*, 9-24.

[4] Hans, M., and Lowman, A. (2002) Biodegradable nanoparticles for drug delivery and targeting, *Current Opinion in Solid State and Materials Science 6*, 319-327.

[5] Cho, K., Wang, X., Nie, S., and Shin, D. M. (2008) Therapeutic nanoparticles for drug delivery in cancer, *Clinical cancer research 14*, 1310-1316.

[6] Mousa, S. A., and Bharali, D. J. (2011) Nanotechnology-based detection and targeted therapy in cancer: nano-bio paradigms and applications, *Cancers 3*, 2888-2903.
[7] Steichen, S. D., Caldorera-Moore, M., and Peppas, N. A. (2013) A review of current nanoparticle and targeting moieties for the delivery of cancer therapeutics, *European Journal of Pharmaceutical Sciences 48*, 416-427.
[8] Anselmo, A. C., and Mitragotri, S. (2014) An overview of clinical and commercial impact of drug delivery systems, *Journal of Controlled Release 190*, 15-28.
[9] Ross, J. S., Schenkein, D. P., Pietrusko, R., Rolfe, M., Linette, G. P., Stec, J., Stagliano, N. E., Ginsburg, G. S., Symmans, W. F., and Pusztai, L. (2004) Targeted therapies for cancer 2004, *American journal of clinical pathology 122*, 598-609.
[10] Rouge, N., Buri, P., and Doelker, E. (1996) Drug absorption sites in the gastrointestinal tract and dosage forms for site-specific delivery, *International journal of pharmaceutics 136*, 117-139.
[11] Nguyen, K. T. (2011) Targeted nanoparticles for cancer therapy: promises and challenge.
[12] Jain, R. K. (2005) Normalization of tumor vasculature: an emerging concept in antiangiogenic therapy, *Science 307*, 58-62.
[13] Natarajan, K., Bhullar, J., Shukla, S., Burcu, M., Chen, Z.-S., Ambudkar, S. V., and Baer, M. R. (2013) The Pim kinase inhibitor SGI-1776 decreases cell surface expression of P-glycoprotein (ABCB1) and breast cancer resistance protein (ABCG2) and drug transport by Pim-1-dependent and-independent mechanisms, *Biochemical pharmacology 85*, 514-524.
[14] Guertin, A. D., O'Neil, J., Stoeck, A., Reddy, J. A., Cristescu, R., Haines, B. B., Hinton, M. C., Dorton, R., Bloomfield, A., and Nelson, M. (2016) High Levels of Expression of P-glycoprotein/Multidrug Resistance Protein Result in Resistance to Vintafolide, *Molecular cancer therapeutics 15*, 1998-2008.
[15] Leslie, E. M., Deeley, R. G., and Cole, S. P. (2005) Multidrug resistance proteins: role of P-glycoprotein, MRP1, MRP2, and BCRP (ABCG2) in tissue defense, *Toxicology and applied pharmacology 204*, 216-237.
[16] Sandow, N., Kim, S., Raue, C., Päsler, D., Klaft, Z.-J., Antonio, L. L., Hollnagel, J. O., Kovacs, R., Kann, O., and Horn, P. (2015) Drug resistance in cortical and hippocampal slices from resected tissue of epilepsy patients: no significant impact of p-glycoprotein and multidrug resistance-associated proteins, *Frontiers in neurology 6*.
[17] Daniels, T. R., Delgado, T., Helguera, G., and Penichet, M. L. (2006) The transferrin receptor part II: targeted delivery of therapeutic agents into cancer cells, *Clinical immunology 121*, 159-176.
[18] Huang, Y. F., Shangguan, D., Liu, H., Phillips, J. A., Zhang, X., Chen, Y., and Tan, W. (2009) Molecular assembly of an aptamer–drug conjugate for targeted drug delivery to tumor cells, *ChemBioChem 10*, 862-868.
[19] Mitchison, T. J. (2012) The proliferation rate paradox in antimitotic chemotherapy, *Molecular biology of the cell 23*, 1-6.
[20] Chari, R. V. (2007) Targeted cancer therapy: conferring specificity to cytotoxic drugs, *Accounts of chemical research 41*, 98-107.
[21] Maeda, H., Bharate, G., and Daruwalla, J. (2009) Polymeric drugs for efficient tumor-targeted drug delivery based on EPR-effect, *European Journal of Pharmaceutics and Biopharmaceutics 71*, 409-419.
[22] Naidu, M. U. R., Ramana, G. V., Rani, P. U., Suman, A., and Roy, P. (2004) Chemotherapy-induced and/or radiation therapy-induced oral mucositis-complicating the treatment of cancer, *Neoplasia 6*, 423-431.
[23] Griffin, A., Butow, P., Coates, A., Childs, A., Ellis, P., Dunn, S., and Tattersall, M. (1996) On the receiving end V: patient perceptions of the side effects of cancer chemotherapy in 1993, *Annals of oncology 7*, 189-195.
[24] Mills, J. K., and Needham, D. (1999) Targeted drug delivery, *Expert Opinion on Therapeutic Patents 9*, 1499-1513.

[25] Maeda, H., Sawa, T., and Konno, T. (2001) Mechanism of tumor-targeted delivery of macromolecular drugs, including the EPR effect in solid tumor and clinical overview of the prototype polymeric drug SMANCS, *Journal of controlled release 74*, 47-61.
[26] Juliano, R. (1978) Drug delivery systems: a brief review, *Canadian journal of physiology and pharmacology 56*, 683-690.
[27] Chourasia, M., and Jain, S. (2003) Pharmaceutical approaches to colon targeted drug delivery systems, *J Pharm Pharm Sci 6*, 33-66.
[28] Sahoo, S. K., and Parveen, S. (2006) Nanomedicine: Clinical Applications of Polyethylene Glycol Conjugated Proteins and Drugs, *Clinical pharmacokinetics*, 965-988.
[29] Allen, T. M., and Cullis, P. R. (2004) Drug delivery systems: entering the mainstream, *Science 303*, 1818-1822.
[30] Nikalje, A. (2015) Nanotechnology and its Applications in Medicine, *Med chem 5*, 081-089.
[31] Sun, X., Li, F., Shen, G., Huang, J., and Wang, X. (2014) Aptasensor based on the synergistic contributions of chitosan–gold nanoparticles, graphene–gold nanoparticles and multi-walled carbon nanotubes-cobalt phthalocyanine nanocomposites for kanamycin detection, *Analyst 139*, 299-308.
[32] Boland, C. R., Sinicrope, F. A., Brenner, D. E., and Carethers, J. M. (2000) Colorectal cancer prevention and treatment, *Gastroenterology 118*, S115-S128.
[33] Laurie, J. A., Moertel, C., Fleming, T. R., Wieand, H., Leigh, J., Rubin, J., McCormack, G., Gerstner, J., Krook, J., and Malliard, J. (1989) Surgical adjuvant therapy of large-bowel carcinoma: an evaluation of levamisole and the combination of levamisole and fluorouracil. The North Central Cancer Treatment Group and the Mayo Clinic, *Journal of Clinical Oncology 7*, 1447-1456.
[34] Moertel, C. G., Fleming, T. R., Macdonald, J. S., Haller, D. G., Laurie, J. A., Goodman, P. J., Ungerleider, J. S., Emerson, W. A., Tormey, D. C., and Glick, J. H. (1990) Levamisole and fluorouracil for adjuvant therapy of resected colon carcinoma, *New England Journal of Medicine 322*, 352-358.
[35] Moertel, C. G., Fleming, T. R., Macdonald, J. S., Haller, D. G., Laurie, J. A., Tangen, C. M., Ungerleider, J. S., Emerson, W. A., Tormey, D. C., and Glick, J. H. (1995) Fluorouracil plus levamisole as effective adjuvant therapy after resection of stage III colon carcinoma: a final report, *Annals of internal medicine 122*, 321-326.
[36] Ali, S. L., and Florey, K. (1989) Analytical profiles of drug substances, In *Nifedipine*, Academic Press, New York.
[37] Rutman, R. J., Cantarow, A., and Paschkis, K. E. (1954) Studies in 2-Acetylaminofluorene Carcinogenesis, *Cancer Research 14*, 119-123.
[38] Heidelberger, C., Chaudhuri, N., Danneberg, P., Mooren, D., Griesbach, L., DUSCHINSKY, R., Schnitzer, R., Pleven, E., and Scheiner, J. (1957) Fluorinated pyrimidines, a new class of tumour-inhibitory compounds, *Nature 179*, 663-666.
[39] Chabner, B. A., and Longo, D. L. (2011) *Cancer chemotherapy and biotherapy: principles and practice*, Lippincott Williams & Wilkins.
[40] Ma, T., Zhu, Z.-G., Ji, Y.-B., Zhang, Y., Yu, Y.-Y., Liu, B.-Y., Yin, H.-R., and Lin, Y.-Z. (2004) Correlation of thymidylate synthase, thymidine phosphorylase and dihydropyrimidine dehydrogenase with sensitivity of gastrointestinal cancer cells to 5-fluorouracil and 5-fluoro-2'-deoxyuridine, *World journal of gastroenterology 10*, 172-176.
[41] Beumer, J. H., Eiseman, J. L., Parise, R. A., Joseph, E., Holleran, J. L., Covey, J. M., and Egorin, M. J. (2006) Pharmacokinetics, metabolism, and oral bioavailability of the DNA methyltransferase inhibitor 5-fluoro-2′-deoxycytidine in mice, *Clinical cancer research 12*, 7483-7491.
[42] Howell, S. B., Mansfield, S. J., and Taetle, R. (1981) Significance of variation in serum thymidine concentration for the marrow toxicity of methotrexate, *Cancer chemotherapy and pharmacology 5*, 221-226.
[43] Lockhart, P. B., and Sonis, S. T. (1981) Alterations in the Oral Mucosa Caused by Chemotherapeutic Agents, *The Journal of dermatologic surgery and oncology 7*, 1019-1025.

[44] Pico, J.-L., Avila-Garavito, A., and Naccache, P. (1998) Mucositis: its occurrence, consequences, and treatment in the oncology setting, *The Oncologist 3*, 446-451.
[45] Stringer, A. M., Gibson, R. J., Logan, R. M., Bowen, J. M., Yeoh, A. S., Hamilton, J., and Keefe, D. M. (2009) Gastrointestinal microflora and mucins may play a critical role in the development of 5-fluorouracil-induced gastrointestinal mucositis, *Experimental Biology and Medicine 234*, 430-441.
[46] Roco, M. C. (2003) Nanotechnology: convergence with modern biology and medicine, *Current opinion in biotechnology 14*, 337-346.
[47] Niemeyer, C. (1999) Progress in "engineering up" nanotechnology devices utilizing DNA as a construction material, *Applied Physics A: Materials Science & Processing 68*, 119-124.
[48] Schummer, J. (2004) "Societal and ethical implications of nanotechnology": meanings, interest groups, and social dynamics, *Techné: Research in Philosophy and Technology 8*, 56-87.
[49] McDonough, W., and Braungart, M. (1998) The next industrial revolution, *The Atlantic Monthly 282*.
[50] Sobolev, K., and Gutiérrez, M. F. (2005) How nanotechnology can change the concrete world, *American Ceramic Society Bulletin 84*, 14.
[51] Alivisatos, A. P. (1996) Perspectives on the physical chemistry of semiconductor nanocrystals, *The Journal of Physical Chemistry 100*, 13226-13239.
[52] Sutherland, A. J. (2002) Quantum dots as luminescent probes in biological systems, *Current Opinion in Solid State and Materials Science 6*, 365-370.
[53] Nie, S., Xing, Y., Kim, G. J., and Simons, J. W. (2007) Nanotechnology applications in cancer, *Annu. Rev. Biomed. Eng. 9*, 257-288.
[54] West, J. L., and Halas, N. J. (2000) Applications of nanotechnology to biotechnology: Commentary, *Current opinion in Biotechnology 11*, 215-217.
[55] Jain, P. K., Lee, K. S., El-Sayed, I. H., and El-Sayed, M. A. (2006) Calculated absorption and scattering properties of gold nanoparticles of different size, shape, and composition: applications in biological imaging and biomedicine, *J. Phys. Chem. B 110*, 7238-7248.
[56] Niemeyer, C. M. (2001) Semi-synthetic nucleic acid–protein conjugates: applications in life sciences and nanobiotechnology, *Reviews in Molecular Biotechnology 82*, 47-66.
[57] Wang, X., Yang, L., Chen, Z. G., and Shin, D. M. (2008) Application of nanotechnology in cancer therapy and imaging, *CA: a cancer journal for clinicians 58*, 97-110.
[58] Kreuter, J., Ramge, P., Petrov, V., Hamm, S., Gelperina, S. E., Engelhardt, B., Alyautdin, R., Von Briesen, H., and Begley, D. J. (2003) Direct evidence that polysorbate-80-coated poly (butylcyanoacrylate) nanoparticles deliver drugs to the CNS via specific mechanisms requiring prior binding of drug to the nanoparticles, *Pharmaceutical research 20*, 409-416.
[59] Mukherjee, S. (2010) *The emperor of all maladies: a biography of cancer*, Simon and Schuster.
[60] Ferlay, J., Soerjomataram, I., Dikshit, R., Eser, S., Mathers, C., Rebelo, M., Parkin, D. M., Forman, D., and Bray, F. (2015) Cancer incidence and mortality worldwide: sources, methods and major patterns in GLOBOCAN 2012, *International journal of cancer 136*, E359-E386.
[61] Hanahan, D., and Weinberg, R. A. (2011) Hallmarks of cancer: the next generation, *cell 144*, 646-674.
[62] Pai, R., Soreghan, B., Szabo, I. L., Pavelka, M., Baatar, D., and Tarnawski, A. S. (2002) Prostaglandin E2 transactivates EGF receptor: a novel mechanism for promoting colon cancer growth and gastrointestinal hypertrophy, *Nature medicine 8*, 289-293.
[63] Gupta, G. P., and Massagué, J. (2006) Cancer metastasis: building a framework, *Cell 127*, 679-695.
[64] Kannagi, R., Izawa, M., Koike, T., Miyazaki, K., and Kimura, N. (2004) Carbohydrate-mediated cell adhesion in cancer metastasis and angiogenesis, *Cancer science 95*, 377-384.
[65] Fidler, I. J. (2002) Critical determinants of metastasis, In *Seminars in cancer biology*, pp 89-96, Elsevier.
[66] Bissell, M. J., and Hines, W. C. (2011) Why don't we get more cancer? A proposed role of the microenvironment in restraining cancer progression, *Nature medicine 17*, 320-329.
[67] Bae, Y. H., and Park, K. (2011) Targeted drug delivery to tumors: Myths, reality and possibility, *Journal of Controlled Release 153*, 198-205.

[68] Albain, K. S., Swann, R. S., Rusch, V. W., Turrisi, A. T., Shepherd, F. A., Smith, C., Chen, Y., Livingston, R. B., Feins, R. H., and Gandara, D. R. (2009) Radiotherapy plus chemotherapy with or without surgical resection for stage III non-small-cell lung cancer: a phase III randomised controlled trial, *The Lancet 374*, 379-386.
[69] Miller, K. D., Siegel, R. L., Lin, C. C., Mariotto, A. B., Kramer, J. L., Rowland, J. H., Stein, K. D., Alteri, R., and Jemal, A. (2016) Cancer treatment and survivorship statistics, 2016, *CA: a cancer journal for clinicians*.
[70] Groenewald, C., Konstantinidis, L., and Damato, B. (2013) Effects of radiotherapy on uveal melanomas and adjacent tissues, *Eye 27*, 163-171.
[71] Lewitzki, V., Andratschke, N., Kuhnt, T., and Hildebrandt, G. (2015) Radiation myelitis after hypofractionated radiotherapy with concomitant gefitinib, *Radiation Oncology 10*, 29.
[72] Redgrove, H. S. (2014) *Alchemy: ancient and modern*, Lulu. com.
[73] Blum, J. D. (2013) Mesmerized by mercury, *Nature chemistry 5*, 1066-1066.
[74] Yamada, M., Foote, M., and Prow, T. W. (2015) Therapeutic gold, silver, and platinum nanoparticles, *Wiley Interdisciplinary Reviews: Nanomedicine and Nanobiotechnology 7*, 428-445.
[75] HUDSON, D. Proven Benefits of Nano Gold Colloidal.
[76] Khan, A., Rashid, R., Murtaza, G., and Zahra, A. (2014) Gold nanoparticles: synthesis and applications in drug delivery, *Tropical journal of pharmaceutical research 13*, 1169-1177.
[77] Biju, V. (2014) Chemical modifications and bioconjugate reactions of nanomaterials for sensing, imaging, drug delivery and therapy, *Chemical Society Reviews 43*, 744-764.
[78] Bao, G., Mitragotri, S., and Tong, S. (2013) Multifunctional nanoparticles for drug delivery and molecular imaging, *Annual review of biomedical engineering 15*, 253-282.
[79] Sun, T., Zhang, Y. S., Pang, B., Hyun, D. C., Yang, M., and Xia, Y. (2014) Engineered nanoparticles for drug delivery in cancer therapy, *Angewandte Chemie International Edition 53*, 12320-12364.
[80] Almeida, J. P. M., Figueroa, E. R., and Drezek, R. A. (2014) Gold nanoparticle mediated cancer immunotherapy, *Nanomedicine: Nanotechnology, Biology and Medicine 10*, 503-514.
[81] Niikura, K., Matsunaga, T., Suzuki, T., Kobayashi, S., Yamaguchi, H., Orba, Y., Kawaguchi, A., Hasegawa, H., Kajino, K., and Ninomiya, T. (2013) Gold nanoparticles as a vaccine platform: influence of size and shape on immunological responses in vitro and in vivo, *ACS nano 7*, 3926-3938.
[82] Papasani, M. R., Wang, G., and Hill, R. A. (2012) Gold nanoparticles: the importance of physiological principles to devise strategies for targeted drug delivery, *Nanomedicine: Nanotechnology, Biology and Medicine 8*, 804-814.
[83] Connor, E. E., Mwamuka, J., Gole, A., Murphy, C. J., and Wyatt, M. D. (2005) Gold nanoparticles are taken up by human cells but do not cause acute cytotoxicity, *Small 1*, 325-327.
[84] Daniel, M.-C., and Astruc, D. (2004) Gold nanoparticles: assembly, supramolecular chemistry, quantum-size-related properties, and applications toward biology, catalysis, and nanotechnology, *Chemical reviews 104*, 293-346.
[85] Morshed, R. A., Muroski, M. E., Dai, Q., Wegscheid, M. L., Auffinger, B., Yu, D., Han, Y., Zhang, L., Wu, M., and Cheng, Y. (2016) Cell-Penetrating Peptide-Modified Gold Nanoparticles for the Delivery of Doxorubicin to Brain Metastatic Breast Cancer, *Molecular pharmaceutics 13*, 1843-1854.
[86] Ding, X., Liow, C. H., Zhang, M., Huang, R., Li, C., Shen, H., Liu, M., Zou, Y., Gao, N., and Zhang, Z. (2014) Surface plasmon resonance enhanced light absorption and photothermal therapy in the second near-infrared window, *Journal of the American Chemical Society 136*, 15684-15693.
[87] Sershen, S., Westcott, S., Halas, N., and West, J. (2000) Temperature-sensitive polymer–nanoshell composites for photothermally modulated drug delivery, *Journal of biomedical materials research 51*, 293-298.
[88] Zhang, Z., Wang, J., Nie, X., Wen, T., Ji, Y., Wu, X., Zhao, Y., and Chen, C. (2014) Near infrared laser-induced targeted cancer therapy using thermoresponsive polymer encapsulated gold nanorods, *Journal of the American Chemical Society 136*, 7317-7326.

[89] Conde, J., Dias, J. T., Grazú, V., Moros, M., Baptista, P. V., and Jesus, M. (2014) Revisiting 30 years of biofunctionalization and surface chemistry of inorganic nanoparticles for nanomedicine.
[90] Kim, K. Y. (2007) Nanotechnology platforms and physiological challenges for cancer therapeutics, *Nanomedicine: Nanotechnology, Biology and Medicine 3*, 103-110.
[91] Eustis, S., and El-Sayed, M. A. (2006) Why gold nanoparticles are more precious than pretty gold: noble metal surface plasmon resonance and its enhancement of the radiative and nonradiative properties of nanocrystals of different shapes, *Chemical society reviews 35*, 209-217.
[92] Han, G., Ghosh, P., and Rotello, V. M. (2007) Functionalized gold nanoparticles for drug delivery.
[93] Corti, C. W., Holliday, R. J., and Thompson, D. T. (2002) Developing new industrial applications for gold: gold nanotechnology, *Gold Bulletin 35*, 111-117.
[94] Kim, K.-S., Demberelnyamba, D., and Lee, H. (2004) Size-selective synthesis of gold and platinum nanoparticles using novel thiol-functionalized ionic liquids, *Langmuir 20*, 556-560.
[95] Paciotti, G. F., Kingston, D. G., and Tamarkin, L. (2006) Colloidal gold nanoparticles: a novel nanoparticle platform for developing multifunctional tumor-targeted drug delivery vectors, *Drug development research 67*, 47-54.
[96] Zhang, Z., Jia, J., Lai, Y., Ma, Y., Weng, J., and Sun, L. (2010) Conjugating folic acid to gold nanoparticles through glutathione for targeting and detecting cancer cells, *Bioorganic & medicinal chemistry 18*, 5528-5534.
[97] Bergen, J. M., Von Recum, H. A., Goodman, T. T., Massey, A. P., and Pun, S. H. (2006) Gold nanoparticles as a versatile platform for optimizing physicochemical parameters for targeted drug delivery, *Macromolecular bioscience 6*, 506-516.
[98] Orendorff, C. J., Sau, T. K., and Murphy, C. J. (2006) Shape-Dependent Plasmon-Resonant Gold Nanoparticles, *Small 2*, 636-639.
[99] Link, S., and El-Sayed, M. A. (1999) Size and temperature dependence of the plasmon absorption of colloidal gold nanoparticles, *The Journal of Physical Chemistry B 103*, 4212-4217.
[100] Loo, C., Lin, A., Hirsch, L., Lee, M.-H., Barton, J., Halas, N., West, J., and Drezek, R. (2004) Nanoshell-enabled photonics-based imaging and therapy of cancer, *Technology in cancer research & treatment 3*, 33-40.
[101] O'Neal, D. P., Hirsch, L. R., Halas, N. J., Payne, J. D., and West, J. L. (2004) Photo-thermal tumor ablation in mice using near infrared-absorbing nanoparticles, *Cancer letters 209*, 171-176.
[102] Ghosh, S. K., and Pal, T. (2007) Interparticle coupling effect on the surface plasmon resonance of gold nanoparticles: from theory to applications, *Chemical reviews 107*, 4797-4862.
[103] Huang, X., El-Sayed, I. H., Qian, W., and El-Sayed, M. A. (2006) Cancer cell imaging and photothermal therapy in the near-infrared region by using gold nanorods, *Journal of the American Chemical Society 128*, 2115-2120.
[104] Pissuwan, D., Niidome, T., and Cortie, M. B. (2011) The forthcoming applications of gold nanoparticles in drug and gene delivery systems, *Journal of controlled release 149*, 65-71.
[105] Caruso, F. (2006) *Colloids and colloid assemblies: synthesis, modification, organization and utilization of colloid particles*, John Wiley & Sons.
[106] Chorom, M., and Rengasamy, P. (1995) Dispersion and zeta potential of pure clays as related to net particle charge under varying pH, electrolyte concentration and cation type, *European Journal of Soil Science 46*, 657-665.
[107] Ji, X., Song, X., Li, J., Bai, Y., Yang, W., and Peng, X. (2007) Size control of gold nanocrystals in citrate reduction: the third role of citrate, *Journal of the American Chemical Society 129*, 13939-13948.
[108] Frens, G. (1973) Controlled nucleation for the regulation of the particle size in monodisperse gold suspensions, *Nature 241*, 20-22.
[109] Ojea-Jiménez, I., and Puntes, V. (2009) Instability of cationic gold nanoparticle bioconjugates: the role of citrate ions, *Journal of the American Chemical Society 131*, 13320-13327.
[110] Sun, Y., and Xia, Y. (2002) Shape-controlled synthesis of gold and silver nanoparticles, *Science 298*, 2176-2179.

[111] Liao, H., and Hafner, J. H. (2005) Gold nanorod bioconjugates, *Chemistry of Materials 17*, 4636-4641.
[112] Kommareddy, S., and Amiji, M. (2007) Poly (ethylene glycol)–modified thiolated gelatin nanoparticles for glutathione-responsive intracellular DNA delivery, *Nanomedicine: nanotechnology, biology and medicine 3*, 32-42.
[113] Shenoy, D., Fu, W., Li, J., Crasto, C., Jones, G., Dimarzio, C., Sridhar, S., and Amiji, M. (2006) Surface functionalization of gold nanoparticles using hetero-bifunctional poly (ethylene glycol) spacer for intracellular tracking and delivery, *International journal of nanomedicine 1*, 51.
[114] Bhattacharya, R., Patra, C. R., Earl, A., Wang, S., Katarya, A., Lu, L., Kizhakkedathu, J. N., Yaszemski, M. J., Greipp, P. R., and Mukhopadhyay, D. (2007) Attaching folic acid on gold nanoparticles using noncovalent interaction via different polyethylene glycol backbones and targeting of cancer cells, *Nanomedicine: Nanotechnology, Biology and Medicine 3*, 224-238.
[115] Srivastava, S., Verma, A., Frankamp, B. L., and Rotello, V. M. (2005) Controlled assembly of protein–nanoparticle composites through protein surface recognition, *Advanced Materials 17*, 617-621.
[116] Giljohann, D. A., Seferos, D. S., Daniel, W. L., Massich, M. D., Patel, P. C., and Mirkin, C. A. (2010) Gold nanoparticles for biology and medicine, *Angewandte Chemie International Edition 49*, 3280-3294.
[117] Mizrahy, S., and Peer, D. (2012) Polysaccharides as building blocks for nanotherapeutics, *Chemical Society Reviews 41*, 2623-2640.
[118] Gbenebor, O., Adeosun, S., Lawal, G., and Jun, S. (2016) Role of CaCO 3 in the physicochemical properties of crustacean-sourced structural polysaccharides, *Materials Chemistry and Physics 184*, 203-209.
[119] De Carvalho, M., Stamford, T., Pereira, E., Dos Santos, P., and Sampaio, F. (2011) Chitosan as an oral antimicrobial agent, *Formatex 2012*, 13.
[120] Prabaharan, M., and Mano, J. F. (2004) Chitosan-Based Particles as Controlled Drug Delivery Systems, *Drug Delivery 12*, 41-57.
[121] Hamman, J. H. (2010) Chitosan based polyelectrolyte complexes as potential carrier materials in drug delivery systems, *Marine drugs 8*, 1305-1322.
[122] Nicol, S. (1991) Life after death for empty shells, *New Scientist 129*, 46-48.
[123] Berscht, P. C., Nies, B., Liebendörfer, A., and Kreuter, J. (1994) Incorporation of basic fibroblast growth factor into methylpyrrolidinone chitosan fleeces and determination of the in vitro release characteristics, *Biomaterials 15*, 593-600.
[124] SINGH, D. K., and RAY, A. R. (2000) Biomedical applications of chitin, chitosan, and their derivatives, *Journal of Macromolecular Science, Part C: Polymer Reviews 40*, 69-83.
[125] Singla, A., and Chawla, M. (2001) Chitosan: Some pharmaceutical and biological aspects-an update, *Journal of Pharmacy and Pharmacology 53*, 1047-1067.
[126] Agnihotri, S. A., Mallikarjuna, N. N., and Aminabhavi, T. M. (2004) Recent advances on chitosan-based micro- and nanoparticles in drug delivery, *Journal of Controlled Release 100*, 5-28.
[127] Arias, J. L. (2008) Novel strategies to improve the anticancer action of 5-fluorouracil by using drug delivery systems, *Molecules 13*, 2340-2369.
[128] Ilium, L. (1998) Chitosan and its use as a pharmaceutical excipient, *Pharmaceutical research 15*, 1326-1331.
[129] Aider, M. (2010) Chitosan application for active bio-based films production and potential in the food industry: Review, *LWT-Food Science and Technology 43*, 837-842.
[130] Kauss, H., Jeblick, W., and Domard, A. (1989) The degrees of polymerization and N-acetylation of chitosan determine its ability to elicit callose formation in suspension cells and protoplasts of Catharanthus roseus, *Planta*, 385-392.
[131] Wenling, C., Duohui, J., Jiamou, L., Yandao, G., Nanming, Z., and Xiufang, Z. (2005) Effects of the degree of deacetylation on the physicochemical properties and Schwann cell affinity of chitosan films, *Journal of biomaterials applications 20*, 157-177.

[132] Liu, W. G., and De Yao, K. (2002) Chitosan and its derivatives—a promising non-viral vector for gene transfection, *Journal of Controlled Release 83*, 1-11.
[133] Hejazi, R., and Amiji, M. (2003) Chitosan-based gastrointestinal delivery systems, *Journal of controlled release 89*, 151-165.
[134] Zhang, Y., Li, J., Shen, Y., Wang, M., and Li, J. (2004) Poly-L-lysine functionalization of single-walled carbon nanotubes, *The Journal of Physical Chemistry B 108*, 15343-15346.
[135] Dos, A., Schimming, V., Chan-Huot, M., and Limbach, H.-H. (2010) Effects of hydration on the acid–base interactions and secondary structures of poly-l-lysine probed by 15 N and 13 C solid state NMR, *Physical Chemistry Chemical Physics 12*, 10235-10245.
[136] Tomczak, M. M., Glawe, D. D., Drummy, L. F., Lawrence, C. G., Stone, M. O., Perry, C. C., Pochan, D. J., Deming, T. J., and Naik, R. R. (2005) Polypeptide-templated synthesis of hexagonal silica platelets, *Journal of the American Chemical Society 127*, 12577-12582.
[137] Haque, T., Chen, H., Ouyang, W., Martoni, C., Lawuyi, B., Urbanska, A. M., and Prakash, S. (2005) Superior cell delivery features of poly (ethylene glycol) incorporated alginate, chitosan, and poly-L-lysine microcapsules, *Molecular Pharmaceutics 2*, 29-36.
[138] Shukla, R., Bansal, V., Chaudhary, M., Basu, A., Bhonde, R. R., and Sastry, M. (2005) Biocompatibility of gold nanoparticles and their endocytotic fate inside the cellular compartment: a microscopic overview, *Langmuir 21*, 10644-10654.
[139] Koo, A. N., Lee, H. J., Kim, S. E., Chang, J. H., Park, C., Kim, C., Park, J. H., and Lee, S. C. (2008) Disulfide-cross-linked PEG-poly (amino acid) s copolymer micelles for glutathione-mediated intracellular drug delivery, *Chemical Communications*, 6570-6572.
[140] Matsumura, Y., and Maeda, H. (1986) A new concept for macromolecular therapeutics in cancer chemotherapy: mechanism of tumoritropic accumulation of proteins and the antitumor agent smancs, *Cancer research 46*, 6387-6392.
[141] Yuan, F. (1998) Transvascular drug delivery in solid tumors, In *Seminars in radiation oncology*, pp 164-175, Elsevier.
[142] Greish, K. (2010) Enhanced permeability and retention (EPR) effect for anticancer nanomedicine drug targeting, *Cancer Nanotechnology: Methods and Protocols*, 25-37.
[143] Maeda, H., Wu, J., Sawa, T., Matsumura, Y., and Hori, K. (2000) Tumor vascular permeability and the EPR effect in macromolecular therapeutics: a review, *Journal of controlled release 65*, 271-284.
[144] Bamrungsap, S., Zhao, Z., Chen, T., Wang, L., Li, C., Fu, T., and Tan, W. (2012) Nanotechnology in therapeutics: a focus on nanoparticles as a drug delivery system, *Nanomedicine 7*, 1253-1271.
[145] Danhier, F., Feron, O., and Préat, V. (2010) To exploit the tumor microenvironment: Passive and active tumor targeting of nanocarriers for anti-cancer drug delivery, *Journal of Controlled Release 148*, 135-146.
[146] Brigger, I., Dubernet, C., and Couvreur, P. (2002) Nanoparticles in cancer therapy and diagnosis, *Advanced drug delivery reviews 54*, 631-651.
[147] Fenart, L., Casanova, A., Dehouck, B., Duhem, C., Slupek, S., Cecchelli, R., and Betbeder, D. (1999) Evaluation of effect of charge and lipid coating on ability of 60-nm nanoparticles to cross an in vitro model of the blood-brain barrier, *Journal of pharmacology and experimental therapeutics 291*, 1017-1022.
[148] Allen, T. M., and Chonn, A. (1987) Large unilamellar liposomes with low uptake into the reticuloendothelial system, *FEBS Letters 223*, 42-46.
[149] Jones, A., and Harris, A. L. (1997) New developments in angiogenesis: a major mechanism for tumor growth and target for therapy, *The cancer journal from Scientific American 4*, 209-217.
[150] Jang, S. H., Wientjes, M. G., Lu, D., and Au, J. L.-S. (2003) Drug delivery and transport to solid tumors, *Pharmaceutical research 20*, 1337-1350.
[151] Hori, K., Suzuki, M., Tanda, S., and Saito, S. (1991) Characterization of heterogeneous distribution of tumor blood flow in the rat, *Japanese journal of cancer research 82*, 109-117.

[152] Haley, B., and Frenkel, E. (2008) Nanoparticles for drug delivery in cancer treatment, In *Urologic Oncology: Seminars and original investigations*, pp 57-64, Elsevier.
[153] Jain, R. K. (2001) Delivery of molecular and cellular medicine to solid tumors, *Advanced drug delivery reviews 46*, 149-168.
[154] Owens, D. E., and Peppas, N. A. (2006) Opsonization, biodistribution, and pharmacokinetics of polymeric nanoparticles, *International journal of pharmaceutics 307*, 93-102.
[155] Chithrani, B. D., and Chan, W. C. (2007) Elucidating the mechanism of cellular uptake and removal of protein-coated gold nanoparticles of different sizes and shapes, *Nano letters 7*, 1542-1550.
[156] Heuser, J., and Reese, T. (1973) Evidence for recycling of synaptic vesicle membrane during transmitter release at the frog neuromuscular junction, *The Journal of cell biology 57*, 315-344.
[157] Wang, G., Norton, A. S., Pokharel, D., Song, Y., and Hill, R. A. (2013) KDEL peptide gold nanoconstructs: promising nanoplatforms for drug delivery, *Nanomedicine: Nanotechnology, Biology and Medicine 9*, 366-374.

CHAPTER 3

Chitosan functionalized gold nanoparticles in the delivery of the anticancer drug, 5-Fluorouracil, *in vitro*

L.L. David[1] and M. Singh[1*]

[1]Non-Viral Gene Delivery Laboratory, Discipline of Biochemistry, School of Life Sciences, University of KwaZulu-Natal, Private Bag X54001, Durban, South Africa

[*]Corresponding author: Moganavelli Singh, email: singhm1@ukzn.ac.za

Abstract

Gold nanoparticles (AuNPs) have emerged as potential vehicles for drug delivery due to their favorable attributes such as their apparent low toxicity, high surface area, optical properties, biocompatibility, high loading capacity, ease of synthesis and modification. Most anticancer drugs available do provide some benefit but are rapidly metabolized in the body after administration, reducing their effectiveness. In addition, many of them produce unpleasant and severe side effects. Hence, there is a need for a safe and effective drug delivery system that will ensure sustained and controlled drug release to the desired tumor site. In this study, AuNPs were chemically synthesized and functionalized using two different methods, with the cationic polymer chitosan for delivery of the anticancer drug 5-fluorouracil (5-FU). All nanoparticles and their nano-complexes were fully characterized using UV-vis spectroscopy, ICP, FTIR, TEM and Nanoparticle Tracking Analysis (NTA).

The methods of encapsulation and linear binding of the polymer to the AuNPs were investigated and revealed that the encapsulation method had a superior drug binding efficiency compared to the linear method. Drug release studies over a 7-hour period showed that there was a steady and controlled release of the drug. *In vitro* cytotoxicity assays, using the MTT and SRB assays were carried out on three human cancer cell lines, viz. Caco-2 (colon adenocarcinoma), HEPG2 (hepatocellular carcinoma), MCF-7 (breast adenocarcinoma) and a non-cancer cell line, HEK293 (embryonic kidney). This study, displayed a clear specificity of the nanocomplexes towards the cancer cell lines with little or no significant toxicity observed in the non-cancer cell line. This highlights the immense potential of these cationic polymer functionalized AuNPs in providing safe and efficient drug delivery with limited side effects.

Key Words: Drug delivery, 5-fluorouracil, Gold nanoparticles, Chitosan, Encapsulation, Linear binding

3.1 Introduction

Cancer is one of the leading causes of mortality in the Unites States, with more than ten million individuals diagnosed each year. Even developing countries, including South Africa have seen an unprecedented increase in cancer cases and mortality in recent years. The mechanism through which cancer develops is thought to be a complex, multistep process, involving a number of cellular physiological systems and genetic alterations, including cell signaling pathways, replication and apoptosis [1, 2]. This intricacy and heterogeneity encourages the aggressive growth of cancerous cells resulting in significant morbidity and mortality in patients[3, 4]. In the United States, colon cancer represents approximately forty percent of all cases diagnosed annually and is the third leading cause of death in males and the fourth leading cause in females [5-9].

Cancer begins as a growth localized to an organ or tissue in the body, and progresses to form clumps of cells that can detach and migrate to distant organs or tissues via the vascular or lymphatic systems, a process termed metastasis. At this stage the treatment of the disease becomes more complex and poses various additional obstacles[10]. With regard to colon cancer, colonic adenomas undergo conversion to colonic cancer over an extended period time [11]. Initially the mass develops as a soft polypoid tumor, growing in the direction of the lumen of the colon, leading to ulceration and hemorrhage[12]. Current methods of treatment are dependent on the outcomes of clinical and pathological staging, determined through morphologic diagnostic tools, including radiological and histopathological examinations. Common cancer treatment regimens include surgical resection of the tumor followed by either radiation or chemotherapy or a tailored combination of both[10, 13]. Notwithstanding the numerous advances in these conventional methods of treatment, cancer treatment options are not optimal.

Conventional methods of treatment possess their own limitations including nonspecific distribution of anticancer agents, resulting in the destruction of both healthy and cancerous tissue, multiple drug resistance and below optimal concentrations of anticancer complexes at the site of action [3, 14, 15]. In view of the above impediments, the key to successful cancer treatment lies in the delivery of anticancer complexes, at optimum concentrations to the site of tumor formation, thus targeting the activity of the drug towards cancerous tissue and minimizing its effect on normal healthy tissue. Nanotechnology, a multidisciplinary science, is seen as an important technology by scientists to combat the ever increasing problems facing successful cancer treatment [16]. In recent

years, the field of nanotechnology has been progressing rapidly. According to the metric scale, a nanometer is in reference to the size of an object being one billionth of a meter. The term of nanotechnology was first coined by Norio Taniguchi[17] in 1974, and was said to involve the processing, separation, deformation and synthesis of new materials by one atom or molecule[18].

Progress in the field of nanotechnology has resulted in an increase in its applications in medicine and industry. Nanoparticle size is key to understanding the applications it is best suited towards. In the medical field, nanotechnology is applied in the synthesis of vectors and therapeutic diagnostic tools, to enhance imaging, sensing[19], and for targeted drug and gene delivery[20, 21]. Nanotechnology has resulted in an improvement in the sensitivity of established techniques, leading to a lowering of the risks of cytotoxicity towards healthy tissue, commonly associated with conventional radiation and chemotherapy. Nanoparticles themselves are fast becoming powerful tools in the fight against serious conditions such as cancer [22].

When nanotechnology is used in the diagnosis, treatment and control of various conditions, it is termed nanomedicine. Nanomedicine, although a relatively new field, can be dated back decades to the first recorded use in medicine of lipid vesicles (later called liposomes) in 1965 [23], and quantum dot bio conjugates in 1994[24, 25]. Quantum dots fluoresce under exposure to UV light, and when injected can easily enter cancerous tissue, allowing visualization of the tumor during procedures such as magnetic resonance imaging (MRI)[26]. As research in this area advances, it is becoming clear that nanoparticles offer unique properties which include but not limited to, enhanced permeability and greater retention times. Thus, the prevalence of nanotechnology in the medical field is increasing.

The size of nanoparticles ensures that they are more readily taken up by cells when used as nanovectors for gene delivery [27]. Furthermore, nanoparticles possess a functional surface, that allow for the binding and adsorption of a variety of compounds, making them suitable drug delivery vehicles[28-30]. This nanocomplex formation affords protection to the drug from degradation *in vivo*, improves bioavailability and enables the prolonged release of the anticancer agent[31].

Among the various nanoparticles under study today, noble metal nanoparticles show great promise due to their unique optical properties[32], non-toxicity and high levels of biocompatibility[33], and in the case of the gold nanoparticles (AuNP's) the relatively inert core[34]. In addition, AuNP's with core sizes ranging from 1-150 nm have been easily synthesized with controlled dispersity [35], giving

the advantage of cheap and ease of synthesis. The ability of AuNP's to successfully convert light or radio frequency into heat[36], has been exploited for the thermal destruction of targeted cancer cells. These properties allow for tailored treatment options in cancer therapy, such as treatment of cancerous cells using drugs such as 5-Fluorouracil, together with photothermal therapy. Such applications could improve the recovery rates in colorectal and associated cancers.

Nanoparticles boast a high surface to volume ratio, allowing for increased loading of targeting and therapeutic materials[37]. However, one of the major obstacles faced by researchers, is the tendency of gold nanoparticles to agglomerate during reduction from its metal salts. It is important to control the size of AuNPs, since an increase in size of nanoparticles have shown limitations in their use as drug delivery vectors [38], where particles with sizes ranging from 10 to 100 nm were most effective in the treatment of cancer and related diseases. Nanoparticles within this size range are readily taken up by cells. Hence, there is a need to prevent the agglomeration of gold nanoparticles, possibly by the use of a stabilizing agent [39-41].

Cationic polymers such as chitosan are popular, and have been used as stabilizing agents, mainly due to their high biocompatibility, biodegradability, non-toxicity, and the added advantage of containing NH_2 and OH groups which allow for the binding of drugs and other molecules [42-45]. The combination of chitosan and nanoparticles in the form of nanocomplex matrices provide a larger surface area, allowing higher concentrations of drugs to be loaded onto the nanocomposite. These matrices also generate an environment which is conducive to long term stability for use as a drug delivery vector [46].

Of the various anticancer agents available presently, 5-Fluorouracil (5-FU) was selected. It is a broad spectrum anticancer agent, which can be used alone or in combination with other drugs in chemotherapy. Whilst this drug has shown to be very effective in eliminating cancerous tissue, it shows no specificity. It exhibits high levels of cytotoxicity, therefore destroying healthy tissue in the process, limiting its use in the treatment of cancer[47]. The aim of introducing gold nanoparticles is to bring about a reduction in the cytotoxic effects towards non-cancerous tissue and an overall increase in anticancer activity in cancerous tissue.

To the best of our knowledge, there is very limited research which has been published on the cytotoxic effects of 5-FU loaded chitosan conjugated gold nanoparticle (CS-AuNP) nanocomposites and their cytotoxic effects towards HepG2, HEK293, MCF-7 and Caco-2 cell

lines. This study involves investigation of the encapsulation and linear binding methods of 5-FU onto CS-AuNP nanocomposites, to determine, which method offers greater biocompatibility, and efficiency in delivery of the drug *in vitro.* Furthermore, their respective drug release profiles and anticancer activities were examined, noting dose dependency and cell specificity.

3.2 Materials

Gold (III) chloride trihydrate (M_w: 393.83 g mol^{-1}, HAuCl4.3H2O), chitosan ≥ 75% deacetylated (M_w: 1000-5000), Polysorbate 80 (Tween 80, Mw: 1,310 g mol^{-1}, $C_{64}H_{124}O_{26}$), Sodium triphosphate (Mw: 367.86 g mol^{-1}, $Na_5P_3O_{10}$) 5-Fluorouracil (M_w: 130.1 g mol^{-1}, $C_4H_3FN_2O_2$), Sulforodhamine B (SRB Dye, Mw: 558.67 g mol^{-1}, $C_{27}H_{30}N_2O_7S_2$), Acridine Orange hemi (zinc chloride) salt [3,6-Bis(dimethylamino) acridine hydrochloride zinc chloride double salt] (Mw: 265.36, g $mol^{-1,}$ $C_{17}H_{19}N_3$), and dialysis Tubing (MWCO= 1000 Daltons) were supplied by Sigma-Aldrich Chemical Co., (St. Louis, USA). Sodium citrate tribasic dehydrate, phosphate-buffered saline tablets [PBS, (140mM NaCl, 10mM phosphate buffer, 3mM KCl)], 3-[(4,5-dimethylthiazol-2-yl)-2,5-diphenyl tetrazolium bromide] (MTT), ethidium bromide, glacial acetic acid, and dimethyl sulfoxide [DMSO], were supplied by Merck (Darmstadt, Germany). The human cells, embryonic kidney (HEK293), colorectal adenocarcinoma (Caco-2), hepatocellular carcinoma (HepG2) and breast adenocarcinoma (MCF-7) were obtained from the American type culture collection (Pty) Ltd, Manassas, Virginia, USA. Sterile Fetal Bovine Serum (FBS) was supplied by Hyclone GE Healthcare (Utah, USA). Eagle's Minimum Essential Medium (EMEM) with L-glutamine (4.5 g ml^{-1}), Penicillin/ Streptomycin/ Amphotericin B (100x) antibiotic mixture [Amphotericin B (25 mcg ml^{-1}), NaCl (8.5 mg L^{-1}) Potassium penicillin (10 000 Units mL^{-1}), Streptomycin sulphate (10 000 mcg ml^{-1})] and trypsin-versene-EDTA mixture [versene-EDTA (200 mg L^{-1}), Trypsin (170 000 U L^{-1})] were supplied by Lonza Bio Whittaker (Verviers, Belgium). All sterile tissue culture plasticware were obtained from Corning Inc., (New York, USA). All other reagents were of analytical grade and ultrapure (18 MOhm) water (Milli-Q Academic, Millipore, France) was used throughout.

3.3 Methods

3.3.1 Preparation of colloidal gold nanoparticles (AuNPs)

AuNPs were chemically synthesized using an adaptation of the Turkevich method, involving the chemical reduction of Gold (III) chloride trihydrate ($H[AuCl_4]$) with sodium citrate ($NaC_6H_5O_7$). Briefly, 25 ml of 18 MOhm water in a round bottom flask was heated under constant stirring to a temperature of 85-95 ˚C. To this was added 375 µl of a 3 x 10^{-2} M of H(AuCl4) solution, followed by the addition of 1 ml of 1% sodium citrate, directly into the vortex of the solution. An immediate a color change from a pale yellow to dark blue after 5 minutes and finally to a deep wine red after 15 minutes of constant heating and stirring was observed. Solution was stirred for a further 5 minutes, thereafter cooled to room temperature and stored in a dark bottle at room temperature. The final concentration of the aqueous colloidal AuNPs was 0.45 x 10^{-3} M. The conjugation of chitosan and 5-FU was achieved using two different methods as outlined in 3.3.2 and 3.3.3.

3.3.2 Synthesis of 5-FU encapsulated CS-AuNP nanocomplex

Approximately, 2.5 ml of 5-FU solution (3.8 mM in 18 MOhm water) was added to 2.5 ml of chitosan solution (0.75 mg ml^{-1} in 2% acetic acid) with constant mixing. Thereafter, Tween 80 (0.5% $^{v}/_{v}$) was added, and pH maintained between 4.6-4.8. Sodium tripolyphosphate (TPP) (1.25 ml) was then added to obtain a Chitosan: TPP ratio of (2:1 $^{v}/_{v}$). After gentle stirring for 180 minutes, to ensure adequate adsorption of 5-FU onto the nanoparticles, 2 ml of colloidal AuNP solution (0.45 x 10^{-3} M), was added dropwise to 2 ml of 5-FU/Chitosan nanoparticles under gentle constant stirring.

3.3.3 Linear Synthesis of 5-FU:CS-AuNP nanocomplex

Approximately, 2.5 ml of 5-FU solution (3.8 mM) was added to 2.5 ml of chitosan (0.75 mg ml^{-1} in 2% acetic acid). After gently stirring for 180 minutes, 2 ml of colloidal AuNP solution (0.45 x 10^{-3} M) was added dropwise to 2 ml of the 5-FU/ CS solution under gentle constant stirring for a further 120 minutes.

3.3.4 UV-vis spectrophotometry analysis

UV-vis spectrophotometric analysis was conducted on colloidal solutions of all synthesized nanoparticles and noncomplexes to determine their absorption spectra, allowing for the correlation of the data with that of literature, thereby confirming their successful synthesis. The expected surface plasmon resonance (SPR) absorption of the gold nanoparticles is at 520 nm, with any shift in the absorption spectra indicating successful conjugation of the polymer and/or drug. Solutions were measured using a Biomate 3 spectrophotometer (Thermo Fischer Scientific Inc., Waltham, Massachusetts, USA). All samples were sonicated and vortexed prior to analysis to ensure uniformity of the solution.

3.3.5 Transmission Electron Microscopy (TEM)

To determine the size and ultrastructural morphology of all nanoparticles, TEM studies were conducted. Approximately, 10 µl of the respective nanoparticle/ nanocomplex samples was placed onto a 400-mesh carbon coated copper grid (Ted Pella Inc. Redding, USA), and allowed to air dry at room temperature for 1 hour. Thereafter, samples were viewed at 60 000x magnification using a JEOL-JEM T1010 (Jeol, Tokyo, Japan) electron microscope without warming above -150°C, at an acceleration voltage of 100 kV. Images were captured using the iTEM Soft Imaging Systems (SIS) Megaview III fitted with a side-mounted 3-megapixel digital camera.

3.3.6 Nanoparticle Tracking Analysis (NTA)

For accurate representation of size distribution and zeta potential of all nanoparticles and nanocomplexes, analysis was performed using NTA (Nanosight NS-500, Malvern Instruments, UK) at 25°C. Approximately, 1 ml of a 1:500 dilutions (in 18 MOhm water) of each sample was evaluated. The instrument was first primed and flushed, and the zero position on the camera set. All samples were run in triplicate.

3.3.7 Inductively coupled plasma-optical emission spectroscopy analysis (ICP)

Quantification and elemental detection of the Au concentration present in the colloidal AuNP solution was determined through inductively coupled plasma-optical emission spectroscopy (ICP-

OES). This was performed on a Perkin Elmer optima 5300 DV optical emission spectrometer. A standard curve between 1 – 20 ppm, was set up from an Au standard stock solution of 100 ppm.

3.3.8 Fourier transform infra-red analysis (FTIR)

FTIR was employed to confirm the presence of essential groups and bonds in the nanoparticles, through visualization of the presence of specific peaks. The spectrum was run using 200 µl of the respective sample in a Spectrum Perkin Elmer spectrophotometer, and the respective IR spectra were obtained using Spectrum Analysis Software.

3.3.9 Encapsulation efficiency

Approximately, 2 ml of each nanocomplex (encapsulated and linear) were dialyzed (MWCO=1000 Da), against 15 ml PBS for 12 hours at 37˚ C. Initial absorbance readings pre-dialysis, for each nanocomplex (1 ml) were obtained at 266 nm. Following the 12-hour incubation, 1 mL of each dialyzed sample was analyzed, and reading taken as the total bound 5-FU. The following equation was used to determine the encapsulation efficiency of 5-FU:

Encapsulation efficiency (%) = (Total 5-FU)- (Bound 5-FU)/ (Total 5-FU) x 100

3.3.10 Drug release studies

To determine the controlled ability of the nanocomplexes to release 5-FU over a period of time, and at pH 4 and pH 7, drug release studies were performed. Approximately, 2 mL of each nanocomplex (encapsulated and linear) were dialyzed (MWCO= 1000 Da) against PBS (5 ml) for 12 hours at 37˚C. At hourly intervals, a 2 µl sample was removed and analyzed on a Nanodrop oneC, UV-vis spectrophotometer (Thermo-Fischer Scientific Inc., Waltham, Massachusetts, USA) at 266 nm. These readings were used to generate a drug release profile for the respective nanocomplexes under the different pH conditions.

3.3.11 Reconstitution, propagation and maintenance of cell lines *in vitro*

All tissue culture related studies were conducted under sterile conditions in an Airvolution Class II biosafety laminar flow hood. Cryopreserved cells were thawed in a 37˚C water bath and then

centrifuged at 3000 rpm for 60 seconds. The cell pellet was re-suspended in 1 ml of complete medium (EMEM containing 10% ($^{v}/_{v}$) FBS and antibiotics (100 U ml^{-1} penicillin, 100 µg ml^{-1} streptomycin), warmed to 37˚C. Cells were then propagated and maintained in 25 cm^2 tissue culture flasks containing 5 ml of medium, at 37˚C in a HEPA class 100 Steri-Cult CO_2 incubator (Thermo-Fisher Corporation, Waltham, Massachusetts, USA). The medium of reconstituted cells was changed after 24 hours to remove any traces of the cryopreservatant. The growth of cells was monitored daily under a Nikon TMS inverted microscope (Nikon Corp, Tokyo, Japan). Depending on the growth of cells, spent medium was replenished, cells subcultured for propagation or cell culture assays or cells were cryopreserved.

3.3.12 Trypsinization

Medium and cell culture reagents were first warmed to 37˚C in a water bath. Cells were washed with 5 ml of PBS (pH of 7.5), and 1 ml of trypsin-versene was added to cells. Trypsinization was carried out at 37˚C, with constant monitoring under an inverted microscope. Trypsinization involves the action of the proteolytic enzyme trypsin, which catalyzes the degradation of cellular proteins which allow the cells to attach to culture flasks. Once cells were seen to be "rounding off", trypsinization was stopped by the addition of 1 ml of complete medium containing serum that inhibits the action of the enzyme. The flask was then gently tapped against the palm of the hand to dislodge all the cells. Cells were then split into separate culture flasks, multiwell plates or alternatively cryopreserved.

3.3.13 Cryopreservation

Following trypsinization cells were centrifuged at 3000 rpm for 1 minute. Pelleted cells were then re-suspended in a solution containing 0.9 ml of complete medium and 0.1 ml of DMSO cryopreservation medium), mixed by vortexing and dispensed into sterile 2 ml cryogenic vials. The vials were placed into a Nalgene™ "Mr Frosty" Cryo 1˚C freezing container, containing isopropanol. Cells were frozen at a rate of -1 ˚C per minute to a final temperature of -70 ˚C, and then stored in a -80 ˚C biofreezer (Nuaire, Lasec Laboratory and Scientific equipment), for short term storage or in liquid N_2 for long term storage.

3.3.14 MTT cytotoxicity assay

Confluent cells were trypsinized and seeded into clear 96- well plates at seeding densities between 2.4 x 10^4 - 2.9 x 10^4 cells per well, and incubated at 37˚C for 24 hours to allow for attachment of cells. Thereafter, spent medium was replaced with 200 µl of fresh medium, followed by addition of the respective nanoparticles (AuNP's, Au-CS, Au-CS:5-FU Encapsulated, Au-CS:5-FU Linear and CS:5-FU) at different concentrations as set out in Table 3.1. Positive controls containing cells only, were included and recorded as 100 % survival. Assays were conducted in triplicate. Cells were incubated for 48 hours at 37˚C in 5% CO_2. Thereafter, the medium was removed and replaced with 100 µl fresh medium and 100 µl of MTT reagent (5 mg/ml in PBS), and cells incubated for 4 hours at 37 ˚C. The medium containing MTT was then removed, and 200 µl of DMSO was added to each well, to solubilize the insoluble formazan crystals. The absorbance was then read on a Mindray MR-96A microplate reader (Vacutec, Hamburg, Germany) at 570 nm, using DMSO as a blank. The cell viability (%) was calculated using the following equation:
(Abs of treated – Abs of control/ Abs of control) x 100%.

Table 3.1. Ratios of respective nanoparticles and nanocomposites used in cytotoxicity assays

Ratio	AuNP's	Au-CS (1:1)	Au-CS-5FU Encapsulated	Au-CS-5FU Linear	CS Encapsulated 5-FU control	CS Linear 5-FU control
	1:0	1:1	2:1:1	2:1:1	1:1	1:1
1	0.134 µg	3.88 µg	0.275 µg	0.275 µg	1.866 µg	1.555 µg
2	0.268 µg	7.77 µg	0.549 µg	0.549 µg	3.732 µg	3.110 µg
3	0.402 µg	11.7 µg	0.884 µg	0.884 µg	5.598 µg	4.665 µg
4	0.536 µg	15.5 µg	1.090 µg	1.090 µg	7.464 µg	6.221 µg

3.3.15 SRB cytotoxicity assay

This assay was set up as for the MTT assay (3.3.14, Table 3.1). After the 48-hour incubation, 50 µl of TCA (50%) was gently layered onto the cells, taking care not to dislodge cells. The plates were then incubated for 1 hour at 4˚C, followed by washing (3x) with 18 MOhm water, to remove excess serum and fixative agent. Plates were then dried at 40˚C for 1 hour, followed by the addition of 100 µl of SRB dye (0.4% $^{w}/_{v}$ in 1% acetic acid) to each well, and incubation for 30 minutes in

the dark at room temperature. Excess dye was removed by washing (3x) with 1% acetic acid. The protein bound dye was solubilized with 200 µl of 10 mM Tris base, and plates read on a Mindray MR-96A microplate reader at 565 nm using Tris base as the blank. Cell viability was calculated is in 3.3.14.

3.3.16 Mechanism of cell death - Apoptosis Assay

This assay is a rapid fluorescent technique for the detection of cell apoptosis *in vitro*, and uses the dual dye system of acridine orange and ethidium bromide. The dyes were each prepared to a concentration of 100 $mg.ml^{-1}$ in PBS and mixed at a ratio of 1:1, prior to the start of the assay. Cells were seeded into clear 24-well plates at a density of 1.2 x 10^5 cells per well, and incubated at 37˚C for 24 hours. Spent medium was then replenished with 400 µl of fresh medium and respective nanoparticles (Au-CS:5-FU encapsulated and Au-CS:5-FU linear) were added at a mass of 0.917 µg and 0.983 µg. Positive controls containing untreated cells were used. Assay was done in triplicate. Cells were incubated for 48 hours at 37˚C in 5% CO_2, thereafter washed with 100 µl of cold PBS, followed by the addition of 15 µl of the dye solution to each well. Cells were viewed under an Olympus fluorescent microscope (200x magnification), fitted with a CC12 fluorescent camera (Olympus Co., Tokyo, Japan). The apoptotic indices were calculated according to the following equation:

Apoptotic Index = Number of Apoptotic cells/ total number of cells counted.

3.3.17 Statistical analysis

All data has been presented as mean ± standard deviation (± SD n=3). The Dunnetts post hoc test was used for the MTT and SRB assay. Statistical significance of the tests was set at **$p<0.01$ and *<0.05. Each of the experimental values were compared to their corresponding control. The software used for statistical analysis was GraphPad Instat 3.

3.4 Results and discussion

3.4.1 UV-vis studies

The UV-vis spectra obtained for the AuNP's, Au-CS, Au-CS:5-FU encapsulated and Au-CS:5-FU linear bound nanocomplexes are shown in Figure 3.1. The AuNP's exhibited a single narrow peak absorbance band at 522 nm, which corresponded to the surface plasmon excitation of small spherical monodispersed and well-separated AuNPs, that peak in the 522-525 nm range[48]. The presence of a single visible peak, indicates that there were very low levels of by-product present from the sodium citrate reduction reaction, as excess citrate and its oxidation products would appear as a separate peak if they were present in large volumes. For Au-CS a single peak at 524 nm was observed, indicating a shift in SPR due to the polymer conjugation. For Au-CS:5-FU encapsulated and Au-CS:5-FU linear, there were single peaks visible at 528 nm and 530 nm respectively, due to successful conjugation of Au-CS to 5-FU. There was a decrease in the overall absorbance of the nanocomplexes when compared to the colloidal gold nanoparticles, indicating that the nanoparticles are small in size, since smaller nanoparticles possess a reduced mean free path for the electrons, leading to a less pronounced peak. It also suggests that there was a lower concentration gold nanoparticles present in the conjugated samples, as expected.

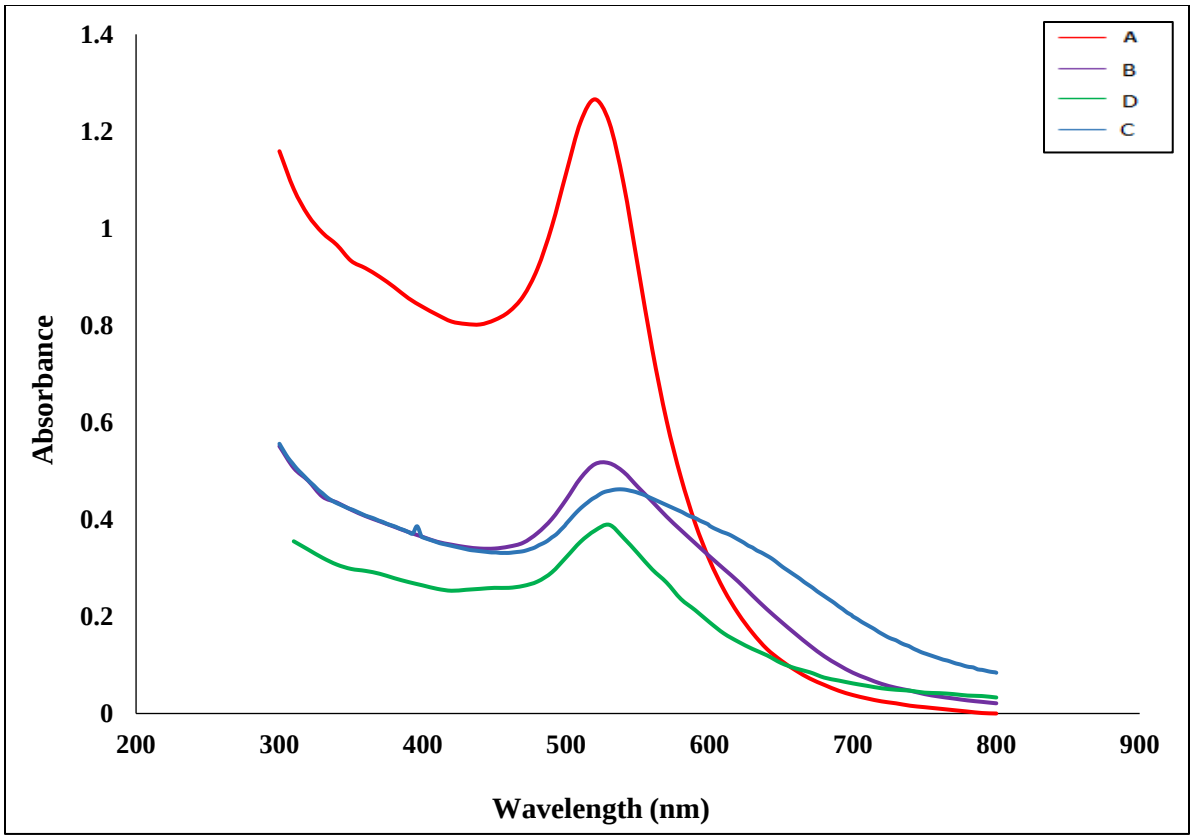

Figure. 3.1 UV-vis Spectra of (A) AuNP, (B) Au-CS, (C) Au-CS:5-FU Encapsulated, (D) Au-CS:5-FU Linear.

3.4.2 ICP-OES and FTIR analysis

The ICP analysis performed was able to confirm the concentration of the synthesized AuNP. Characterization using FTIR, further confirmed that successful conjugation of the polymers to the AuNPs. The FTIR spectrum of Au-CS are shown in Appendix A. The FTIR spectrum of nanocomposites containing chitosan presented with a peak due to N-H, O-H stretching at ~ 3254 cm^{-1}, a peak due to NH_3^+ ~ 1508 cm^{-1} and C-O stretching at ~ 1028. These peaks correspond well to that of pure chitosan as seen in literature.

3.4.3 TEM

The TEM images of the nanoparticles and nanocomplexes are shown in Figure 3.2 (A-D). The AuNP's (Figure 3.2A) appeared uniform in shape and size. They appear as dark spots on a

light background, which is due to the noble metal which has a dense core and therefore reflects the beam of electrons from the TEM. Furthermore, the particles were polydispersed, with very little large scale agglomeration. These results were further supported by the UV-vis studies, which indicated that the colloidal solution consisted of nanoparticles which were small in size, less than 100 nm in diameter. For Au-CS (Figure 3.2 B), a layer of chitosan can be vaguely seen in the background surrounding each AuNP. This supports the UV studies, that the binding of chitosan to AuNP was successful. The molecules show a small level of aggregation; which is to be expected. The Au-CS:5-FU encapsulated nanocomplexes (Figure 3.2C) appear to be slightly smaller in size than the Au-CS:5-FU linear nanocomplexes (Figure 3.2D). This was confirmed from the NTA analysis (3.4.4.). The nanocomplexes however show a greater level of dispersion, indicating colloidal stability and the potential to function better in the delivery of the drug to cancer cells due to lower levels of aggregation.

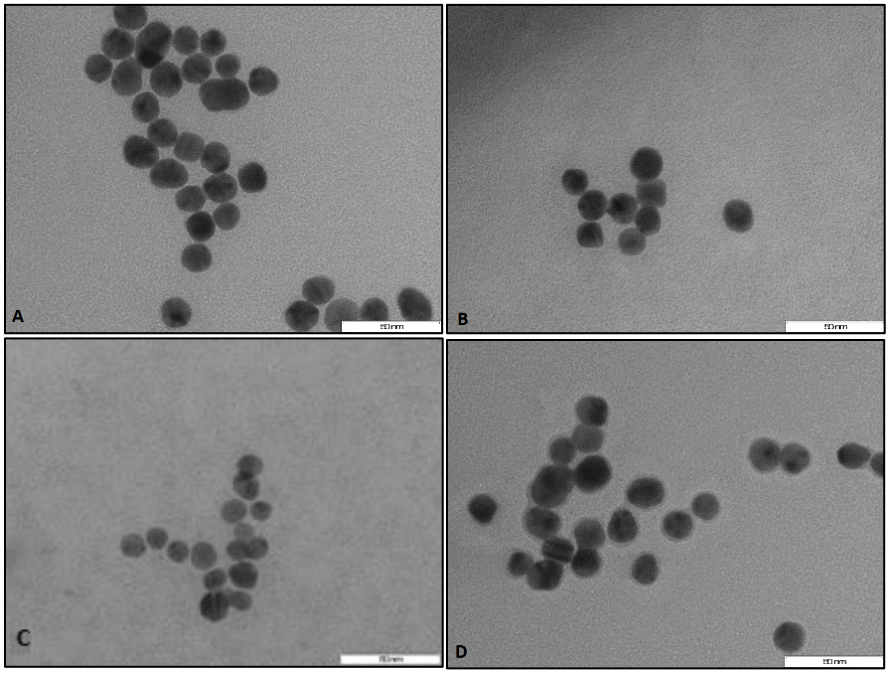

Figure 3.2 TEM imaging of (A) Au nanoparticles, (B) Au-Chitosan, (C) encapsulated Au-Chitosan:5FU (D) linear Au-Chitosan:5-FU. Bar = 50 nm.

3.4.4 Nanoparticle Tracking Analysis (NTA)

NTA was used to accurately determine nanoparticle and nanocomplex size distribution, colloidal stability and zeta potential, as shown in Table 3.2. The results indicate that the AuNP's had a mean diameter of 65.9 nm ± 9.8, indicating that the method employed could successfully synthesize

nanoparticles under 100 nm. Zeta potential is the surface charge in a particular solvent with a specific ionic strength, and is a measure of the repulsive forces which are present. A large zeta potential value either positive or negative is a good indicator of long term colloidal stability. The AuNP's had a low zeta potential value of -7.3 mV, which increased to +55 for CS-Au, which suggests that these nanoparticles had good colloidal stability. Furthermore, it is an indication of the strength of the bond between chitosan and AuNP. A shift from an overall negative charge for the AuNPs to large positive zeta potential values in the case of the nanocomplexes is an indication of the successful and strong association between the respective polymers and the surface of the gold nanoparticle. This correlates with the results obtained from the UV-vis and TEM studies. Furthermore, the increase in sizes seen in CS nanocomplexes can be attributed to the binding of chitosan, which interacts efficiently with the gold surface. Upon addition of the anionic drug, 5-FU to the CS-AuNP, there was an increase in the size of each nanocomplex, encapsulated and linear, from 69.6 nm to 90.4 nm and 95.3 nm, respectively. This also confirms that the higher positive zeta potential value of CS-AuNP:5-FU linear allowed for a stronger, more stable interaction between chitosan and the drug. Furthermore, as evidenced from EM studies the linear method produced slightly larger nanocomplexes than with the encapsulation method (95.3 nm vs 90.4 nm).

Table 3.2. Size distribution and Zeta potential analysis of AuNP and its nanocomplexes.

Sample	Nanoparticle size (nm)	Zeta potential (mV)
AuNP	65.9 ± 9.8	-7.3 ± 1.6
AuNP-CS	69.6 ± 15.2	+55 ± 1.2
AuNP-CS:5-FU Encap	90.4 ± 1.5	+8.3 ± 1.3
AuNP-CS:5-FU Linear	95.3 ± 12.2	+27.2 ± 1.5

3.4.5 Encapsulation efficiency

The encapsulation efficiency was determined through UV-vis spectrometry, from the absorption spectra of nanocomplexes containing 5-FU before and after dialysis. The amount of free drug was calculated from the absorption measurements, which was in turn used to calculate the amount of drug bound to nanoparticles. The encapsulation efficiency of 5-FU into the Au-CS nanocomplex

was calculated to be 89.95%, whilst the binding efficiency of Au-CS:5-FU using the linear method was found to be 72.45 %. This confirms that the encapsulation method was superior to the linear method in the binding of 5-FU. Nevertheless, a binding efficiency of 72.45 % achieved using the linear method still provided a relatively high level of entrapment of 5-FU into the nanocomplex.

3.4.6 Drug release studies

Cancerous cells have a lower pH value, compared to normal tissue[49]. It has been reported [50] that 5-FU is released quickly and continuously at a pH value around 5, due to the gel-sol transition that takes place, releasing 5-FU. A drug release analysis was done spectrophotometrically at pH 7 and 4, and measured at 266 nm since 5-FU peaks between 266 - 271 nm. The results (Figure 3.3) show that at pH 7.0, the linear bound nanocomposite, released the drug at a quicker rate and in higher volumes compared to the encapsulated nanocomposite. Release of the drug in high volumes under neutral pH, may result in non-specific cytotoxic effects towards healthy tissue or the expelling of the drug from the body before any therapeutic effect may occur, which can be avoided by the encapsulation method. At pH 4.0, both nanocomposites released the drug, however a more controlled release was seen for the encapsulated nanocomposite, compared to the linear bound nanocomposite, indicating the effective release of the drug under acidic conditions, which is highly favourable due to biology of cancerous cells. The encapsulated nanocomposite was shown to be more effective at binding the drug in higher volumes and releasing the drug in a controlled manner under appropriate conditions. Approximately, 30% and 41% of the drug was released from encapsulated and linear bound nanocomplexes respectively at a pH of 4.0. Hence, whilst both nanocomposites are capable of sustained release of the drug over a period of time, the encapsulated nanocomplex was shown to possess a more favorable release profile.

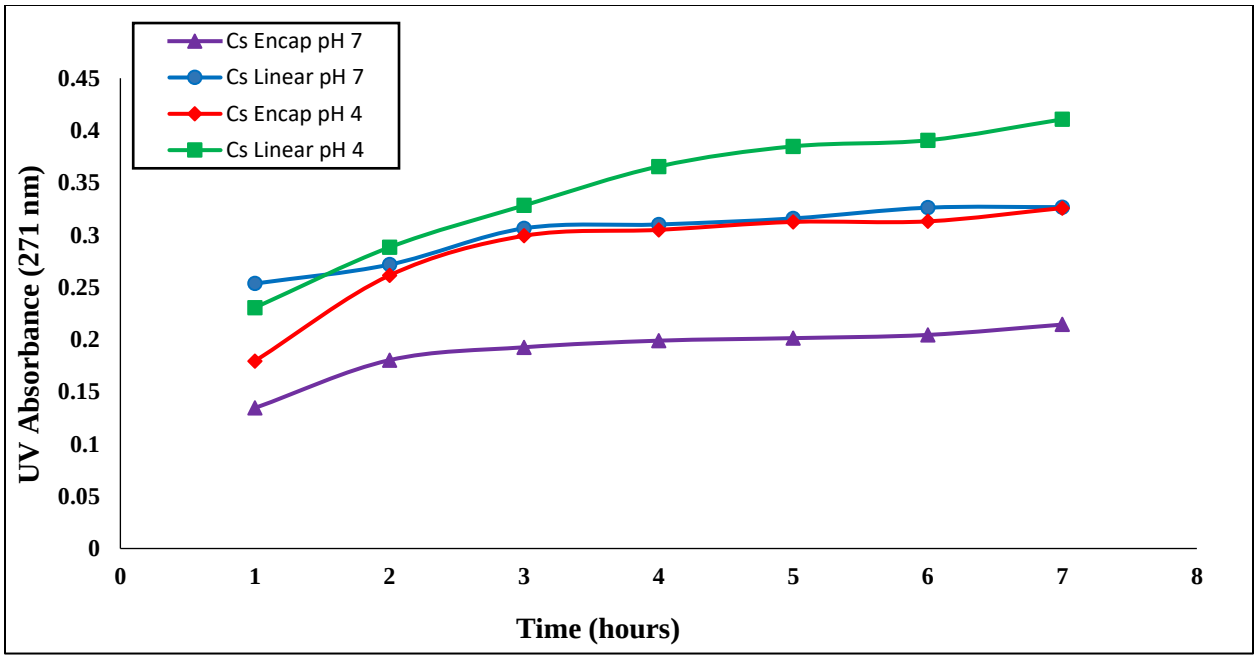

Figure 3.3 Drug release profile of 5-FU from nanocomplexes in the encapsulated and linear method at pH 4.0 and 7.0

3.4.7 *In vitro* Cytotoxicity analysis

3.4.7.1 MTT Assay

The cytotoxicity of the respective nanocomplexes was investigated using the MTT assay, a quantitative colorimetric assay, relying on the premise that viable cells retain their mitochondrial enzyme activity and reduce the tetrazolium salt into intensely colored insoluble formazan products. One of the attractive features of using gold as a delivery vehicle is that due to its chemically inert core, it is essentially non-toxic to cells[51]. The toxicity profile of AuNP and its nanocomplexes at selected ratios (Table 3.1) were evaluated in the four human cell lines viz. HepG2, HEK293, Caco-2 and MCF-7. The amount of 5-FU used as controls were determined from the concentration of 5-FU present in the encapsulated and linear bound nanocomplexes (1.52 mM), together with the calculated percentage binding efficiency. Figures 3.4-3.7 depict the cytotoxicity profiles of these nanoparticles and nanocomplexes in the four cell lines. A similar trend of little or no cytotoxicity was observed for the AuNP and Au-CS with the AuNPs showing increased cell viability with increased concentration of the nanoparticle. Polymer complexes conjugated to 5-FU, however all

showed a greater cytotoxic effect and a dose dependent profile, with encapsulated nanocomposites inducing greater cell death (>70% in all cell lines), compared to linear bound nanocomposite. The drug controls showed limited cytotoxicity towards the cancerous cell lines, when compared to the nanocomposites of Au-CS:5-FU both encapsulated and linear. This data combined illustrates that whilst the nanoparticles and nanocomplexes were not cytotoxic to cells, upon the addition of 5-FU they become much more efficient drug delivery vectors. The HEK293 cell line was used as a control cell line, to test the cytotoxicity of the nanocomposites towards a non-cancerous cell line. It was further anticipated that the use of AuNP would reduce the cytotoxic effects in this cell line, whilst increasing the overall anticancer activity of the drug towards the non-cancerous cell line. AuNP's did not have any significant cytotoxic action on the HEK293 cell line, the same was true for the Au-Cs nanocomplexes. Overall there was in increase in the percentage cell viability from ratio 1 to 4 for these complexes. Drug containing nanocomposites, show a decrease in cell viability from ratio 1 to 4, indicating a dose dependent profile in the HEK293 cells. This trend is also seen in the other three cell lines, with different degrees of cytotoxicity achieved. The encapsulated AuNP-CS:5-FU complexes showed the greatest anticancer activity across all four cell lines cell lines with close to 70% cell death occurring mostly at the highest concentration. The linear bound AuNP-CS:5-FU complexes however displayed the best balance of anticancer activity towards the cancerous cell lines and reduced cytotoxic effects in the HEK293 cell line resulting in approximately 65% cell death at the highest ratio for the cancerous cell lines and 60 % cell death for the HEK293 cell lines compared to the approximately 80% cell death exhibited by the encapsulated nanocomplex. However, the nanocomposites consisting of CS:5-FU via encapsulation and linear binding methods revealed a lower anticancer activity in all cell lines compared to their respective polymer-AuNP:5FU complexes. This clearly indicates that the presence of the AuNP in the complex, significantly increased the activity of the anticancer drug. This could be due to efficient cellular uptake due to the small size and positive surface charge of the nanoparticles, in addition to the slow controlled release of the drug over a period of time, allowing for a more pronounced effect on the cells.

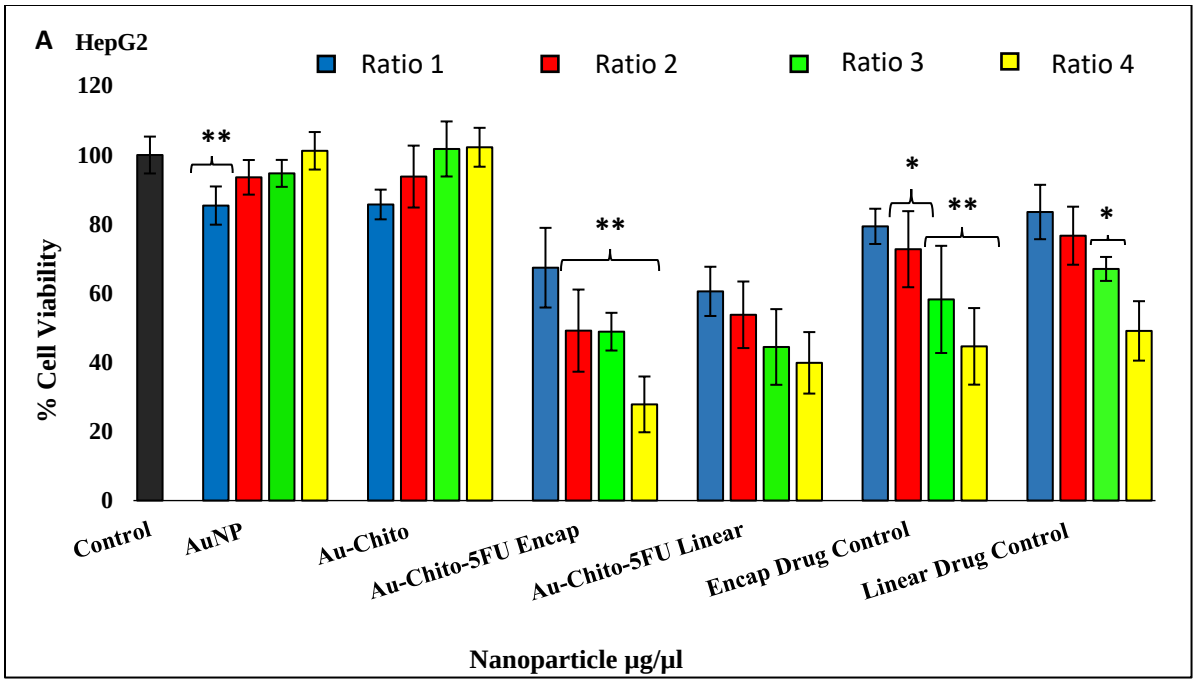

Figure 3.4 MTT cytotoxicity assay of nanoparticles and nanocomplexes in the HepG2 cell line. Data represented as means ± SD (n=3), * p<0.05, **p<0.01 were considered statistically significant, Ratios as laid out in Table 3.1.

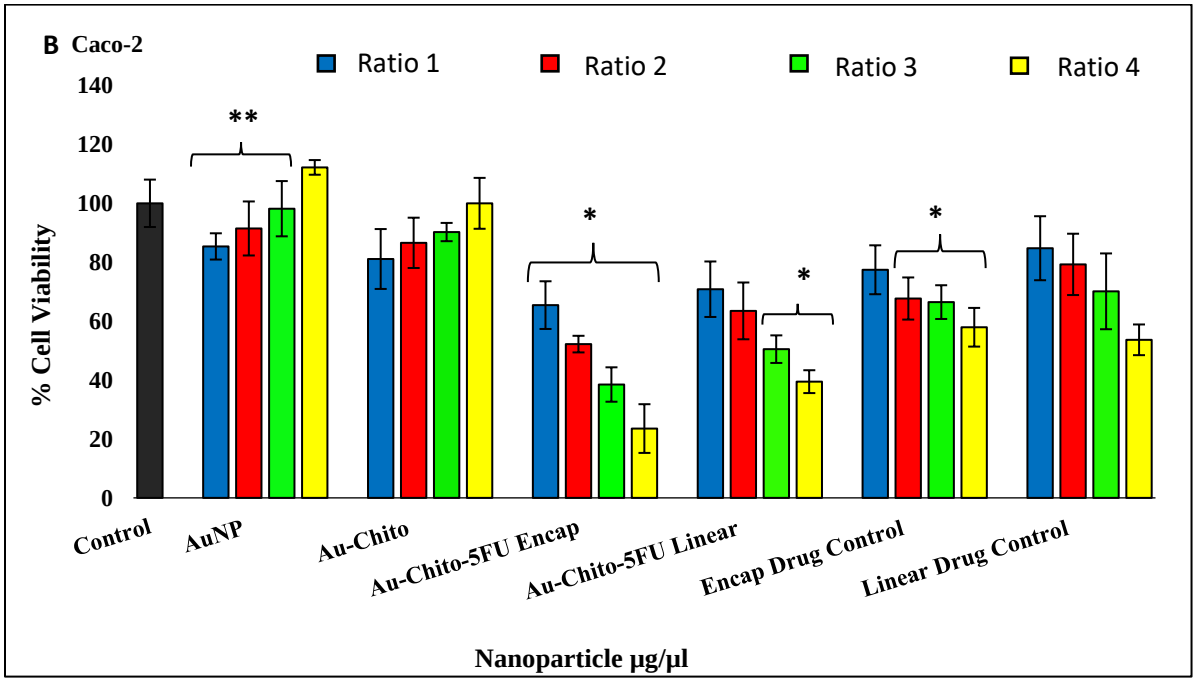

Figure 3.5 MTT cytotoxicity assay of nanoparticles and nanocomplexes in the Caco-2 cell line. Data represented as means ± SD (n=3), * p<0.05, **p<0.01 were considered statistically significant, Ratios as laid out in Table 3.1.

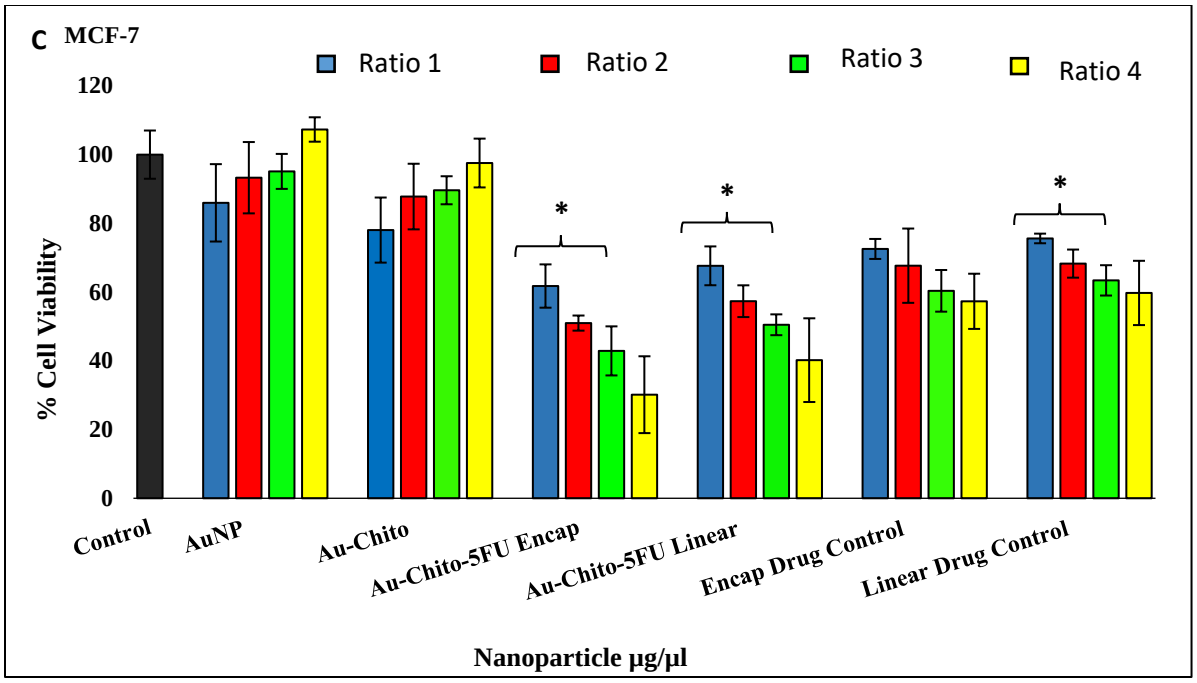

Figure 3.6 MTT cytotoxicity assay of nanoparticles and nanocomplexes in the MCF-7 cell line Data represented as means ± SD (n=3), * p<0.05, **p<0.01 were considered statistically significant, Ratios as laid out in Table 3.1.

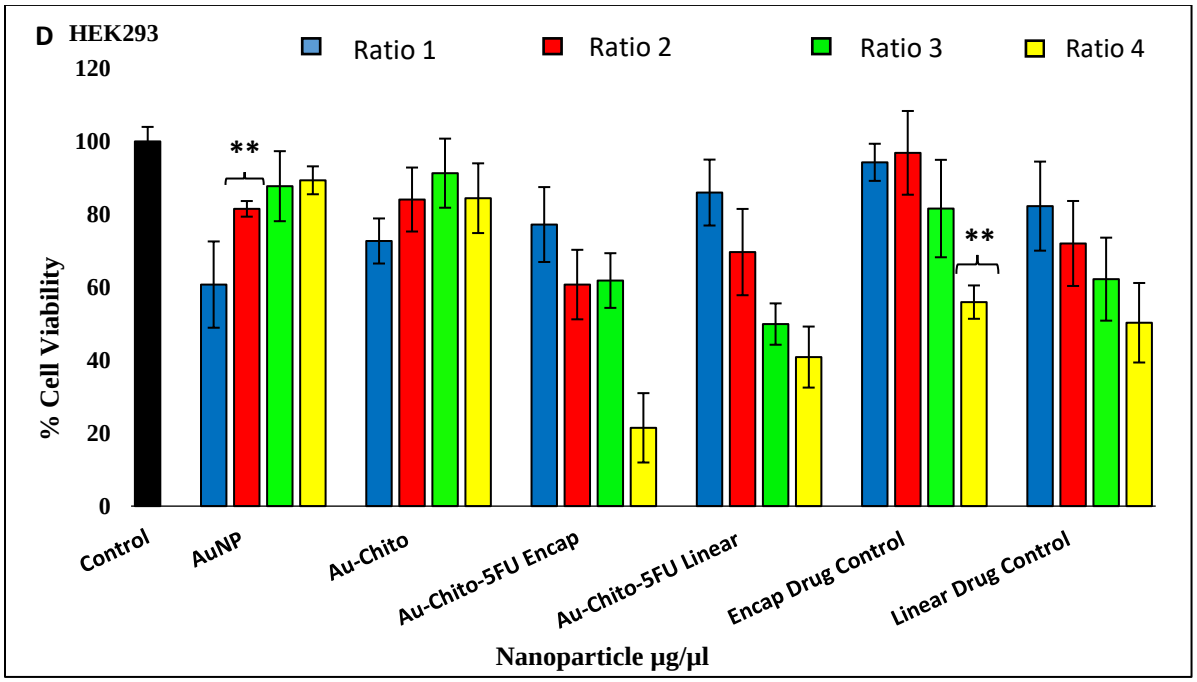

Figure 3.7 MTT cytotoxicity assay of nanoparticles and nanocomplexes in the HEK293 cell line Data represented as means ± SD (n=3), * p<0.05, **p<0.01 were considered statistically significant, Ratios as laid out in Table 3.1.

3.4.7.2 Sulforhodamine B (SRB) Assay

To correlate the results obtained from the MTT assay, a second cytotoxicity assay was performed with the same nanoparticles and nanocomplexes. The SRB cytotoxicity assay is a sensitive, quantitative assay which involves the staining of cellular proteins by sulforhodamine B (SRB). The SRB dye is an is an anionic aminoxanthene, which binds to the basic amino acid residues of proteins through electrostatic interactions under mildly acidic conditions. The SRB assay provides a measure of drug induced cytotoxicity, with much greater sensitivity[52]. Figures 3.8-3.11, depict the cytotoxicity profiles for the SRB assay in the four cell lines. A similar trend for AuNP's and Au-CS as in the MTT assay was observed, viz. with an increasing cell viability lined to increasing concentration. However, the AuNP-CS:5-FU nanocomplexes and the CS:5-FU nanocomplexes all showed a dose dependent activity with decreased viability across all three cell lines as concentration increased. Encapsulated Au-CS:5-FU showed the greatest anticancer activity with the exception of the Caco-2 cell line at the highest concentration, and correlates with data from the MTT assay. The HepG2 cells (Figure 3.8), least tolerated the nanocomplexes, with a significant decrease in the cell viability (~80% cell death) at the highest ratio. Linear bound nanocomposites showed lower cell death, indicating a lesser ability to deliver the anticancer agent successfully to the cell lines, compared to encapsulated complexes. This is also evident in the Caco-2 and MCF-7 cell lines. This assay further confirmed that the inclusion of AuNP in the delivery system played a significant role in the level of anticancer activity observed, and that encapsulated nanocomplexes were more efficient than their linear bound counterparts. The SRB assay results hence correlate with the data obtained in the MTT assay.

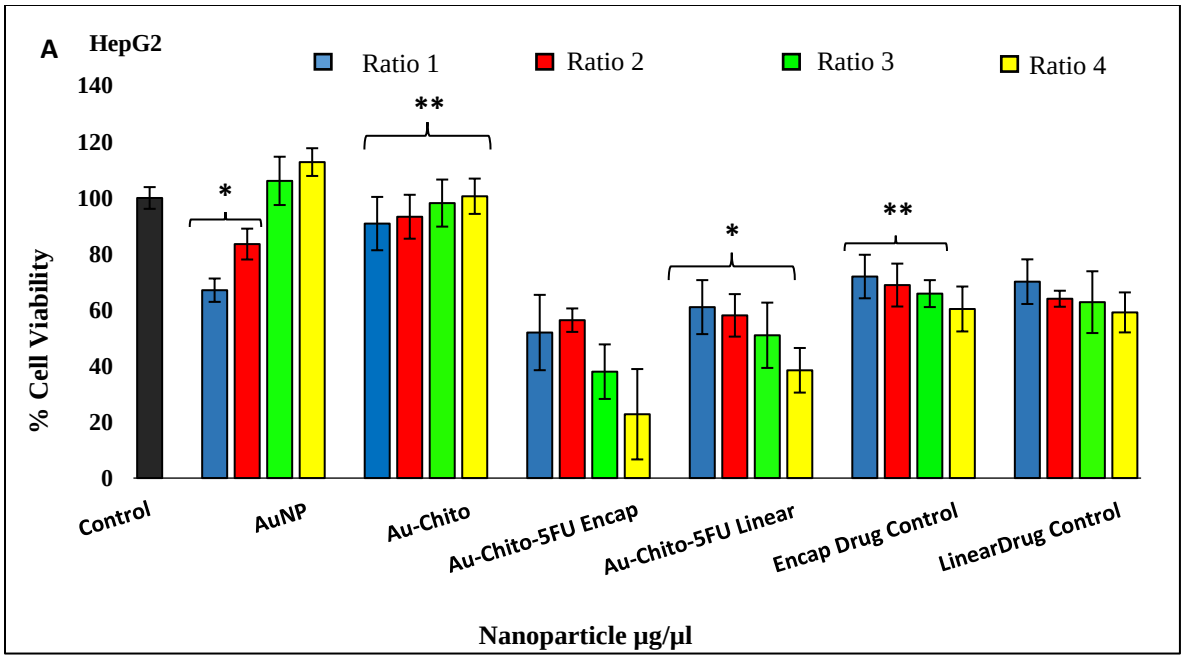

Figure 3.8 SRB cytotoxicity assay of nanoparticles and nanocomplexes in the HepG2 cell line. Data represented as means ± SD (n=3), * p<0.05, **p<0.01 were considered statistically significant, Ratios as laid out in Table 3.1.

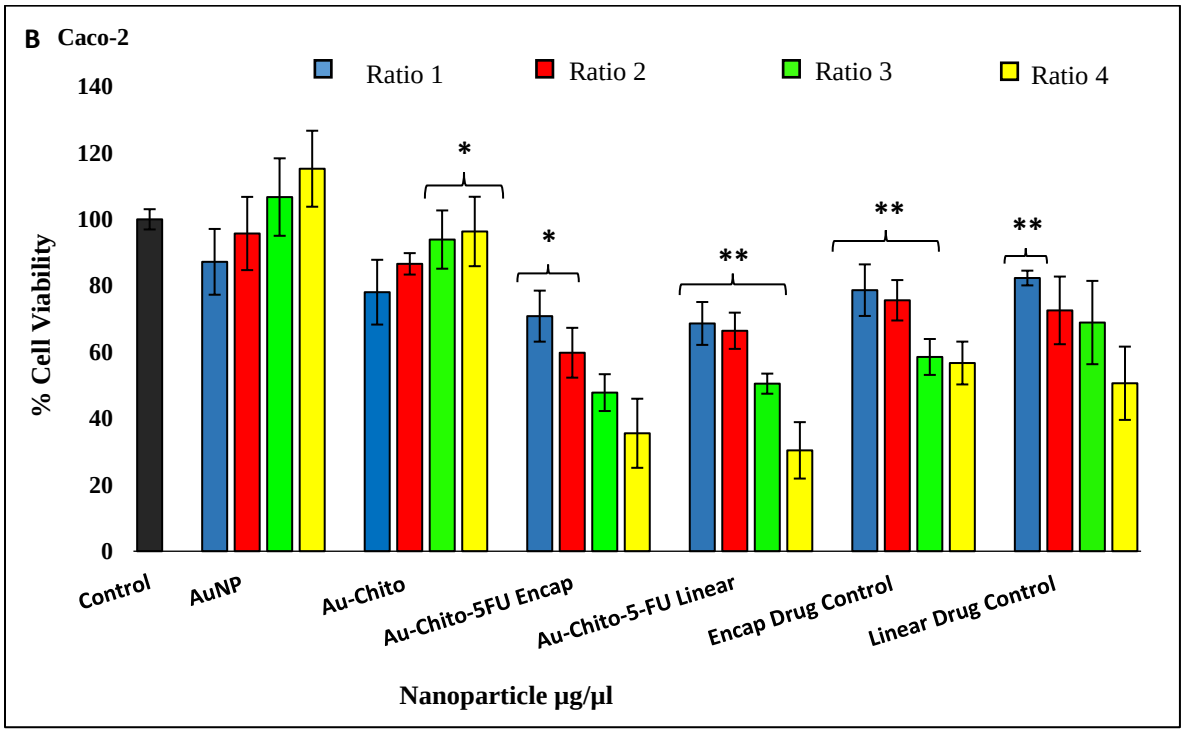

Figure 3.9 SRB **c**ytotoxicity assay of nanoparticles and nanocomplexes in the Caco-2 cell line Data represented as means ± SD (n=3), * p<0.05, **p<0.01 were considered statistically significant, Ratios as laid out in Table 3.1.

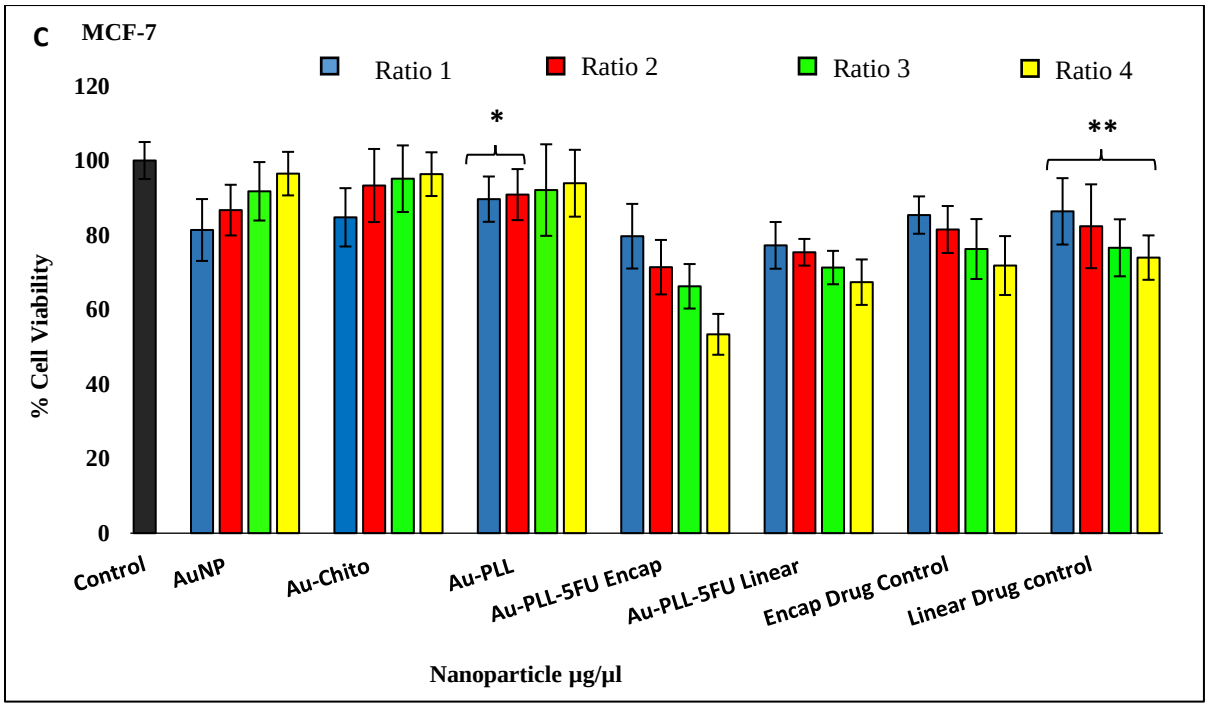

Figure 3.10 SRB **c**ytotoxicity assay of nanoparticles and nanocomplexes in the MCF-7 cell line Data represented as means ± SD (n=3), * p<0.05, **p<0.01 were considered statistically significant, Ratios as laid out in Table 3.1.

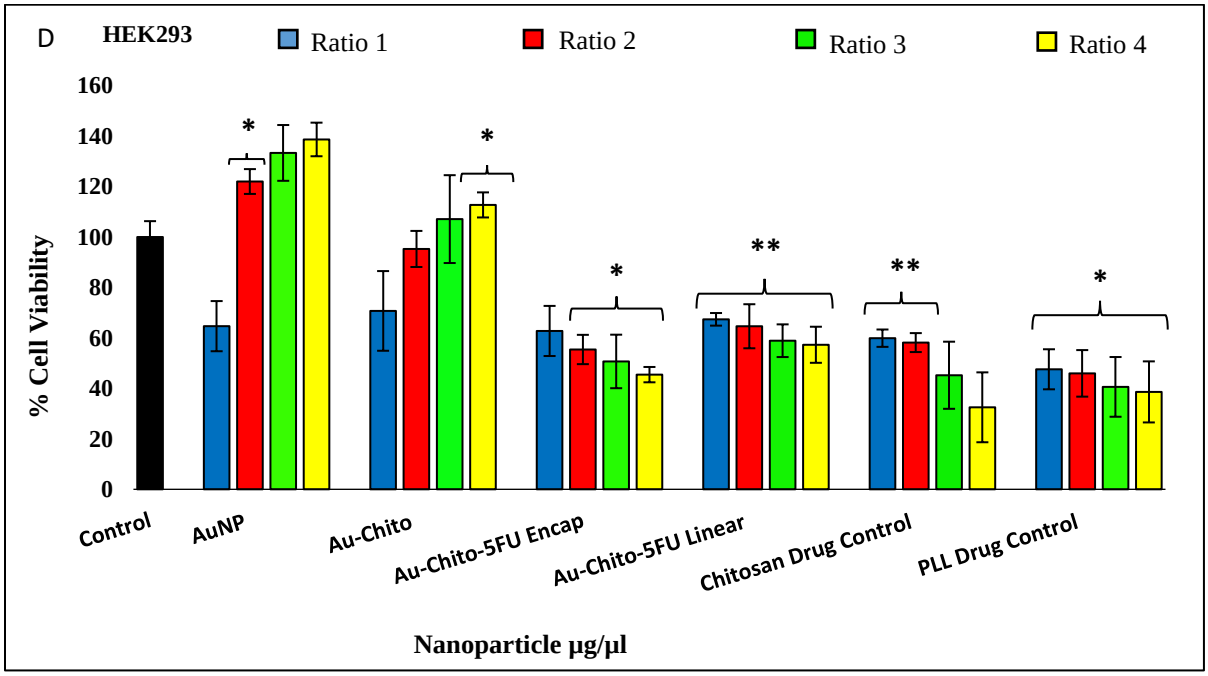

Figure 3.11 SRB **c**ytotoxicity assay of nanoparticles and nanocomplexes in the HEK293 cell line Data represented as means ± SD (n=3), * p<0.05, **p<0.01 were considered statistically significant, Ratios as laid out in Table 3.1.

3.4.8 Mechanism of cell death – Apoptosis studies

Apoptosis studies was conducted to determine the mechanism of cell death resulting from exposure to the two nanocomposites viz. encapsulated and linear bound CS-AuNP:5-FU, which produced the most significant anticancer activities in the MTT and SRB assays. The dual acridine orange/ethidium bromide (AO/EB) assay allows for the sensitive fluorescent detection of live, early and late apoptotic cells and necrotic cells. The principle behind this technique is that acridine orange stains live cells, by intercalating with the cell's DNA to emit a green fluorescence, while, ethidium bromide stains dead cells resulting in the emission of a yellow to red fluorescence, which is dependent on the stage of apoptosis [53]. Hence, viable cells will fluoresce green, with early apoptotic cells fluorescing a brighter hue of green, late apoptotic cells will fluoresce orange with a condensed chromatin visible, and necrotic cells will also fluoresce orange but with no chromatin condensation visible [54]. Apoptotic features were visible in all four of the cell lines (Figure 3.12) with the nanocomplexes showing higher levels of apoptotic induction towards the cancerous cell lines, as seen from the higher apoptotic indexes calculated (Table 3.3) studies have demonstrated that 5-FU does induce apoptosis in a wide range of cell lines,[55-58] . The apoptotic index was much lower in the control cell line HEK293, compared to the three cancerous cell lines, from the data observed in the drug release, the pH microenvironment of a normal cell is not acidic, possibly aiding in the slow release of the bioactive agent. Nanocomposites containing encapsulated 5-FU showed a higher apoptotic index in all cell lines compared to linear bound nanocomposites. These results correlate with the MTT and SRB cytotoxicity assays, in that the encapsulated nanocomplexes are more effective than the linear bound counterparts in the delivery of the drug 5-FU, and inducing anticancer activity.

Table 3.3. Apoptotic indices for the nanocomposites in HEK293, HepG2, Caco-2 and MCF-7 cell lines

Cell Lines	Apoptotic index	
	Au-CS-5-FU (Encapsulated)	Au-CS-5-FU (Linear)
HEK293	0.111	0.10
HepG2	0.25	0.17
Caco-2	0.64	0.26
MCF-7	0.23	0.19

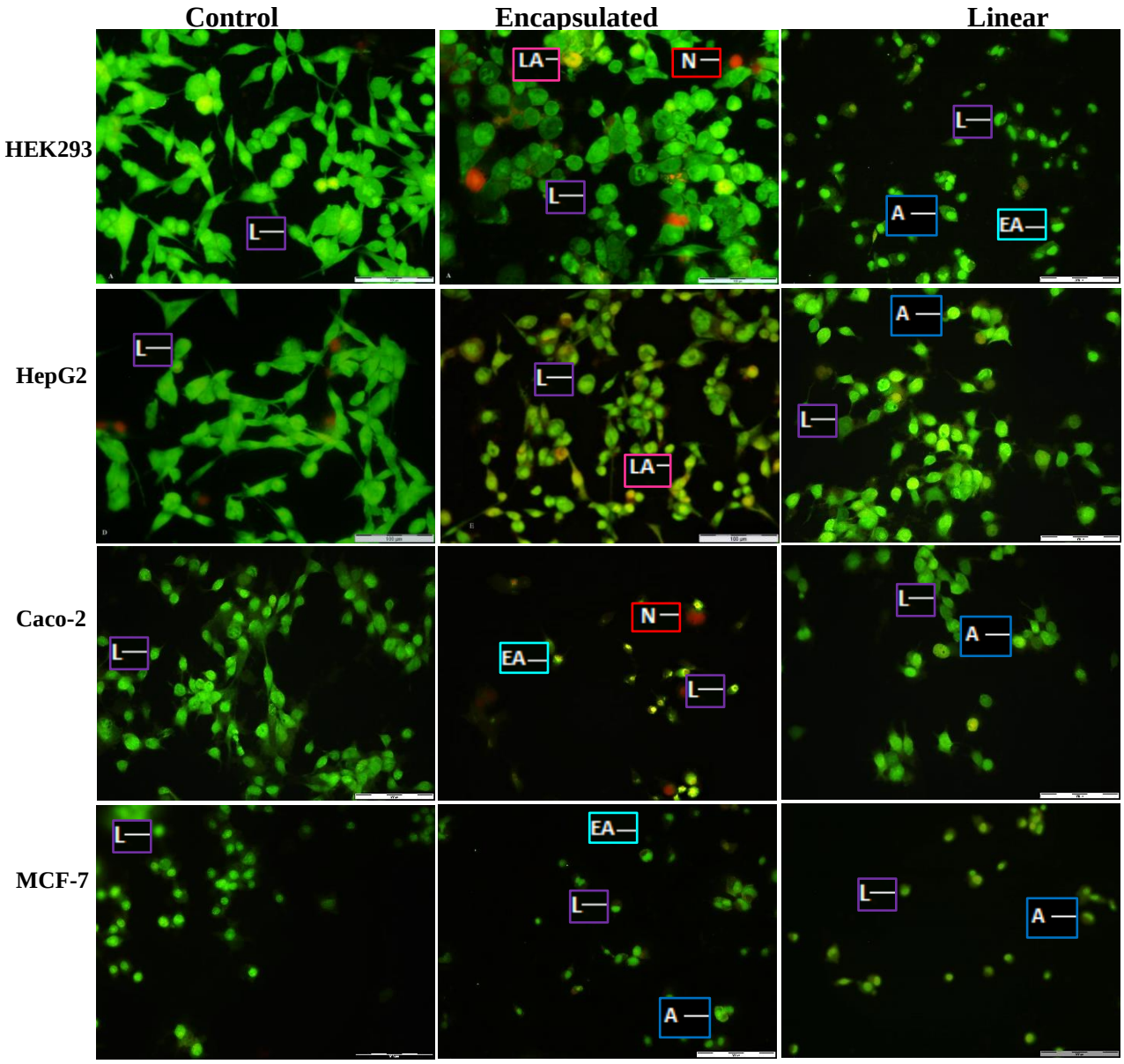

Figure 3.12: Fluorescent images obtained from the dual acridine orange /ethidium bromide apoptosis studies in the HEK293, HepG2, Caco-2 and MCF-7 cell lines at 20x magnification. (L= live cells; A= apoptotic cells; N= necrotic cells; LA= late apoptotic cells; EA = early apoptotic cells)

3.5 Conclusion

Gold nanoparticles were successfully synthesized, through chemical reduction and functionalized with the cationic polymer chitosan. The conjugation of AuNP to CS through the binding of Au to their NH_2 and OH groups, was successful as evidenced from the FTIR, UV-vis, TEM and NTA analysis. Of the two conjugation methods investigated, encapsulation emerged superior, with good colloidal stability, desirable size, higher drug binding efficiency (89.95 %), favorable drug release profile and efficient cellular uptake. The cytotoxicity assays further confirmed the above findings, with high anticancer activity observed in all cell lines. This study confirmed that the use of functionalized gold nanoparticles in drug delivery, enhances the anticancer activity of the bound drug, compared to drug delivery on its own or with a polymer. Overall, these nanocomplexes have shown to be promising drug delivery systems and warrant further optimization and testing in more cell lines and in an *in vivo* system.

3.6 References

[1] Reichert, J. M., and Wenger, J. B. (2008) Development trends for new cancer therapeutics and vaccines, *Drug discovery today 13*, 30-37.

[2] Zou, W. (2005) Immunosuppressive networks in the tumour environment and their therapeutic relevance, *Nature Reviews Cancer 5*, 263-274.

[3] Das, M., Mohanty, C., and Sahoo, S. K. (2009) Ligand-based targeted therapy for cancer tissue, *Expert opinion on drug delivery 6*, 285-304.

[4] Mohanty, C., Das, M., R Kanwar, J., and K Sahoo, S. (2011) Receptor mediated tumor targeting: an emerging approach for cancer therapy, *Current drug delivery 8*, 45-58.

[5] Mateka, J. J., Haniff, M. M., Bainey, R. S., and Iliou, C. B. (2013) Interesting trends in incidence and mortality rates of colorectal cancer in the United States of America, *Journal of Gastrointestinal & Digestive System 2013*.

[6] Lee, Y.-C., Lee, Y.-L., Chuang, J.-P., and Lee, J.-C. (2013) Differences in survival between colon and rectal cancer from SEER data, *PloS one 8*, e78709.

[7] Pisani, P., Parkin, D., and Ferlay, J. (1993) Estimates of the worldwide mortality from eighteen major cancers in 1985. Implications for prevention and projections of future burden, *International journal of cancer 55*, 891-903.

[8] Society, A. C. (2011) Colorectal Cancer Facts & Figures 2011-2013, American Cancer Society Atlanta, GA.

[9] Hastings, J. B. (1974) Mass screening for colorectal cancer, *The American Journal of Surgery 127*, 228-233.

[10] Singhal, S., Nie, S., and Wang, M. D. (2010) Nanotechnology applications in surgical oncology, *Annual review of medicine 61*, 359.

[11] Fauci, A., Braunwald, E., Kaspe, D., Hauser, L., Longo, D., and Jameson, J. (2008) Gastrointestinal cancer, *Harrison's, Principles of Internal Medicine. Mc Graw Hill, New York*.

[12] Lippman, M. (2008) oncology and Hematology, *Fauci A. Branwald E, et al, editors. Harrison's principles of internal medicine*, 479-747.

[13] Wang, X., Yang, L., Chen, Z. G., and Shin, D. M. (2008) Application of nanotechnology in cancer therapy and imaging, *CA: a cancer journal for clinicians 58*, 97-110.
[14] Sahoo, S. K., and Parveen, S. (2006) Nanomedicine: Clinical Applications of Polyethylene Glycol Conjugated Proteins and Drugs, *Clinical pharmacokinetics*, 965-988.
[15] Parveen, S., and Sahoo, S. K. (2008) Polymeric nanoparticles for cancer therapy, *Journal of drug targeting 16*, 108-123.
[16] Vasir, J. K., and Labhasetwar, V. (2007) Biodegradable nanoparticles for cytosolic delivery of therapeutics, *Advanced drug delivery reviews 59*, 718-728.
[17] Taniguchi, N. (1974) On the basic concept of nano-technology Proceedings of the International Conference on Production Engineering Tokyo Part II Japan Society of Precision Engineering.
[18] Singh, M., Singh, S., Prasad, S., and Gambhir, I. (2008) Nanotechnology in medicine and antibacterial effect of silver nanoparticles, *Digest Journal of Nanomaterials and Biostructures 3*, 115-122.
[19] Lim, S. Y., Shen, W., and Gao, Z. (2015) Carbon quantum dots and their applications, *Chemical Society Reviews 44*, 362-381.
[20] Bertrand, N., Wu, J., Xu, X., Kamaly, N., and Farokhzad, O. C. (2014) Cancer nanotechnology: the impact of passive and active targeting in the era of modern cancer biology, *Advanced drug delivery reviews 66*, 2-25.
[21] Sanna, V., Pala, N., and Sechi, M. (2014) Targeted therapy using nanotechnology: focus on cancer, *International journal of nanomedicine 9*, 467.
[22] Grodzinski, P., Silver, M., and Molnar, L. K. (2014) Nanotechnology for cancer diagnostics: promises and challenges, *Expert review of molecular diagnostics*.
[23] Bangham, A., Standish, M. M., and Watkins, J. (1965) Diffusion of univalent ions across the lamellae of swollen phospholipids, *Journal of molecular biology 13*, 238-IN227.
[24] Alivisatos, A. P. (1996) Semiconductor clusters, nanocrystals, and quantum dots, *Science 271*, 933.
[25] Bruchez, M., Moronne, M., Gin, P., Weiss, S., and Alivisatos, A. P. (1998) Semiconductor nanocrystals as fluorescent biological labels, *science 281*, 2013-2016.
[26] Zhu, S., Song, Y., Zhao, X., Shao, J., Zhang, J., and Yang, B. (2015) The photoluminescence mechanism in carbon dots (graphene quantum dots, carbon nanodots, and polymer dots): current state and future perspective, *Nano Research 8*, 355-381.
[27] Liu, Y., Rohrs, J., and Wang, P. (2014) Development and challenges of nanovectors in gene therapy, *Nano LIFE 4*, 1441007.
[28] Xiao, H., Qi, R., Liu, S., Hu, X., Duan, T., Zheng, Y., Huang, Y., and Jing, X. (2011) Biodegradable polymer− cisplatin (IV) conjugate as a pro-drug of cisplatin (II), *Biomaterials 32*, 7732-7739.
[29] Xiao, H., Yan, L., Zhang, Y., Qi, R., Li, W., Wang, R., Liu, S., Huang, Y., Li, Y., and Jing, X. (2012) A dual-targeting hybrid platinum (IV) prodrug for enhancing efficacy, *Chemical communications 48*, 10730-10732.
[30] Xiao, H., Song, H., Yang, Q., Cai, H., Qi, R., Yan, L., Liu, S., Zheng, Y., Huang, Y., and Liu, T. (2012) A prodrug strategy to deliver cisplatin (IV) and paclitaxel in nanomicelles to improve efficacy and tolerance, *Biomaterials 33*, 6507-6519.
[31] Sivasankar, M., and Kumar, B. P. (2010) Role of nanoparticles in drug delivery system, *International Journal of Research in Pharmaceutical and Biomedical Sciences 1*, 41-66.
[32] Lokina, S., Stephen, A., Kaviyarasan, V., Arulvasu, C., and Narayanan, V. (2014) Cytotoxicity and antimicrobial activities of green synthesized silver nanoparticles, *European journal of medicinal chemistry 76*, 256-263.
[33] Fan, Y.-L., Fan, B.-Y., Li, Q., Di, H.-X., Meng, X.-Y., and Ling, N. (2013) Preparation of 5-fluorouracil-loaded nanoparticles and study of interaction with gastric cancer cells, *Asian Pacific journal of cancer prevention: APJCP 15*, 7611-7615.
[34] Rana, S., Bajaj, A., Mout, R., and Rotello, V. M. (2012) Monolayer coated gold nanoparticles for delivery applications, *Advanced drug delivery reviews 64*, 200-216.
[35] Zhao, P., Li, N., and Astruc, D. (2013) State of the art in gold nanoparticle synthesis, *Coordination Chemistry Reviews 257*, 638-665.

[36] Trivedi, N., Patel, N., Upadhyay, U., and Sha, S. (2012) Gold nanoparticulate drug delivery system: a review, *Pharmacie Globale International Journal of Comphrehesive Pharmacy 3*, 1-5.
[37] Biju, V. (2014) Chemical modifications and bioconjugate reactions of nanomaterials for sensing, imaging, drug delivery and therapy, *Chemical Society Reviews 43*, 744-764.
[38] Shimizu, T., Teranishi, T., Hasegawa, S., and Miyake, M. (2003) Size evolution of alkanethiol-protected gold nanoparticles by heat treatment in the solid state, *The Journal of Physical Chemistry B 107*, 2719-2724.
[39] Kumar, S. V., and Ganesan, S. (2011) Preparation and characterization of gold nanoparticles with different capping agents, *International Journal of Green Nanotechnology 3*, 47-55.
[40] Li, D., and Kaner, R. B. (2006) Shape and aggregation control of nanoparticles: not shaken, not stirred, *Journal of the American Chemical Society 128*, 968-975.
[41] Goel, A., and Rani, N. (2012) Effect of PVP, PVA and POLE surfactants on the size of iridium nanoparticles, *Open Journal of Inorganic Chemistry 2*, 67.
[42] Božanić, D. K., Trandafilović, L. V., Luyt, A. S., and Djoković, V. (2010) 'Green'synthesis and optical properties of silver–chitosan complexes and nanocomposites, *Reactive and functional polymers 70*, 869-873.
[43] Pauliukaite, R., Ghica, M. E., Fatibello-Filho, O., and Brett, C. M. (2010) Electrochemical impedance studies of chitosan-modified electrodes for application in electrochemical sensors and biosensors, *Electrochimica Acta 55*, 6239-6247.
[44] Schroeder, B. R., Ghare, M. I., Bhattacharya, C., Paul, R., Yu, Z., Zaleski, P. A., Bozeman, T. C., Rishel, M. J., and Hecht, S. M. (2014) The disaccharide moiety of bleomycin facilitates uptake by cancer cells, *Journal of the American Chemical Society 136*, 13641-13656.
[45] Yu, Z., Schmaltz, R. M., Bozeman, T. C., Paul, R., Rishel, M. J., Tsosie, K. S., and Hecht, S. M. (2013) Selective tumor cell targeting by the disaccharide moiety of bleomycin, *Journal of the American Chemical Society 135*, 2883-2886.
[46] Singh, J., Roychoudhury, A., Srivastava, M., Solanki, P. R., Lee, D. W., Lee, S. H., and Malhotra, B. (2014) A dual enzyme functionalized nanostructured thulium oxide based interface for biomedical application, *Nanoscale 6*, 1195-1208.
[47] Arias, J. L. (2008) Novel strategies to improve the anticancer action of 5-fluorouracil by using drug delivery systems, *Molecules 13*, 2340-2369.
[48] Shalkevich, N., Shalkevich, A., Si-Ahmed, L., and Bürgi, T. (2009) Reversible formation of gold nanoparticle–surfactant composite assemblies for the preparation of concentrated colloidal solutions, *Physical Chemistry Chemical Physics 11*, 10175-10179.
[49] Kato, Y., Ozawa, S., Miyamoto, C., Maehata, Y., Suzuki, A., Maeda, T., and Baba, Y. (2013) Acidic extracellular microenvironment and cancer, *Cancer cell international 13*, 1.
[50] Chandran, P. R., and Sandhyarani, N. (2014) An electric field responsive drug delivery system based on chitosan–gold nanocomposites for site specific and controlled delivery of 5-fluorouracil, *RSC Advances 4*, 44922-44929.
[51] Jain, S., Hirst, D., and O'sullivan, J. (2014) Gold nanoparticles as novel agents for cancer therapy, *The British journal of radiology*.
[52] Skehan, P., Storeng, R., Scudiero, D., Monks, A., McMahon, J., Vistica, D., Warren, J. T., Bokesch, H., Kenney, S., and Boyd, M. R. (1990) New colorimetric cytotoxicity assay for anticancer-drug screening, *Journal of the National Cancer Institute 82*, 1107-1112.
[53] Bezabeh, T., Mowat, M., Jarolim, L., Greenberg, A., and Smith, I. (2001) Detection of drug-induced apoptosis and necrosis in human cervical carcinoma cells using 1 H NMR spectroscopy, *Cell death and differentiation 8*, 219-224.
[54] C Maiyo, F., Moodley, R., and Singh, M. (2016) Cytotoxicity, Antioxidant and Apoptosis Studies of Quercetin-3-O Glucoside and 4-(β-D-Glucopyranosyl-1→ 4-α-L-Rhamnopyranosyloxy)-Benzyl Isothiocyanate from Moringa oleifera, *Anti-Cancer Agents in Medicinal Chemistry (Formerly Current Medicinal Chemistry-Anti-Cancer Agents) 16*, 648-656.

[55] Nita, M. E., Nagawa, H., Tominaga, O., Tsuno, N., Fujii, S., Sasaki, S., Fu, C., Takenoue, T., Tsuruo, T., and Muto, T. (1998) 5-Fluorouracil induces apoptosis in human colon cancer cell lines with modulation of Bcl-2 family proteins, *British journal of cancer 78*, 986.
[56] Eichhorst, S. T., Müerköster, S., Weigand, M. A., and Krammer, P. H. (2001) The chemotherapeutic drug 5-fluorouracil induces apoptosis in mouse thymocytes in vivo via activation of the CD95 (APO-1/Fas) system, *Cancer research 61*, 243-248.
[57] Hwang, J.-T., Ha, J., and Park, O. J. (2005) Combination of 5-fluorouracil and genistein induces apoptosis synergistically in chemo-resistant cancer cells through the modulation of AMPK and COX-2 signaling pathways, *Biochemical and biophysical research communications 332*, 433-440.
[58] Kondo, M., Nagano, H., Wada, H., Damdinsuren, B., Yamamoto, H., Hiraoka, N., Eguchi, H., Miyamoto, A., Yamamoto, T., and Ota, H. (2005) Combination of IFN-α and 5-fluorouracil induces apoptosis through IFN-α/β receptor in human hepatocellular carcinoma cells, *Clinical cancer research 11*, 1277-1286.

CHAPTER 4

An *in vitro* study of poly-l-lysine functionalized gold nanoparticles in anticancer drug delivery

L.L. David[1] and M. Singh[1*]

[1]Non-Viral Gene Delivery Laboratory, Discipline of Biochemistry, School of Life Sciences, University of KwaZulu-Natal, Private Bag X54001, Durban, South Africa

[*]Corresponding author: Moganavelli Singh, email: singhm1@ukzn.ac.za

Abstract

The formulation of safe and efficient drug delivery systems, which are able to overcome the many limitations and hurdles faced by conventional methods, is seen as the next step towards successfully treating diseases such as cancer. Nanoparticles have gained much attention due to their desirable characteristics, facile synthesis and their adaptability in applications across various fields. Of these nanoparticles, the noble metal gold, has emerged superior due to characteristics such as high surface to volume ratio, relative ease of synthesis and low toxicity to name a few. Through the chemical reduction of gold (III) chloride trihydrate with sodium citrate, AuNPs were synthesized and functionalized with poly-l-lysine (PLL), a cationic polymer and an anticancer agent 5-fluorouracil (5-FU). Subsequent nanocomplexes and nanocomposites were fully characterized through UV-vis spectroscopy, ICP, FTIR, TEM and nanoparticle tracking analysis (NTA).

Nanocomplexes consisting of PLL:5-FU were synthesized via two methods viz. encapsulation and linear binding, followed by their conjugation to AuNPs. Nanocomplexes prepared by the encapsulation method displayed better binding and drug release, protection of the drug, and greater anticancer activity in the cancer cell lines, HepG2, Caco-2 and MCF-7 compared to the linear binding method, probably. Cytotoxicity analysis was carried out using the MTT and SRB assays in all cell lines to provide a detailed cytotoxicity profile. Overall, studies revealed that both methods of formulation were significantly effective in delivering the anticancer agent to the cancer cell lines, with little cytotoxicity observed towards the non-cancer cell line.

Key Words: Drug delivery, Nanoparticles, Gold, Poly-l-lysine, 5-Fluorouracil, encapsulation, linear binding

4.1 Introduction

The term nanotechnology refers to the creation, synthesis and manipulation of materials on an atomic scale, often between 1-100 nm[1]. The creation of materials on this scale, results in properties which are unique to nanoparticles, such as size, charge and solubility[2]. For this reason, nanotechnology is viewed by many as having a promising future for the treatment for cancer, considering that the classical forms of treatment, to date have been less than ideal[3]. Most classical anticancer agents such as 5-fluorouracil do not exhibit a specificity towards the tissue they act on, and while they have been shown to be effective in killing cancerous tissue, they have also been known to cause high levels of toxicity towards healthy tissue, limiting their use at high concentrations. This drug specifically has also been shown to present with low bioavailability and solubility[4].

These factors combined resulted in the limited use of these anticancer drugs. Classical therapy strategies have also been faced with obstacles, including low accumulation into tumor tissue and rapid metabolism, resulting in many therapies being ineffective towards the treatment of cancer[5]. Importantly, the use of nanoparticles in drug delivery have been shown to increase bioavailability, and increase retention time. In addition the use of nanoparticles have increased the plasma half-life of cytotoxic drugs, while keeping toxicity to a minimun[6]. These factors have resulted in nanoparticle conjugated cytotoxic drugs being able to overcome drug resistance, through accumulation of the anticancer agents, in high volumes in the tumor regions[7]. The ability to functionalize different targeting ligands onto the surface of nanoparticles, allow for the delivery of specific drugs to organs rich in these ligand specific receptors[8].

The ability to tailor make drug delivery vectors, allow for the use of drugs at much lower concentrations, whilst still resulting in significant anticancer activity, and lower cytotoxicity in healthy tissue. Encapsulation of many hydrophobic drugs increases their solubility and reduces the need for many organic solvents, which have been used in the past to increase the solubility of drugs, leading to increased cytotoxicity. Encapsulation offers the added advantage of preventing the degradation of the drug *in vivo*, thereby allowing for smaller concentrations to be used. It is known that nanoparticles possess large surface to volume ratios, resulting in larger volumes of drugs being conjugated to nanoparticles[9 10].

Various nanoparticles have been investigated for use as drug delivery vehicles including liposomes[11, 12], carbon nanotubes[13], dendrimers,[14] selenium[15] and metallic nanoparticles such as gold[16]. Gold nanoparticles (AuNPs) have shown potential as drug and gene delivery vectors due to their unique optical properties [17], low toxicity and high biocompatibility[18 19]. AuNP's present with a core which is essentially inert, assisting to its low levels of cytotoxicity observed. They have been shown to possess unique properties such as surface plasmon resonance (SPR) and the ability to bind amine and thiol groups[20], allowing for the conjugation of polymers such as poly-l-lysine. Gold nanoparticles readily enter the cell through nonspecific receptor mediated endocytosis[21], resulting in the accumulation of the nanoparticles at the site of the tumor, which present with a leaky, mutated vasculature. These properties allow for alternative or combined therapies, such as photo thermal ablation[22].

The addition of poly-l-lysine (PLL) serves as a stabilizing agent for synthesized AuNPs[23]. It is a cationic polymer with an abundance of primary amino groups, which are primarily responsible for the controlled drug release observed in nanocomposites consisting of PLL[24]. Poly-l-lysine is a biocompatible polymer, which exhibits low toxicity and has a high level of biodegradability[25].

5-Fluorouracil (5-FU), is a broad spectrum anticancer agent, which has been shown to be effective against cancer cells.[26], however like most cytotoxic drugs it shows little specificity, resulting in high cytotoxicity in healthy tissue[27]. Using the combination of AuNPs and PLL conjugated to 5-FU, it was hoped that there would be an increase in anticancer activity towards cancerous cell lines and a reduction in the cytotoxicity towards the control cell line. This study involves a comparison of conjugation protocols with the encapsulation of 5-FU into AuNP-PLL and linearly bound AuNP-PLL:5-FU, to determine, which method offers greater activity of the drug. AuNP-PLL have been prepared with and without the drug 5-FU. The prepared nanocomposites have been fully characterized using UV-vis, TEM, FTIR, ICP and NTA. *In vitro* drug release profiles have been evaluated, and cytotoxicity studies in all four human cell lines have also been assessed.

4.2. Materials

Gold (III) chloride trihydrate (M_w: 393.83 g mol^{-1}, HAuCl4.3H2O), Poly-L-lysine hydrobromide (M_w: 1000-5000), Polysorbate 80 (Tween 80, Mw: 1,310 g mol^{-1}, $C_{64}H_{124}O_{26}$), Sodium triphosphate (Mw: 367.86 g mol^{-1}, $Na_5P_3O_{10}$) 5-Fluorouracil (M_w: 130.1 g mol^{-1}, $C_4H_3FN_2O_2$),

Sulforodhamine B (SRB Dye, Mw: 558.67 g mol^{-1}, $C_{27}H_{30}N_2O_7S_2$), Acridine Orange hemi (zinc chloride) salt [3,6-Bis(dimethylamino) acridine hydrochloride zinc chloride double salt] (Mw: 265.36, g $mol^{-1,}$ $C_{17}H_{19}N_3$), Dialysis Tubing (MWCO= 1000 Daltons) were purchased from Sigma-Aldrich Chemical Co., (St. Louis, USA). Sodium citrate tribasic dehydrate, phosphate-buffered saline tablets [PBS, (140 mM NaCl, 10 mM phosphate buffer, 3 mM KCl)], 3-[(4,5-dimethylthiazol-2-yl)-2,5-diphenyl tetrazolium bromide] (MTT), ethidium bromide, glacial acetic acid, and dimethyl sulfoxide [DMSO], were supplied by Merck (Darmstadt, Germany). The human cells, embryonic kidney (HEK293), colorectal adenocarcinoma (Caco-2), hepatocellular carcinoma (HepG2) and breast adenocarcinoma (MCF-7) were obtained from the American type culture collection (Pty) Ltd, Manassas, Virginia, USA. Sterile Fetal Bovine Serum (FBS) was sourced from Hyclone GE Healthcare (Utah, USA). Eagle's Minimum Essential Medium (EMEM) with L-glutamine (4.5 g ml^{-1}), Penicillin/ Streptomycin/ Amphotericin B (100x) antibiotic mixture [Amphotericin B (25 mcg ml^{-1}), NaCl (8.5 mg L^{-1}) Potassium penicillin (10 000 Units mL^{-1}), Streptomycin sulphate (10 000 mcg ml^{-1})] and Trypsin-versene-EDTA mixture were purchased from Lonza Bio Whittaker (Verviers, Belgium). All sterile tissue culture plasticware were supplied by Corning Inc., (New York, USA). Analytical grade reagents and ultrapure (18 MOhm) water (Milli-Q Academic, Millipore, France) was used throughout.

4.3 Methods

4.3.1 Preparation of colloidal gold nanoparticles (AuNPs)

An adaptation of the Turkevich method was used to synthesize the AuNPs , by reduction of Gold (III) chloride trihydrate ($H[AuCl_4]$) with sodium citrate ($NaC_6H_5O_7$). To 25 ml of 18 MOhm water at a temperature of 85-95 ˚C, was added with stirring, 375 µl of a 3 x 10^{-2} M of H(AuCl4) solution, and 1 ml of 1% sodium citrate. A color change from a pale yellow to dark blue after 5 minutes and eventually to a deep wine red after 15 minutes indicated the formation of the nanoparticles. After 5 minutes, the solution containing a final concentration of 0.45 x 10^{-3} M of the colloidal AuNPs, was cooled and stored at room temperature.

4.3.2 Synthesis of 5-FU encapsulate PLL-AuNP nanocomposites

To 2.5 ml of PLL solution (0.75 mg ml^{-1} in 2% acetic acid) was added 2.5 ml of 5-FU solution (3.8 mM in 18 M Ohm water) with constant mixing. Thereafter, Tween 80 (0.5% $^{v}/_{v}$) was added, and pH maintained between 4.6-4.8. A PLL: TPP complex of ratio 2:1 ($^{v}/_{v}$) was then produced by the addition of 1.25 ml of TPP. After gentle mixing for 180 minutes, to ensure conjugation of 5-FU to the nanoparticles, 2 ml of the synthesized colloidal AuNP solution, was added dropwise to 2 ml of PLL:5-FU nanoparticles under gentle stirring.

4.3.3 Synthesis of 5-FU linear PLL-AuNP nanocomplex

To 2.5 ml of PLL solution (0.75 mg ml^{-1}) was added approximately 2.5 ml of 5-FU solution (3.8 mM) and gently stirred for 180 minutes. Thereafter, 2 ml of the AuNP solution was added dropwise to 2 ml of PLL:5-FU with stirring for 60 minutes.

4.3.4 UV-vis spectrophotometry analysis

To confirm the successful synthesis of the AuNPs and AuNPs-PLL, their absorption spectra was obtained by UV-vis spectroscopy, and correlated with that provided in literature. The expected surface plasmon resonance (SPR) absorption of the gold nanoparticles is at 520 nm, with any shift in the absorption spectra indicating successful conjugation of the biomolecule. Solutions were sonicated and vortexed, and then measured using a Biomate 3 spectrophotometer (Thermo Fischer Scientific Inc., Waltham, Massachusetts, USA).

4.3.5 Transmission Electron Microscopy (TEM)

The size, uniformity and ultrastructural morphology of all the AuNPs and their nanocomplexes were determined by TEM. Approximately, 10 µl of the respective nanoparticle/ nanocomplex samples was added to a 400 mesh carbon coated copper grid (Ted Pella Inc. Redding, USA) and air dried at room temperature for 1 hour. Samples were then viewed in a JEOL-JEM T1010 (Jeol, Tokyo, Japan) electron microscope at 60 000x magnification, with temperature above -150°C, and at an operating acceleration voltage of 100 kV. Images were captured using the iTEM Soft Imaging Systems (SIS) Megaview III fitted with a side-mounted 3-megapixel digital camera.

4.3.6 Nanoparticle Tracking Analysis (NTA)

To determine the accurate size distribution and zeta potential of all nanoparticles and nanocomplexes, analysis was performed at 25°C using a laser based NTA system (Nanosight NS-500, Malvern Instruments, UK). Samples were diluted 1:500 in 18 MOhm water, and 1 ml of each sample was evaluated, after the instrument was primed, flushed, and the camera zero position set. All samples were run in triplicate.

4.3.7 Inductively coupled plasma-optical emission spectroscopy analysis (ICP)

The accurate Au concentration present in the prepared colloidal AuNP solution was determined through inductively coupled plasma-optical emission spectroscopy (ICP-OES). This was performed on a Perkin Elmer optima 5300 DV optical emission spectrometer. A standard curve between 1 – 20 ppm, was set up using a standard Au stock solution of 100 ppm.

4.3.8 Fourier transform infra-red analysis (FTIR)

FTIR was employed to confirm the presence of essential groups and bonds in Au-PLL, as displayed in the obtained spectra. The spectrum was run using 200 µl of the respective sample in a Spectrum Perkin Elmer spectrophotometer, and the respective IR spectra were obtained using Spectrum Analysis Software.

4.3.9 Encapsulation efficiency

Approximately, 2 ml of respective encapsulated and linear Au-PLL:5-FU nanocomplexes were dialyzed (MWCO=1000 Da), against 15 ml PBS for 12 hours at 37˚ C. Absorbance readings at 266 nm, of 1 ml samples were taken pre-dialysis, and at the end of the 12-hour incubation. The encapsulation efficiency of 5-FU was determined using the following equation:

Encapsulation efficiency (%) = (Total 5-FU)- (Bound 5-FU)/ (Total 5-FU) x 100

4.3.10 Drug release studies

Drug release studies were performed at pH 4.0 and pH 7.0, to assess the ability of the nanocomplexes to release 5-FU over a period. Approximately, 2 mL of each Au-PLL:5-FU,

encapsulated and linear, were dialyzed (MWCO= 1000 Da) against 5 ml PBS for 7 hours at 37˚C. Hourly samples of 2 µl sample was removed and analyzed on a Nanodrop oneC, UV-vis spectrophotometer (Thermo Fischer Scientific Inc.,Waltham, Massachusetts,USA) at 266 nm. Readings obtained were used to generate a drug release profile for the respective nanocomplexes under the different pH conditions.

4.3.11 Reconstitution, propagation and maintenance of cell lines *in vitro*

Animal cell culture studies were conducted under sterile conditions in an Airvolution Class II biosafety laminar flow hood. All media and cell culture reagents were first warmed to 37˚C in a water bath, prior to any procedure. Cells were obtained from cryopreserved stick and thawed at 37˚C and then centrifuged at 3000 rpm for 60 seconds. The cell pellet was re-suspended in 1 ml of complete medium (EMEM supplemented with 10% ($^{v}/_{v}$) FBS and antibiotics (100 U ml^{-1} Penicillin, 100 µg ml^{-1} streptomycin), and then dispensed into 25 cm^2 tissue culture flasks containing 5 ml of medium, and incubated at 37˚C in a HEPA class 100 Steri-Cult CO_2 incubator (Thermo-Fisher Corporation, Waltham, Massachusetts, USA). The medium of reconstituted cells was changed after 24 hours to remove any traces of the cryopreservatant. The growth of cells was routinely monitored under a Nikon TMS inverted microscope (Nikon Corp, Tokyo, Japan). The old medium was replenished, cells subcultured for propagation or cell culture assays or cells were cryopreserved, depending on cell growth and assay requirement.

4.3.12 Trypsinization

After cells were washed with 5 ml of PBS (pH 7.5), 1 ml of trypsin-versene was added to cells. Trypsinization was monitored under an inverted microscope. Once cells had “rounded off”, trypsinization was halted by the addition of 1 ml medium containing serum that inhibits the enzyme action. To dislodge all the cells, the flask was gently tapped against the palm of the hand. Cells were then split into separate culture flasks, multiwell plates or alternatively cryopreserved.

4.3.13 Cryopreservation

After trypsinization, cells were pelleted by centrifugation at 3000 rpm for 1 minute, then re-suspended in 0.9 ml of complete medium and 0.1 ml of DMSO, mixed by vortexing and dispensed

into sterile 2 ml cryogenic vials. The vials were inserted into a Nalgene™ "Mr Frosty" Cryo 1˚C freezing container, containing isopropanol. Cells were frozen at a rate of -1 ˚C per minute to a final temperature of -70 ˚C, and then stored in a -80 ˚C biofreezer (Nuaire, Lasec Laboratory and Scientific equipment), for short term storage or in liquid N_2 for long term storage.

4.3.14 MTT cytotoxicity assay

Trypsinized cells were plated into clear 96-well plates at seeding densities between 2.4 x 10^4 - 2.9 x 10^4 cells per well, and incubated at 37˚C for 24 hours to allow for attachment of cells. The old medium was then replenished with 200 µl fresh complete EMEM, followed by addition of the AuNP, Au-PLL, Au-PLL:5-FU encapsulated, Au-PLL:5-FU linear and PLL:5-FU nanocomplexes at concentrations set out in Table 4.1. Positive controls (100 % survival), containing cells only were included and assays were conducted in triplicate. Cells were incubated for 48 hours at 37˚C in 5% CO_2, followed by removal of the old medium and the addition of 100 µl fresh medium and 100 µl of MTT reagent (5 mg/ml in PBS). The cells were incubated for a further 4 hours at 37 ˚C, after which the MTT infused medium was removed, and 200 µl of DMSO was added to each well, to solubilize the insoluble formazan crystals. Absorbance was then read at 570 nm, on a Mindray MR-96A microplate reader (Vacutec, Hamburg, Germany), using DMSO as a blank. The cell viability (%) was calculated using the following equation:
(Abs of treated – Abs of control/ Abs of control) x 100%.

Table 4.1. Ratios of respective nanoparticles and nanocomplexes used in cytotoxicity assays

Ratio	AuNP's	Au-PLL	Au-PPL-5FU Encapsulated	Au-PLL-5FU Linear	PLL Encapsulated 5-FU control	PLL Linear 5-FU control
	1:0	**1:1**	**2:1:1**	**2:1:1**	**1:1**	**1:1**
1	0.134 µg	3.88 µg	0.275 µg	0.275 µg	1.306 µg	1.089 µg
2	0.268 µg	7.77 µg	0.549 µg	0.549 µg	2.612 µg	2.178 µg
3	0.402 µg	11.7 µg	0.884 µg	0.884 µg	3.919 µg	3.267 µg
4	0.536 µg	15.5 µg	1.090 µg	1.090 µg	5.225 µg	4.356 µg

4.3.15 SRB cytotoxicity assay

This samples were set up as for the MTT assay (4.3.14, Table 4.1). Following the 48-hour incubation, 50 µl of TCA (50%) was gently layered onto the cells, taking care not to dislodge cells. After a 1 hour at 4˚C incubation, cells were washed (3x) with 18 MOhm water, to remove excess serum and fixative agent. Plates were then dried at 40˚C for 1 hour, followed by the addition of 100 µl of SRB dye (0.4% $^{w}/_{v}$ in 1% acetic acid) to each well. This was then incubated for 30 minutes at room temperature, in the dark. Excess dye was removed by washing (3x) with 1% acetic acid, and any protein bound dye was solubilized with 200 µl of 10 mM Tris base. Absorbance's were obtained using a Mindray MR-96A microplate reader at 565 nm using Tris base as the blank. Cell viability was calculated is in 4.3.14.

4.3.16 Mechanism of cell death - Apoptosis Assay

The dual acridine orange and ethidium bromide system (1:1 $^{v}/_{v}$ of a 100 mg.ml^{-1} in PBS stock) employed, is a rapid fluorescent technique for the detection of cell apoptosis *in vitro*. Cells were trypsinized and seeded into clear 24-well plates at a density of 1.2 x 10^5 cells per well, and incubated at 37˚C for 24 hours. Medium was thereafter replenished with 400 µl of fresh medium, 0.920 µg and 1.040 µg respective nanocomplexes (Au-PLL:5-FU encapsulated and linear) added. Positive controls containing cells only were used. Assay was done in triplicate. After a 48-hour incubation at 37˚C in 5% CO_2, cells were washed with 100 µl of cold PBS, followed by the addition of 15 µl of the dye solution to each well. Cells were viewed under an Olympus fluorescent microscope (200x magnification), fitted with a CC12 fluorescent camera (Olympus Co., Tokyo, Japan). The apoptotic indices were calculated using the following equation:
Apoptotic Index = Number of Apoptotic cells/ total number of cells counted.

4.3.17 Statistical analysis

All data is presented as mean ± standard deviation (± SD n=3). The Dunnetts post hoc test was used for the MTT and SRB assay. Statistical significance of the tests was set at **$p<0.01$ and *<0.05. Each of the experimental values were compared to their corresponding control. GraphPad Instat 3 software was used for statistical analysis.

4.4 Results and discussion

4.4.1 UV-vis studies

The UV-vis spectra of the AuNPs, and AuNP-PLL are depicted in Figure 4.1. Due to extreme aggregation of nanocomplexes containing 5-FU, these UV spectra could not be easily obtained. However further characterization studies viz. TEM and NTA were able to confirm the successful binding of 5-FU to AuNP-PLL. The AuNPs possess unique optical properties, making it possible to estimate the approximate size of the nanoparticles synthesized. Analysis revealed a single peak for AuNPs at 522 nm (Figure 4.1), and according to literature a peak in the 522- 525 nm range corresponds to the surface plasmon excitation of small, spherical gold nanoparticles which are monodispersed and well separated[28]. The AuNP absorbance value at 522 nm was 1.266, providing an indication of the amount of gold present in the colloidal solution. The AuNP-PLL nanocomplexes presented with a single peak at 526nm, indicating that the AuNPs were successfully conjugated to PLL, which was further confirmed using TEM (Figure 4.2 B).

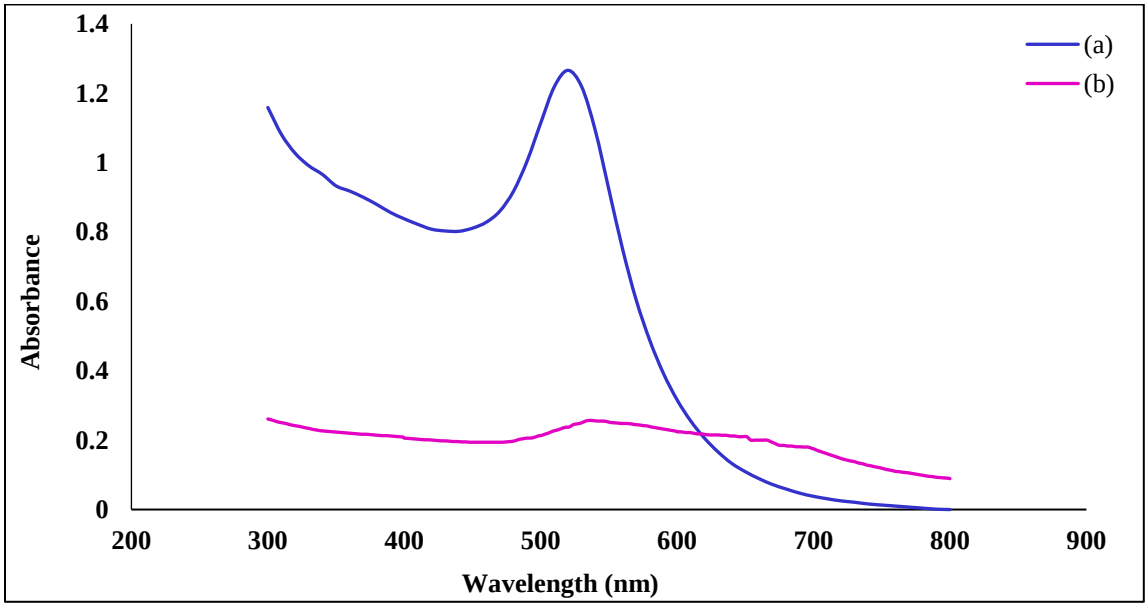

Figure. 4.1 UV-visible spectroscopy of (A) AuNP, and (B) AuNP-PLL.

4.4.2 TEM Imaging

The TEM analysis of the AuNPs and their nanocomplexes are shown in Figure 4.2A-D. Figure 4.2A clearly shows the AuNPs, as being uniform in shape, with good polydispersity, and very little aggregation of the nanoparticles. The AuNP-PLL (Figure 4.2B), can be observed possessing a AuNP core embedded in a matrix of PLL. One of the challenges of using PLL is its tendency to agglomerate. A high level of agglomeration suggests that due to the high loading capacity of the AuNPs, a single PLL molecule may be bound to more than one AuNP, contributing to an increase in agglomeration, a study reported the aggregation of poly-l-lysine which are cationic and the negatively charged nanoparticles. It was discovered that soon after the incorporation of poly-l-lysine with AuNP's, there was the formation of distinct, submicrometer spherical aggregates. Studies involving light scattering revealed that the particles increase in size with an increase in time indicating a dynamic flocculation process[29]. The results from TEM correlate well with this study. The level of agglomeration seen in Figure 4.2B, indicates that due to the increase in size, the nanoparticles may encounter difficulties with respect to cellular uptake, which may impact on the outcomes of the cell viability tests. From the two 5-FU containing nanocomplexes (Figure 4.2C-D), the encapsulation method appears to have produced nanocomplexes with a greater level of dispersion, than in the linear method, with these particles tending to aggregate more. This is possibly due to the binding of a 5-FU molecule to more than one nanoparticle, since linear binding results in the 5-FU molecules being exposed on the exterior of the nanocomplex. However, both methods produced particle of more or less the same size.

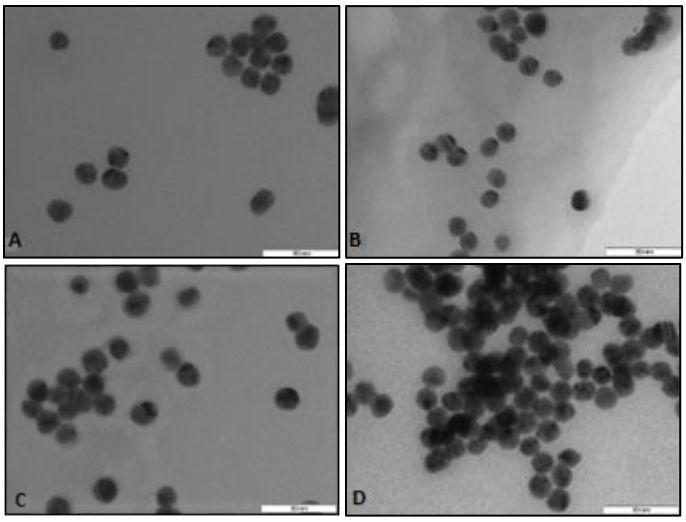

Figure. 4.2 TEM images of (A) Au nanoparticles, (B) AuNP-PLL, (C) Encapsulated AuNP-PLL:5-FU (D) Linear AuNP-PLL:5-FU. Bar = 100 nm.

4.4.3 Nanoparticle tracking analysis (NTA)

NTA provides an accurate assessment of the size distribution, zeta potential and colloidal stability of nanoparticles in solution. The respective nanoparticle and nanocomplex sizes and zeta potential values are shown in Table 4.2. These results indicate that the AuNPs had a mean diameter of 65.9± 9.8 nm, confirming successful synthesis of AuNPs under 100 nm. Zeta potential analysis provides an indication of the long-term stability of the colloidal suspension, a property that is extremely important *in vivo*. A high zeta potential value generally correlates to good colloidal stability. Essentially, zeta potential analysis is a measure of the electrostatic repulsive forces which are present between similarly charged particles in a suspension.

The AuNPs had a zeta potential value of -7.3 mV, which is a relatively low, however on addition of poly-l-lysine, an increase to + 37.2 mV was recorded. This shift from an overall negative zeta potential value to a positive value is an indication of strong ionic bonds formed between the surface of the AuNP and the polymer and correlates well with the results from UV-vis and TEM studies. Furthermore the data correlates with a study in which the concentration of cationic polymer was varied and respective analysis of the zeta potential was carried out, it revealed that as the concentration of polymer increased so did the zeta potential[30]. The polymer was incorporated onto the AuNP for two reasons viz. (1) to act as a stabilizing agent and, (2) to serve as a link between the AuNPs and the anionic drug 5-FU. The shift in zeta potential values also indicate that PLL was successful in stabilizing the nanoparticle, due to larger repulsive forces now existing between the nanoparticles.

The increase in size from 65.9 to 95.3 nm is a further confirmation of PLL successfully binding to the AuNP. Upon addition of encapsulated and linear bound 5-FU, the zeta potential value decreased from + 37.2 mV to + 9.7 mV and + 12.8 mV respectively, showing a correlation between binding efficiency and zeta potential. Size distribution analysis revealed that there was little difference in size, between the two types of nanocomplexes upon addition of 5-FU with sizes of nanocomposites being 101.5 nm and 104.6 nm respectively. This was also noted from the TEM images. There was a slight increase in size for the AuNP-PLL:5-FU nanocomplexes, due to the matrix of PLL- gold nanoparticle flocculation, making it difficult for the drug to be encapsulated efficiently, and limiting interaction with the nanoparticles.

A large zeta potential value is important; however it is not the sole determining factor for a delivery vector, with the ability of a nanocomplex to successfully release the anticancer drug under appropriate conditions is equally important. Hence, drug release studies were performed

Table 4.2. Size distribution and Zeta potential analysis of AuNP and its nanocomplexes.

Sample	Nanoparticle size (nm)	Zeta potential (mV)
AuNP	65.9 ± 9.8	-7.3 ± 1.6
AuNP-PLL	95.3 ± 12.2	+37.2 ± 1.7
AuNP-PLL:5-FU encapsulated	101.5 ± 1.5	+9.7 ± 1.3
AuNP-PLL:5-FU linear	104.6 ± 3.6	+12.8 ± 2.9

4.4.4 ICP-OES and FTIR analysis

The ICP analysis performed could confirm the concentration of the synthesized AuNP. The use of FTIR confirmed the presence of PLL and hence its successful conjugation to the AuNP. The complete FTIR spectrum is shown in Appendix B. The FTIR spectra displayed C-O stretching at ~ 1070 cm^{-1}, C-O-C stretching at ~ 1260 cm^{-1}, CH_2 bending at 1416 cm^{-1}, a peak of NH_3^+ at ~ 1568, C=O and N-H bending at ~ 1655 cm^{-1}. These results correspond well with the peak of pure PLL with minor differences as a result of the interaction with the gold nanoparticles[31].

4.4.5 Encapsulation/ binding efficiency

To determine the efficacy of the two binding methods of 5-FU, samples of the respective nanocomplexes were analyzed by UV-vis spectrometry, before and after dialysis (MWCO= 1000 Da), which was utilized to remove any unbound 5-FU from the nanocomplexes. The amount of free drug was calculated from absorption measurements, with the observed differences in absorptions providing an indication of the amount of drug incorporated into nanocomplex. The binding efficiency in the encapsulation method was calculated to be 61.43%, whilst the linear method provided a binding efficiency of 53.45%. Although, binding above 60% for the can be regarded as good, the PLL associated aggregation probably did affect its ability to efficiently bind the drug.

4.4.6 Drug release studies

Drug release analysis were performed spectrophotometrically, under pH conditions of 7.0 and 4.0, to determine the ability of the nanocomposites to protect and release the 5-FU. In addition to cancerous cells having a leaky cell wall structure, which aids in the entry of nanocomposites, they have been shown to have a lower pH when compared to normal tissue[32]. Many tumors tend to be hypoxic, resulting in a reduction of mitochondrial oxygen consumption and a decrease in the level of ATP production. A decrease in the levels of ATP influences the transport systems involved within cancerous cells. This results in the breakdown of the $NA^{+\,a}$ and K^{+} gradients, depolarization of membranes, an increase in the concentration of $Ca2^{+}$ and decreased cytosolic pH. These factors contribute towards the formation of acidosis in cancerous cells[33]. A study performed by***[34]*****,** states that at a pH around 4-5, 5-FU is released quickly and continuously. The drug 5-FU has been shown to have an absorbance peak between 266 - 271 nm [35]. It is more favorable in therapy for the drug to be delivered continuously, over a period of time rather than in a single dose[36]. At a pH of 7.0, the linearly bound nanocomplex released the drug progressively over time, compared to the encapsulated nanocomplex, which showed a slower, more restrained drug release profile.

If nanocomposites release the drug in high volumes under neutral pH, it may result in severe and unwanted side effects. At a pH of 4.0, a more controlled release was observed for the encapsulated nanocomplex, compared to the linearly bound nanocomplex. This provides an indication that the nanocomplex will be able to effectively release the drug under the acidic conditions in cancerous cells. The 5-FU encapsulated nanocomplexes was shown to be more effective in binding the drug in higher volumes and releasing the drug safely under the appropriate conditions. Both nanocomplexes (encapsulated and linear) released approximately, 22% and 41% of the drug respectively at a pH of 4.0.

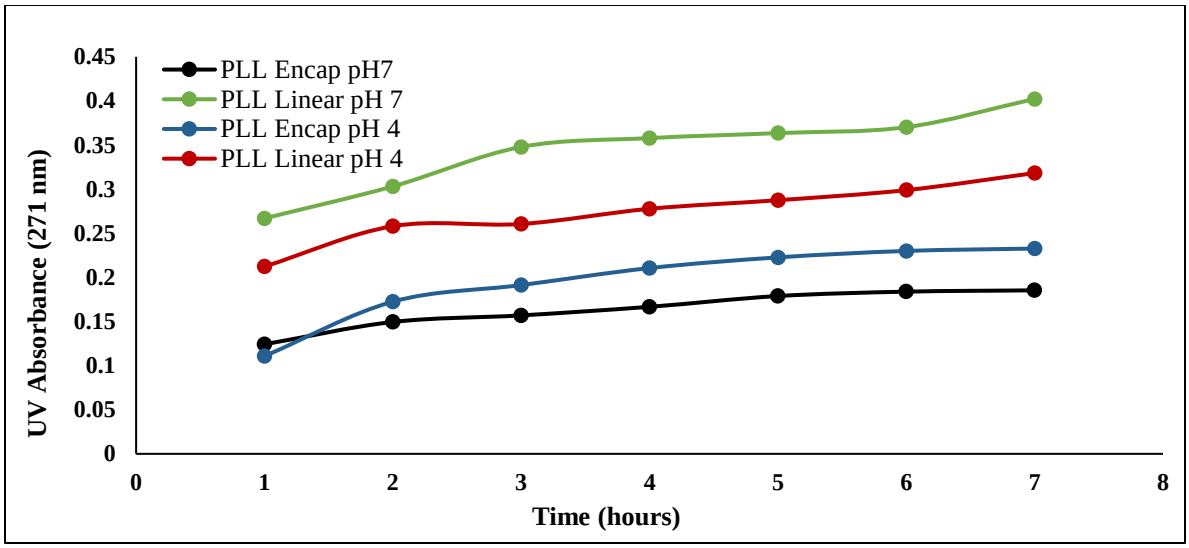

Figure. 4.3 Drug release profile of nanocomposites under pH 4.0 and 7.0

4.4.7 *In vitro* Cytotoxicity Studies

4.4.7.1 MTT Assay

To test the efficiency of the drug loaded nanocomposites in curbing the proliferation of cancerous cells, MTT assays were carried out on three cancer cell lines (HepG2, Caco-2 and MCF-7) and one control non-cancer cell line (HEK293). This assay is a rapid, quantitative, colorimetric assay for determination of the anticancer activity and cytotoxicity of compounds, and in this case nanocomplexes. The principle of the assay is that viable cells will have metabolically active mitochondria, where the cellular oxidoreductase enzymes under specified conditions will catalyze the reduction of the MTT tetrazolium salt into an intensely colored, insoluble formazan product. Gold nanoparticles have been investigated as drug delivery vectors, due to their relative non-toxicity due to the presence of a chemically inert core[37].

Besides positive cell controls the use of PLL:5-FU controls without AuNPs were evaluated. The cytotoxicity profiles of the nanoparticles and nanocomposites are depicted in Figures 4.4 - 4.7. The AuNPs in particular did not show cytotoxicity as expected, and the cell viability increased with increasing AuNP concentration. Numerous studies including Shukla *et al*[20]., Yen *et al*[38, 39]., At the highest ratio, cell viability was actually greater than 100%, which could be indicate that the AuNPs had some growth promoting effect on the cells. However, according to Jaszczyszyn and Gasiorowski, 2008, the penetrated dye in some cell lines are also reduced by non-mitochondrial,

cytosolic or microsomal enzymes. The AuNPs could also have interfered with the enzyme activity leading to an increased absorbance, indicating increased cell survival. Interaction of tested compounds with the MTT is also possible resulting in increased formazan production and higher absorbances[40, 41]. The AuNP-PLL nanocomplex also displayed low cytotoxicity. Therefore, any observed cytotoxicity of the drug containing nanocomplexes would not be due to the presence of the AuNPs or AuNP-PLL.

The cytotoxicity of the AuNP-PLL:5-FU nanocomplex (encapsulated and linearly bound) (Figures 4.4 – 4.7) is dose dependent, with encapsulated PLL-nanocomplexes inducing greater cell death (>70% in HepG2 and HEK293 cells), compared linear bound nanocomposites. This is contrary to reports that PLL-nanocomposites due to aggregation would have greater difficulty entering the cell. The encapsulated nanocomplexes showed far greater anticancer activity across all three of the cancerous cell lines, indicating that the encapsulation method is better for 5-FU delivery, this has been demonstrated in previous studied and correlates well with the data[42, 43]. However, the nanocomplexes prepared by the linear method also showed significant activity, illustrating that both methods are potent enough for anticancer therapy. This data combined illustrates that while AuNP and AuNP-PLL were not cytotoxic to cells, upon the addition of 5-FU they become efficient drug delivery vectors, these results correlate well with [44]. The PLL-5FU controls also showed limited cytotoxicity towards the cancer cells, reinforcing the notion that the combination of AuNP and PLL, significantly improved the anticancer activity of 5-FU.

The encapsulated nanocomplexes did exhibit much cytotoxicity towards the HEK293 cell line (Figure 4.5), with a decrease in cell viability from ratios 1 – 4 noted. This can be observed as a common trend across all four cell lines, with varying degrees of cytotoxicity attained. The encapsulated PLL-AuNP:5-FU nanocomplex displayed the best anticancer activity in the HepG2 cell line resulting in >70% cell death at the highest ratio. The differences in cytotoxicity levels observed can be attributed to the fact that the encapsulated nanoparticles offer a greater degree of protection for the drug, compared to the linear nanocomplexes. Hence, the drug once delivered to the cancer cells, is released under acidic conditions as evidenced by the drug release studies, thereby improving the efficacy of the drug, with greater anticancer activity at a much lower dose.

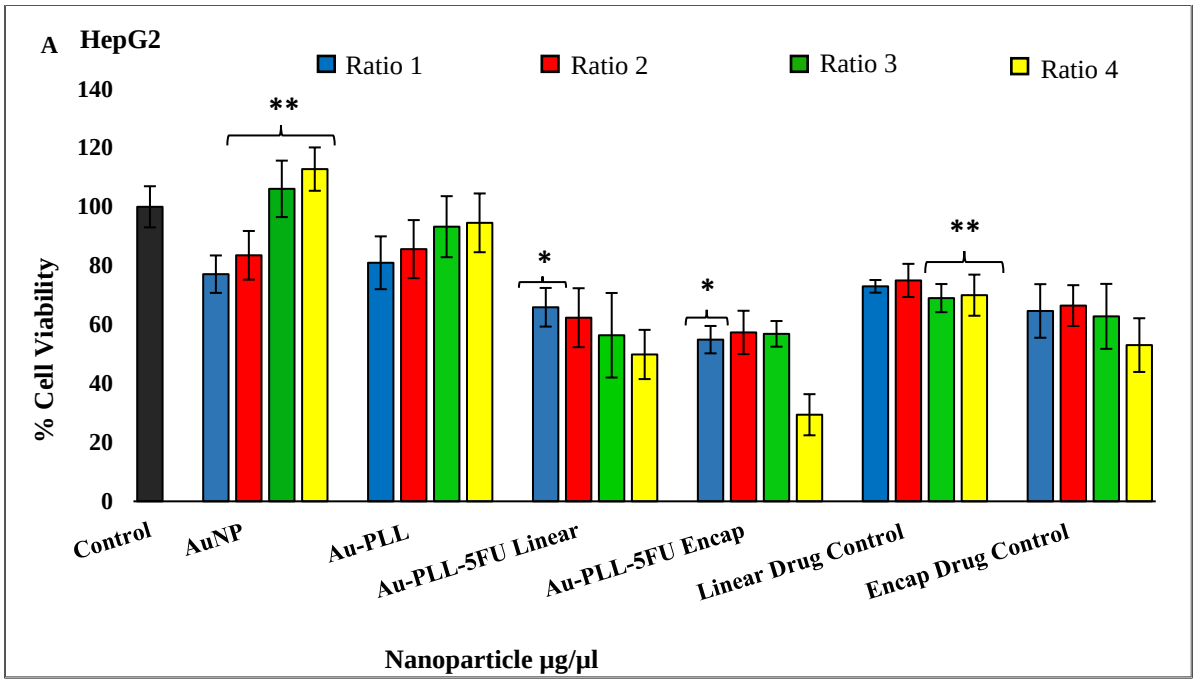

Figure 4.4 MTT Cytotoxicity assay of nanoparticles and nanocomposites in the HepG2 cell line. Data represented as means ± SD (n=3), * p<0.05, **p<0.01 were considered statistically significant, Ratios as laid out in Table 4.1.

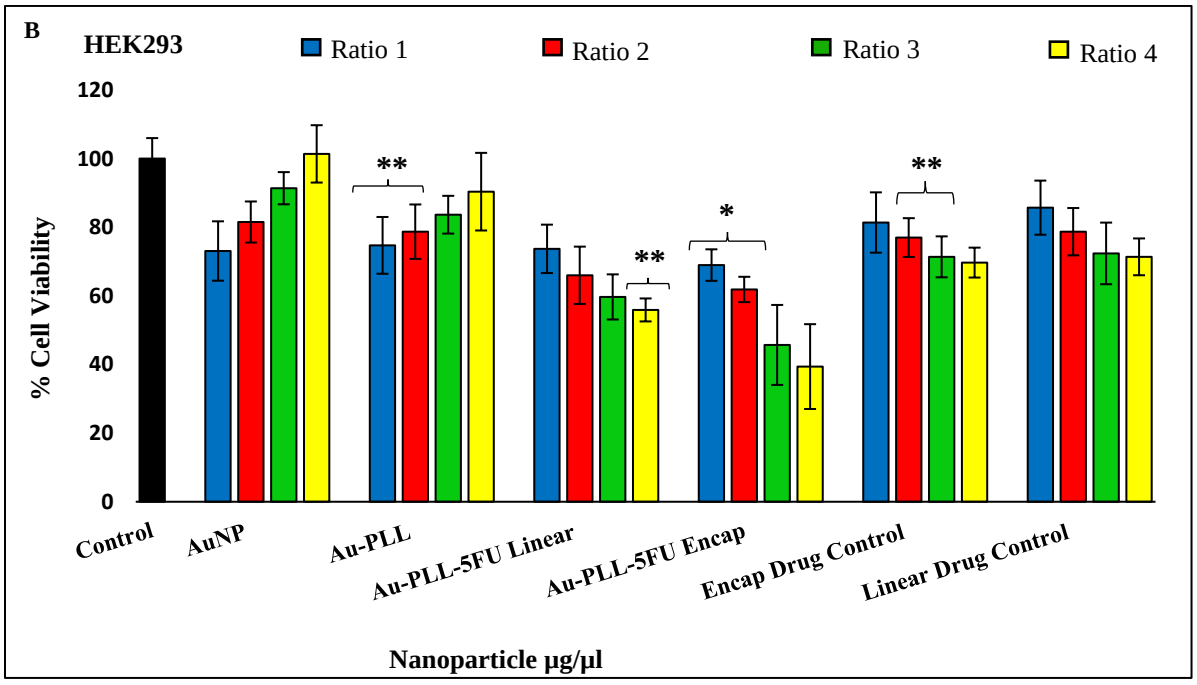

Figure 4.5 MTT Cytotoxicity assay of nanoparticles and nanocomplexes in the HEK293 cell line Data represented as means ± SD (n=3), * p<0.05, **p<0.01 were considered statistically significant, Ratios as laid out in Table 4.1.

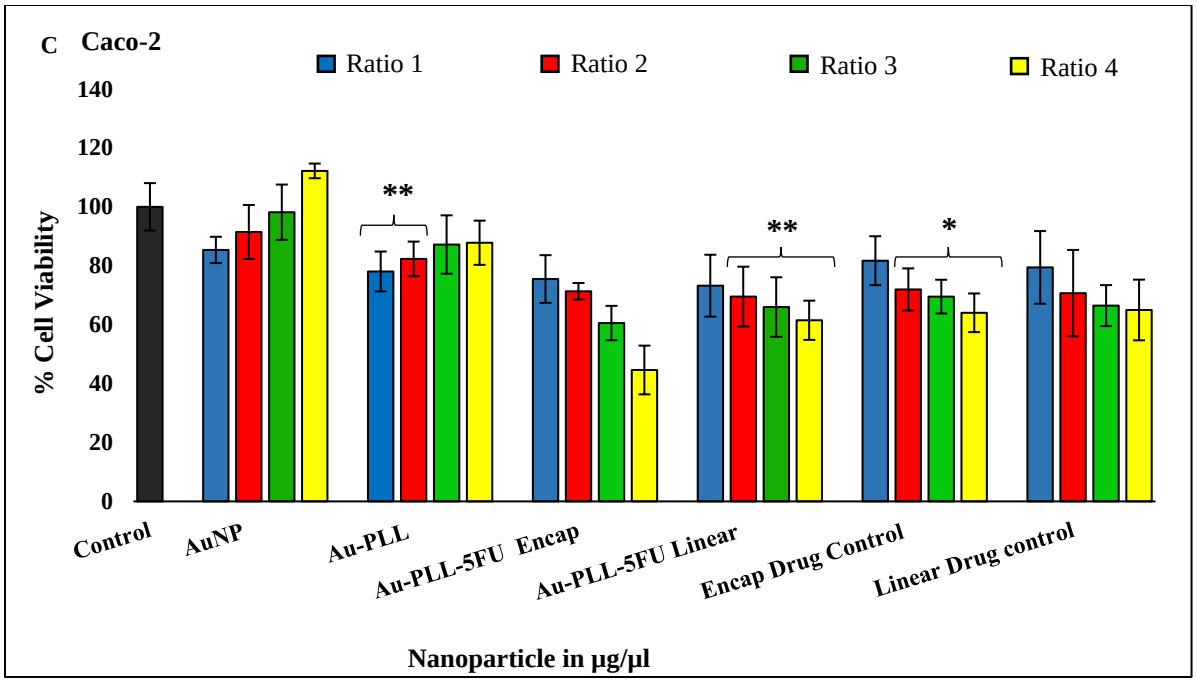

Figure 4.6 MTT Cytotoxicity assay of nanoparticles and nanocomplexes in the Caco-2 cell line Data represented as means ± SD (n=3), * p<0.05, **p<0.01 were considered statistically significant, Ratios as laid out in Table 4.1.

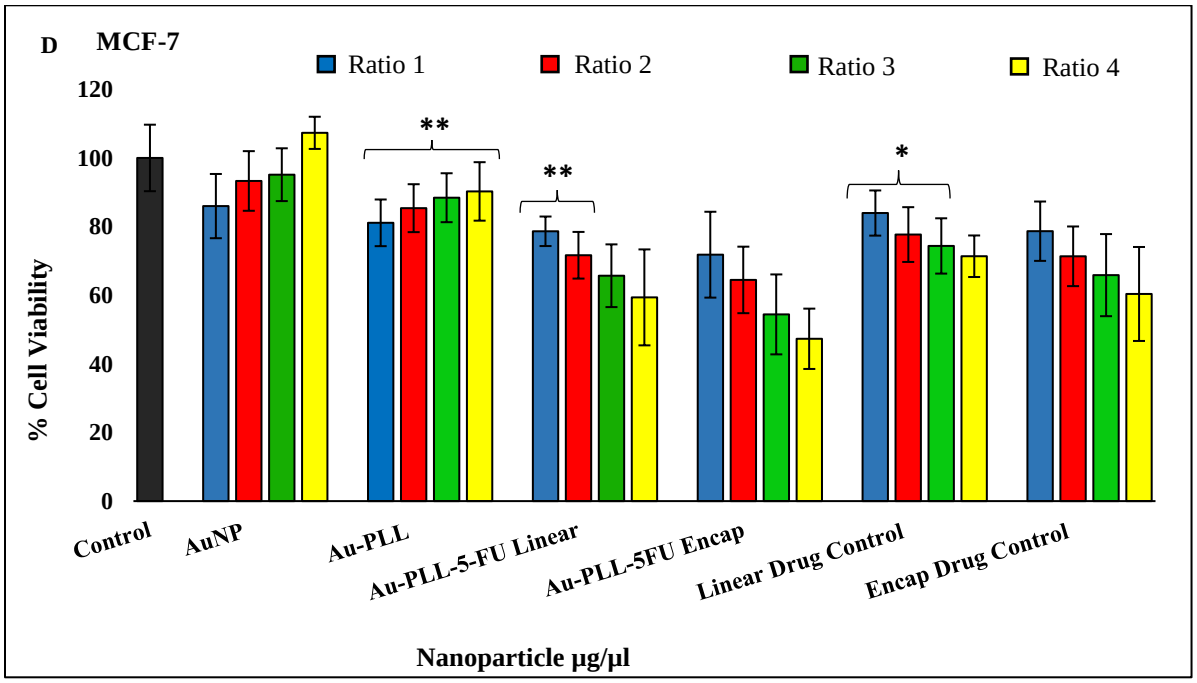

Figure 4.7 MTT Cytotoxicity assay of nanoparticles and nanocomplexes in the MCF-7 cell line Data represented as means ± SD (n=3), * p<0.05, **p<0.01 were considered statistically significant, Ratios as laid out in Table 4.1.

4.4.7.2 Sulforodhamine B (SRB) Assay

The SRB cytotoxicity assay was carried out with the same samples to assess whether there was any significant correlation with the results obtained from the MTT assay. This is because the SRB assay provides a more sensitive measure of drug induced cytotoxicity[45]. This is a quantitative assay, in which cellular proteins are stained by the SRB dye electrostatically binding to the basic amino acid residues present in proteins.

From Figures 4.8-4.11, it can be noted that a similar trend exists as for the MTT assay, with AuNP and AuNP-PLL complexes not exhibiting much cytotoxicity in all cell lines, and upon increasing nanoparticle concentration, there was a concomitant increase in cell viability. Overall, greater cell viability was observed with the SRB assay, compared to the MTT assay, and any observed cytotoxicity attributed to the presence of the anticancer agent 5-FU.

The respective nanocomplexes containing 5-FU exhibited the typical dose dependent activity, resulting in a decrease in cell viability across all three cell lines, with increase concentration. The encapsulated nanocomplexes displayed a greater level of cytotoxicity, compared to their linear counterparts. This closely correlates with the results from the MTT assay. Both the encapsulated and linear nanocomplexes were able to efficiently deliver the 5-FU and bring about a decrease in cell viability, with the latter to a lesser extent. The encapsulated nanocomplex was most effective in the HepG2 cell line, indicating some cell specificity. These results confirm that the inclusion of AuNPs in a drug delivery system, can be beneficial, as in this case it resulted in an increase in cytotoxicity.

Both AuNP or AuNP-PLL were here again well tolerated by the HEK293 cells producing little or no cytotoxicity. Overall, both the MTT and SRB assays showed good correlation, and firmly suggest that the AuNP-PLL:5-FU nanocomplexes are effective in the delivery of the anticancer drug 5-FU.

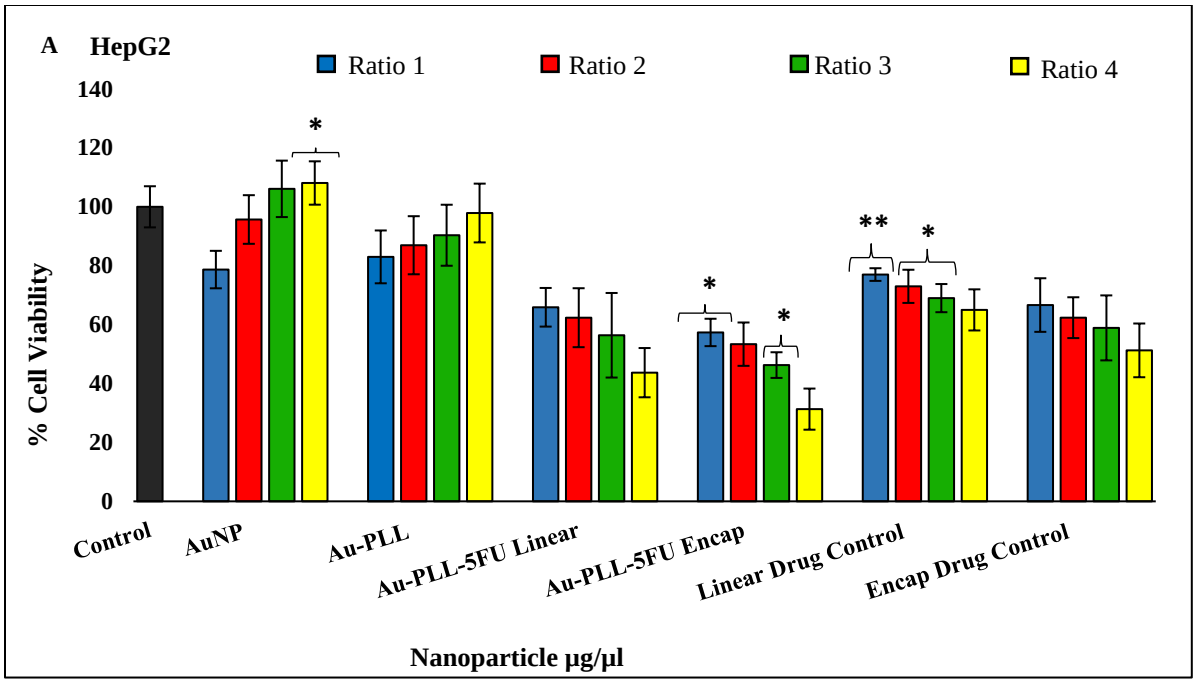

Figure 4.8 SRB cytotoxicity assay of nanoparticles and nanocomplexes in the HepG2 cell line Data represented as means ± SD (n=3), * $p<0.05$, **$p<0.01$ were considered statistically significant, Ratios as laid out in Table 4.1.

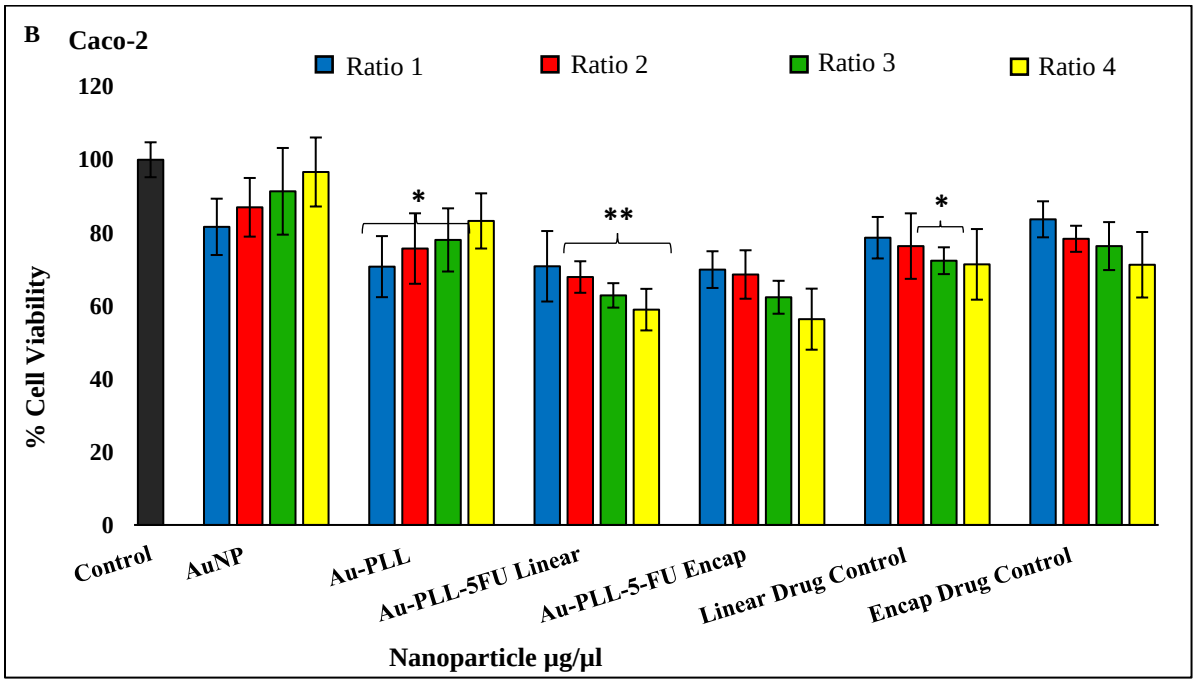

Figure 4.9 SRB cytotoxicity assay of nanoparticles and nanocomplexes in the Caco-2 cell line Data represented as means ± SD (n=3), * $p<0.05$, **$p<0.01$ were considered statistically significant, Ratios as laid out in Table 4.1.

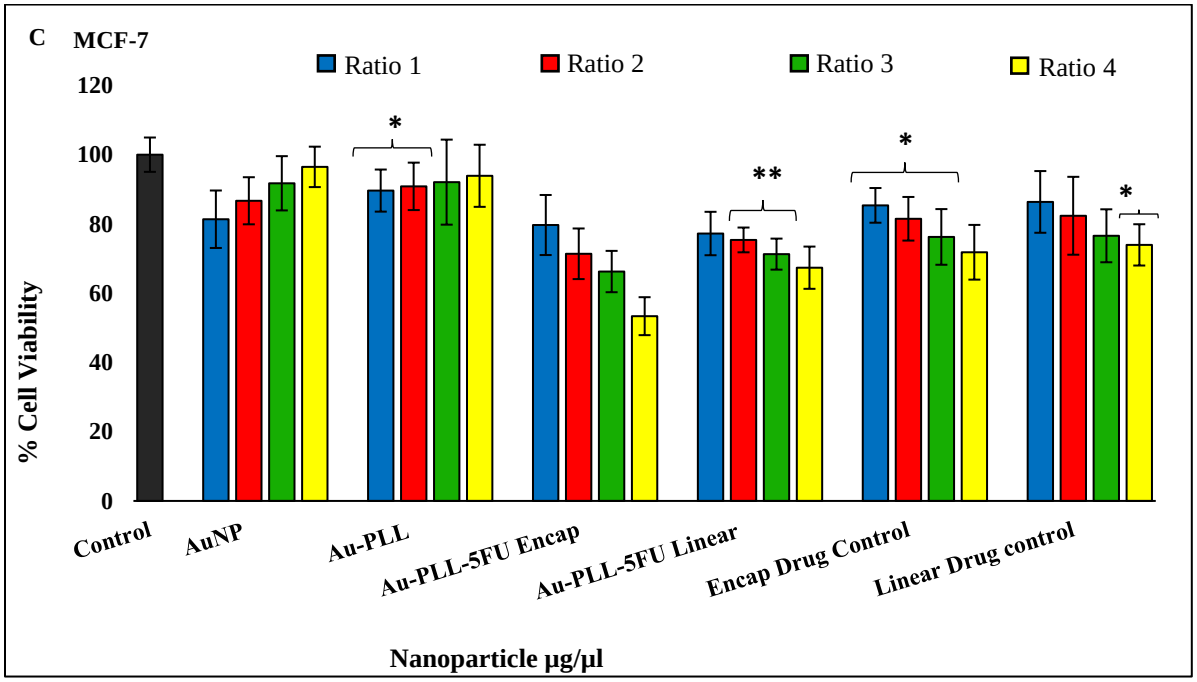

Figure 4.10 SRB cytotoxicity assay of nanoparticles and nanocomplexes in the MCF-7 cell line Data represented as means ± SD (n=3), * p<0.05, **p<0.01 were considered statistically significant, Ratios as laid out in Table 4.1.

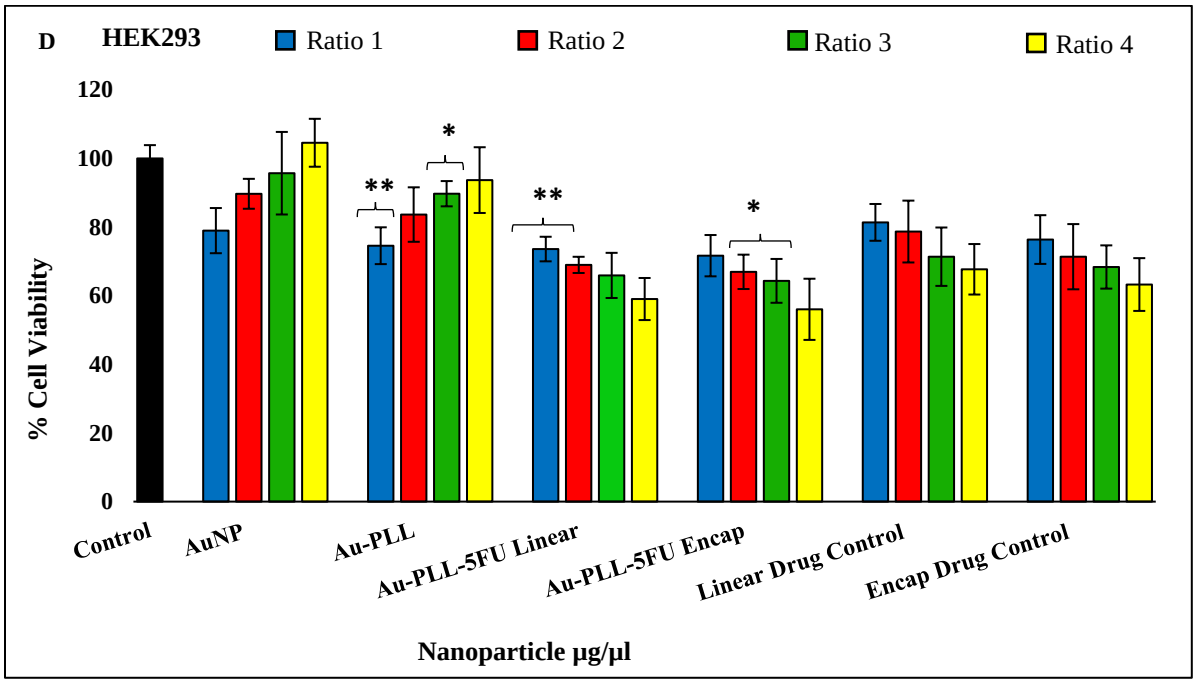

Figure 4.11 SRB cytotoxicity assay of nanoparticles and nanocomplexes in the HEK293 cell line Data represented as means ± SD (n=3), * p<0.05, **p<0.01 were considered statistically significant, Ratios as laid out in Table 4.1.

4.8 Mechanism of cell death – Apoptosis studies

Apoptosis is a programmed cell death and eliminates cells during normal development, and prevents the over-proliferation of cells as in the case of cancer. To further correlate observed cytotoxicity with the respective nanocomplexes, the mechanism of cell death using an apoptosis assay was performed. Some apoptotic features were visible in the cell lines, indicating these nanocomplexes were able to induce apoptosis in the specific cell lines. The calculated apoptotic indices are outlined in Table 4.3. Encapsulated nanocomplexes showed higher levels of apoptotic induction in the cancer cell lines, as inferred from the higher apoptotic index. This correlates well with the data from the MTT and SRB assays. Studies have indicated that 5-Fluorouracil induces apoptosis[46-49], this correlates well with our results, also indicating that the drug was delivered into the cell.

The two dyes used in the assay stain cells from green to red depending on the viability of the cell. Acridine orange stains live and dead cells, while ethidium bromide, stains cells with permeable membranes that allow it to enter and stain the DNA. Hence due to a combination of the two dyes, live cells stain green (L), early apoptotic cells (EA) stain a brighter green, late apoptotic cells (LA) appear orange with condensed chromatin. and necrotic cells (N) also stain orange but have no condensed chromatin.

Table 4.3. Apoptotic indices for the nanocomposites in HEK293, HepG2, Caco-2 and MCF-7 cell lines

Cell Lines	Apoptotic index	
	Au-PLL:5-FU Encapsulated	**Au-PLL:5-FU Linear**
HEK293	0.0625	0.0551
HepG2	0.14	0.132
Caco-2	0.18	0.15
MCF-7	0.17	0.17

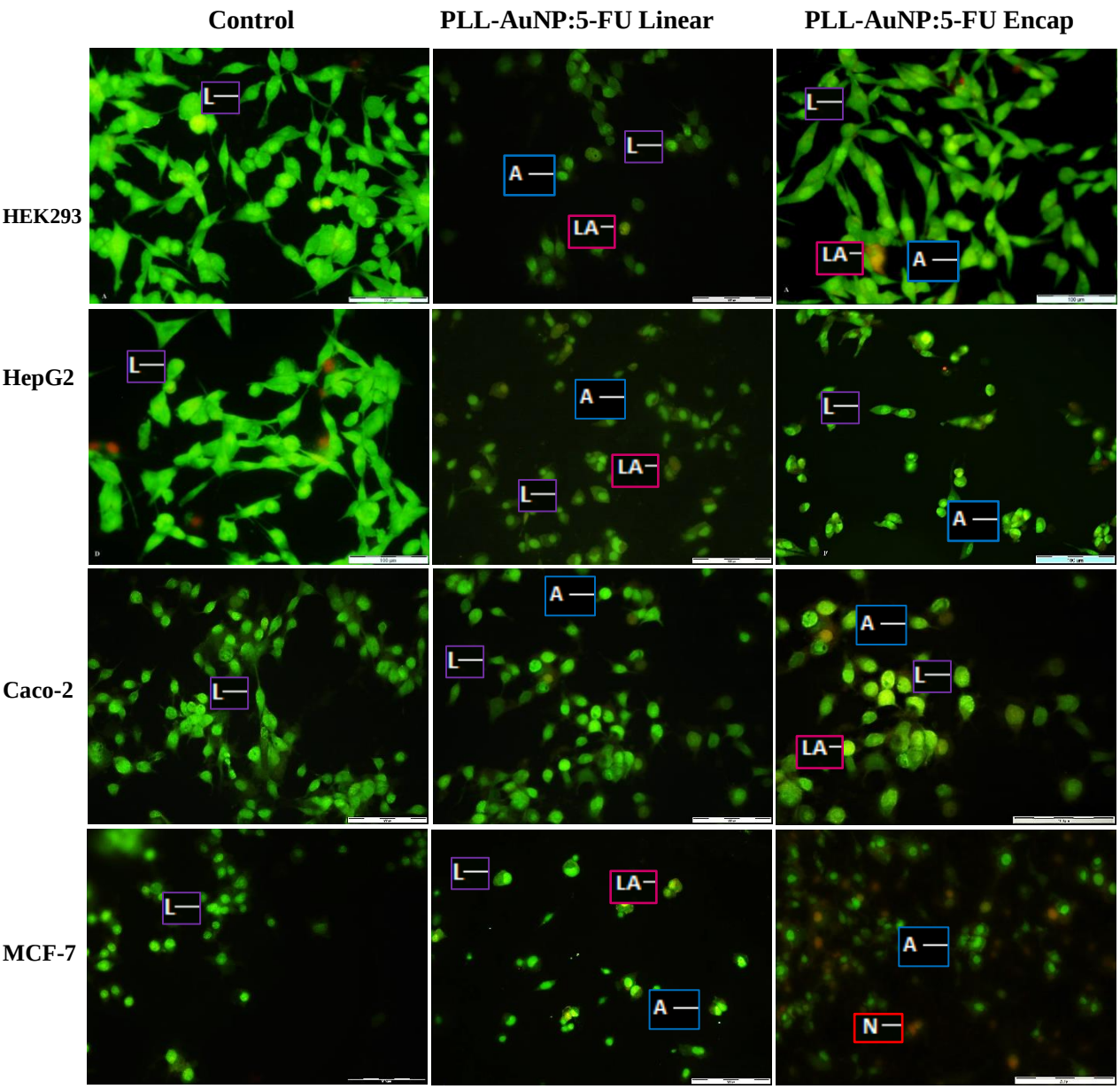

Figure 4.12: Fluorescent images obtained from the dual acridine orange /ethidium bromide apoptosis studies in the HEK293, HepG2, Caco-2 and MCF-7 cell lines at 20x magnification. (L= live cells; A= apoptotic cells; N=necrotic cells; LA= late apoptotic cells)

4.9 Conclusion

Successful AuNP synthesis, functionalization with PLL and binding of 5-FU was achieved and confirmed. From the two 5-FU binding methods, encapsulation of 5-FU in PLL produced higher binding efficiencies (61.43%), and a more sustained drug release profile. The cytotoxicity assays conducted further confirmed the above findings, with cell selectivity and a dose dependent activity observed. Furthermore, the addition of gold into the delivery system significantly enhanced the anticancer activity of the drug especially in the cancer cell lines tested. Overall, this AuNP based drug delivery system has shown immense promise, which augurs well for future *in vivo* studies. However, further optimizations and more cell lines need to be tested to determine the overall pharmacokinetic profile of the system.

4.10 References

[1] Grodzinski, P., Silver, M., and Molnar, L. K. (2014) Nanotechnology for cancer diagnostics: promises and challenges, *Expert review of molecular diagnostics*.

[2] Farrell, D., Ptak, K., Panaro, N. J., and Grodzinski, P. (2011) Nanotechnology-Based Cancer Therapeutics—Promise and Challenge—Lessons Learned Through the NCI Alliance for Nanotechnology in Cancer, *Pharmaceutical Research 28*, 273-278.

[3] Ahmad, M. Z., Akhter, S., Rahman, Z., Akhter, S., Anwar, M., Mallik, N., and Ahmad, F. J. (2013) Nanometric gold in cancer nanotechnology: current status and future prospect, *Journal of Pharmacy and Pharmacology 65*, 634-651.

[4] Anitha, A., Sreeranganathan, M., Chennazhi, K. P., Lakshmanan, V.-K., and Jayakumar, R. (2014) In vitro combinatorial anticancer effects of 5-fluorouracil and curcumin loaded N, O-carboxymethyl chitosan nanoparticles toward colon cancer and in vivo pharmacokinetic studies, *European Journal of Pharmaceutics and Biopharmaceutics 88*, 238-251.

[5] Ortiz, R., Cabeza, L., Arias, J. L., Melguizo, C., Álvarez, P. J., Vélez, C., Clares, B., Áranega, A., and Prados, J. (2015) Poly (butylcyanoacrylate) and Poly (ε-caprolactone) Nanoparticles Loaded with 5-Fluorouracil Increase the Cytotoxic Effect of the Drug in Experimental Colon Cancer, *The AAPS journal 17*, 918-929.

[6] Wang, A. Z., Langer, R., and Farokhzad, O. C. (2012) Nanoparticle delivery of cancer drugs, *Annual review of medicine 63*, 185-198.

[7] Patel, N. R., Pattni, B. S., Abouzeid, A. H., and Torchilin, V. P. (2013) Nanopreparations to overcome multidrug resistance in cancer, *Advanced drug delivery reviews 65*, 1748-1762.

[8] Zhang, Y., Li, J., Lang, M., Tang, X., Li, L., and Shen, X. (2011) Folate-functionalized nanoparticles for controlled 5-fluorouracil delivery, *Journal of colloid and interface science 354*, 202-209.

[9] Biju, V. (2014) Chemical modifications and bioconjugate reactions of nanomaterials for sensing, imaging, drug delivery and therapy, *Chemical Society Reviews 43*, 744-764.

[10] Zhang, L., Gu, F., Chan, J., Wang, A., Langer, R., and Farokhzad, O. (2008) Nanoparticles in medicine: therapeutic applications and developments, *Clinical pharmacology and therapeutics 83*, 761-769.

[11] Allen, T. M., and Cullis, P. R. (2013) Liposomal drug delivery systems: from concept to clinical applications, *Advanced drug delivery reviews 65*, 36-48.

[12] Liu, Y., Ji, M., Wong, M. K., Joo, K.-I., and Wang, P. (2013) Enhanced therapeutic efficacy of iRGD-conjugated crosslinked multilayer liposomes for drug delivery, *BioMed research international 2013*.
[13] Mody, N., Tekade, R. K., Mehra, N. K., Chopdey, P., and Jain, N. K. (2014) Dendrimer, liposomes, carbon nanotubes and PLGA nanoparticles: one platform assessment of drug delivery potential, *Aaps Pharmscitech 15*, 388-399.
[14] Caminade, A.-M., and Turrin, C.-O. (2014) Dendrimers for drug delivery, *Journal of Materials Chemistry B 2*, 4055-4066.
[15] Saji, V. S., Kumeria, T., Gulati, K., Prideaux, M., Rahman, S., Alsawat, M., Santos, A., Atkins, G. J., and Losic, D. (2015) Localized drug delivery of selenium (Se) using nanoporous anodic aluminium oxide for bone implants, *Journal of Materials Chemistry B 3*, 7090-7098.
[16] Cheng, J., Gu, Y.-J., Cheng, S. H., and Wong, W.-T. (2013) Surface functionalized gold nanoparticles for drug delivery, *Journal of biomedical nanotechnology 9*, 1362-1369.
[17] Lokina, S., Stephen, A., Kaviyarasan, V., Arulvasu, C., and Narayanan, V. (2014) Cytotoxicity and antimicrobial activities of green synthesized silver nanoparticles, *European journal of medicinal chemistry 76*, 256-263.
[18] Song, Y., Feng, D., Shi, W., Li, X., and Ma, H. (2013) Parallel comparative studies on the toxic effects of unmodified CdTe quantum dots, gold nanoparticles, and carbon nanodots on live cells as well as green gram sprouts, *Talanta 116*, 237-244.
[19] Fan, Y.-L., Fan, B.-Y., Li, Q., Di, H.-X., Meng, X.-Y., and Ling, N. (2013) Preparation of 5-fluorouracil-loaded nanoparticles and study of interaction with gastric cancer cells, *Asian Pacific journal of cancer prevention: APJCP 15*, 7611-7615.
[20] Shukla, R., Bansal, V., Chaudhary, M., Basu, A., Bhonde, R. R., and Sastry, M. (2005) Biocompatibility of gold nanoparticles and their endocytotic fate inside the cellular compartment: a microscopic overview, *Langmuir 21*, 10644-10654.
[21] Chithrani, B. D., Ghazani, A. A., and Chan, W. C. (2006) Determining the size and shape dependence of gold nanoparticle uptake into mammalian cells, *Nano letters 6*, 662-668.
[22] Jing, L., Liang, X., Deng, Z., Feng, S., Li, X., Huang, M., Li, C., and Dai, Z. (2014) Prussian blue coated gold nanoparticles for simultaneous photoacoustic/CT bimodal imaging and photothermal ablation of cancer, *Biomaterials 35*, 5814-5821.
[23] Silva, A. T., Coelho, A. G., Lopes, L. C. d. S., Martins, M. V., Crespilho, F. N., Merkoçi, A., and Silva, W. C. d. (2013) Nano-assembled supramolecular films from chitosan-stabilized gold nanoparticles and Cobalt (II) phthalocyanine, *Journal of the Brazilian Chemical Society 24*, 1237-1245.
[24] Bernkop-Schnürch, A., and Dünnhaupt, S. (2012) Chitosan-based drug delivery systems, *European Journal of Pharmaceutics and Biopharmaceutics 81*, 463-469.
[25] Chuah, L. H., Roberts, C. J., Billa, N., Abdullah, S., and Rosli, R. (2014) Cellular uptake and anticancer effects of mucoadhesive curcumin-containing chitosan nanoparticles, *Colloids and Surfaces B: Biointerfaces 116*, 228-236.
[26] Llorca, F. C., Esquerdo, G. G., Cervera, G. J., Briceño, G. H., Calduch, B. J., and Del Pino, C. J. (2005) [5-Fluorouracil-induced small bowel toxicity in a patient with colorectal cancer], *Clinical & translational oncology: official publication of the Federation of Spanish Oncology Societies and of the National Cancer Institute of Mexico 7*, 356-357.
[27] Arias, J. L. (2008) Novel strategies to improve the anticancer action of 5-fluorouracil by using drug delivery systems, *Molecules 13*, 2340-2369.
[28] Shalkevich, N., Shalkevich, A., Si-Ahmed, L., and Bürgi, T. (2009) Reversible formation of gold nanoparticle–surfactant composite assemblies for the preparation of concentrated colloidal solutions, *Physical Chemistry Chemical Physics 11*, 10175-10179.
[29] Murthy, V. S., Cha, J. N., Stucky, G. D., and Wong, M. S. (2004) Charge-driven flocculation of poly (L-lysine) gold nanoparticle assemblies leading to hollow microspheres, *Journal of the American Chemical Society 126*, 5292-5299.

[30] Bhumkar, D. R., Joshi, H. M., Sastry, M., and Pokharkar, V. B. (2007) Chitosan Reduced Gold Nanoparticles as Novel Carriers for Transmucosal Delivery of Insulin, *Pharmaceutical Research 24*, 1415-1426.
[31] Jackson, M., Haris, P. I., and Chapman, D. (1989) Conformational transitions in poly(l-lysine): studies using Fourier transform infrared spectroscopy, *Biochimica et Biophysica Acta (BBA) - Protein Structure and Molecular Enzymology 998*, 75-79.
[32] Kato, Y., Ozawa, S., Miyamoto, C., Maehata, Y., Suzuki, A., Maeda, T., and Baba, Y. (2013) Acidic extracellular microenvironment and cancer, *Cancer cell international 13*, 1.
[33] Lang, F. (2007) Mechanisms and significance of cell volume regulation, *Journal of the American College of Nutrition 26*, 613S-623S.
[34] Chandran, P. R., and Sandhyarani, N. (2014) An electric field responsive drug delivery system based on chitosan–gold nanocomposites for site specific and controlled delivery of 5-fluorouracil, *RSC Advances 4*, 44922-44929.
[35] Lin, F.-H., Lee, Y.-H., Jian, C.-H., Wong, J.-M., Shieh, M.-J., and Wang, C.-Y. (2002) A study of purified montmorillonite intercalated with 5-fluorouracil as drug carrier, *Biomaterials 23*, 1981-1987.
[36] Freiberg, S., and Zhu, X. (2004) Polymer microspheres for controlled drug release, *International journal of pharmaceutics 282*, 1-18.
[37] Jain, S., Hirst, D., and O'sullivan, J. (2014) Gold nanoparticles as novel agents for cancer therapy, *The British journal of radiology*.
[38] Yen, H. J., Hsu, S. h., and Tsai, C. L. (2009) Cytotoxicity and immunological response of gold and silver nanoparticles of different sizes, *Small 5*, 1553-1561.
[39] Han, G., Ghosh, P., and Rotello, V. M. (2007) Functionalized gold nanoparticles for drug delivery.
[40] Jaszczyszyn, A., and Gasiorowski, K. (2008) Limitations of the MTT assay in cell viability testing, *Adv. Clin. Exp. Med 17*, 525-529.
[41] Ulukaya, E., Ozdikicioglu, F., Oral, A. Y., and Demirci, M. (2008) The MTT assay yields a relatively lower result of growth inhibition than the ATP assay depending on the chemotherapeutic drugs tested, *Toxicology in vitro 22*, 232-239.
[42] Tiwari, P. M., Vig, K., Dennis, V. A., and Singh, S. R. (2011) Functionalized gold nanoparticles and their biomedical applications, *Nanomaterials 1*, 31-63.
[43] Hu, C.-M. J., Aryal, S., and Zhang, L. (2010) Nanoparticle-assisted combination therapies for effective cancer treatment, *Therapeutic delivery 1*, 323-334.
[44] Brown, S. D., Nativo, P., Smith, J.-A., Stirling, D., Edwards, P. R., Venugopal, B., Flint, D. J., Plumb, J. A., Graham, D., and Wheate, N. J. (2010) Gold nanoparticles for the improved anticancer drug delivery of the active component of oxaliplatin, *Journal of the American Chemical Society 132*, 4678-4684.
[45] Skehan, P., Storeng, R., Scudiero, D., Monks, A., McMahon, J., Vistica, D., Warren, J. T., Bokesch, H., Kenney, S., and Boyd, M. R. (1990) New colorimetric cytotoxicity assay for anticancer-drug screening, *Journal of the National Cancer Institute 82*, 1107-1112.
[46] Eichhorst, S. T., Müerköster, S., Weigand, M. A., and Krammer, P. H. (2001) The chemotherapeutic drug 5-fluorouracil induces apoptosis in mouse thymocytes in vivo via activation of the CD95 (APO-1/Fas) system, *Cancer research 61*, 243-248.
[47] Kondo, M., Nagano, H., Wada, H., Damdinsuren, B., Yamamoto, H., Hiraoka, N., Eguchi, H., Miyamoto, A., Yamamoto, T., and Ota, H. (2005) Combination of IFN-α and 5-fluorouracil induces apoptosis through IFN-α/β receptor in human hepatocellular carcinoma cells, *Clinical cancer research 11*, 1277-1286.
[48] Nita, M. E., Nagawa, H., Tominaga, O., Tsuno, N., Fujii, S., Sasaki, S., Fu, C., Takenoue, T., Tsuruo, T., and Muto, T. (1998) 5-Fluorouracil induces apoptosis in human colon cancer cell lines with modulation of Bcl-2 family proteins, *British journal of cancer 78*, 986.

[49] Hwang, J.-T., Ha, J., and Park, O. J. (2005) Combination of 5-fluorouracil and genistein induces apoptosis synergistically in chemo-resistant cancer cells through the modulation of AMPK and COX-2 signaling pathways, *Biochemical and biophysical research communications 332*, 433-440.

Chapter 5

Conclusion and future work

Chapter Five

5.1 Conclusion

The emergence of new drug delivery systems has increased over the past three decades and show promise to continue on this trajectory, due to advances in nanotechnology and the development of new material. The application of nanomaterial in therapeutics and nanomedicine requires further research if they are going to be effective in *in vivo* applications. Gold nanoparticles (AuNPs) have the potential to form a skeleton around which an efficient and safe drug delivery system can be designed. Other systems such as liposomes have shown promise *in vitro*, however have fallen short in many clinical trials. It is hoped that due to their low toxicity, high loading capacity, ease of synthesis and functionalization, AuNPs could prove to be more efficient *in vivo*. The results obtained in this study provides an insight into the potential of these nanoparticles for future *in vivo* and *in vitro* applications, highlighting the areas in the study that can be further researched.

In this study, spherical, colloidally stable AuNPs of small size (<100 nm) were successfully synthesized. Functionalization of AuNPs with cationic polymers of chitosan and PLL respectively, were achieved, with both showing greater stability, efficient binding (encapsulation and linear) of the anticancer drug, 5-FU, controlled drug release, and favorable cellular uptake probable due to the positive charges imparted by the polymers reacting with the negatively charged cell surface. This study has successfully demonstrated that these functionalized AuNPs can be used to successfully deliver anticancer drugs to different cell lines. In addition, the AuNPs were seemingly non-toxic to any of the human cell lines studied.

Both the AuNP-CS:5-FU and AuNP-PLL:5-FU nanocomplexes, were able to elicit significant cytotoxicity *in vitro*, in both a cell specific and a dose dependent manner. Although, the drug encapsulation method performed slightly better than the linear binding method for both polymers, both methods produced noteworthy results which can be built upon. Overall, AuNP-CS:5-FU nanocomplexes were shown to be more effective as drug delivery carriers, compared to their PLL counterparts. Furthermore, it is apparent that the addition of AuNP to the delivery system resulted in an increase in anticancer activity, as evidenced from the cytotoxicity studies.

The results strongly suggest that these nanocomplexes possess the potential to become efficient drug delivery systems, and to one day be used in drug delivery in clinical trials, for the treatment

of diseases such as cancer, as well as improving the delivery of other drugs and biomolecules across the blood brain barrier to aid in conditions such as depression, anxiety and other mental conditions.

Further research and optimizations to make the nanocomplexes more efficient are warranted. Future work could involve the designing of a targeted delivery system capable of delivering multiple drugs efficiently, with controlled release profiles. A dual treatment system, using a combination of drug delivery and photo thermal ablation therapy is also very appealing, and should be considered. The attachment of polymers such as poly-ethyleneglycol for steric stabilization of the nanoparticle, which shields and protects it, allowing for its prolonged circulation time *in vivo*, should be attempted. Lastly, the mechanism involved in cellular uptake, intracellular trafficking, and the overall fate of the AuNPs after the drug has been delivered need to be evaluated. All this information will add to the designing of a safe, stable and efficient drug delivery system of the future.

Appendix A

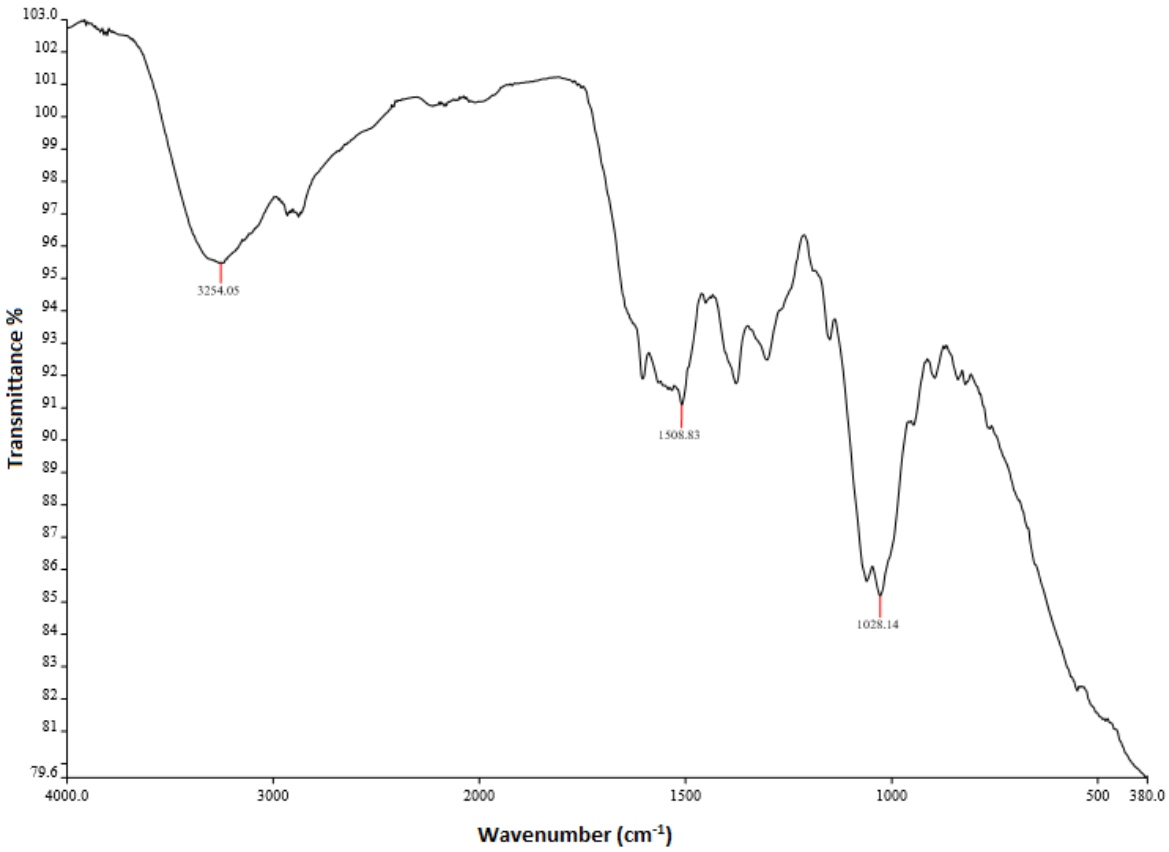
Transmittance %
Wavenumber (cm-1)
3254.05
1508.83
1028.14
103.0
102
101
100
99
98
97
96
95
94
93
92
91
90
89
88
87
86
85
84
83
82
81
79.6
4000.0
3000
2000
1500
1000
500
380.0

Appendix B

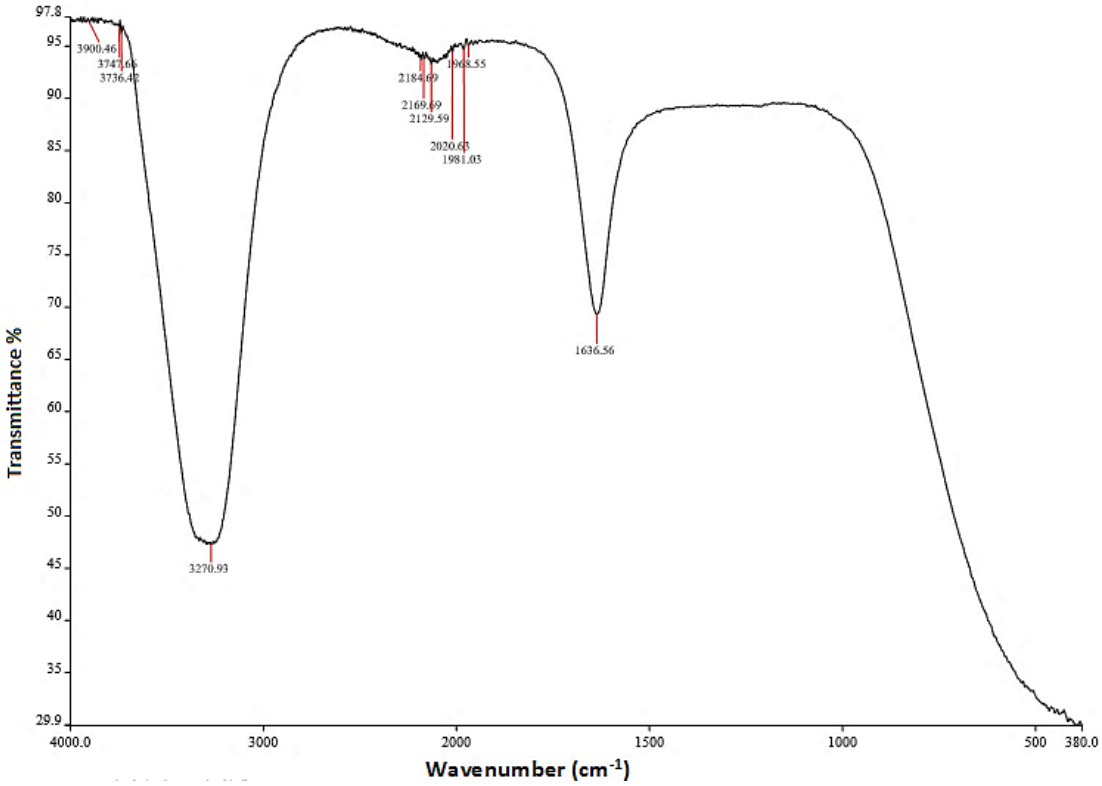
97.8
95
90
85
80
75
70
65
60
55
50
45
40
35
29.9
Transmittance %
3900.46
3747.66
3736.48
3270.93
2184.69
1968.55
2169.69
2129.59
2020.63
1981.03
1636.56
4000.0
3000
2000
1500
1000
500
380.0
Wavenumber (cm-1)